



POZNAN UNIVERSITY OF TECHNOLOGY
FACULTY OF CHEMICAL TECHNOLOGY
Institute of Chemistry and Technical Electrochemistry
Field of study: Chemical Technology



Andrés Camilo Parejo-Tovar

Performance of symmetric and hybrid electrochemical capacitors

Działanie symetrycznych i hybrydowych
kondensatorów elektrochemicznych

DOCTORAL DISSERTATION

Promoter:

Prof. François Béguin

Co-promoter:

Dr. Eng. Paula Ratajczak

Poznan, 2024



Rzeczpospolita
Polska



Fundacja na rzecz
Nauki Polskiej

Unia Europejska
Europejski Fundusz
Rozwoju Regionalnego



Badania do niniejszej pracy prowadzone były w ramach projektu „**Nowa koncepcja zrównoważonego kondensatora opartego o technologię węglowo-jonową – CARBionCAP**” przyznanego przez Fundację na rzecz Nauki Polskiej w ramach programu POWROTY finansowanego ze środków Europejskiego Funduszu Rozwoju Regionalnego w ramach Programu Operacyjnego Inteligentny Rozwój 2014-2020, Oś IV: Zwiększenie potencjału naukowo-badawczego, Działanie 4.4: Zwiększanie potencjału kadrowego sektora B+R.

Kierownik Projektu: dr. inż. Paula Ratajczak

Research for this work was carried out under the project "**New concept of a sustainable capacitor based on carbon-ion technology - CARBionCAP**" awarded by the Foundation for Polish Science under the RETURN program financed by the European Regional Development Fund under the Intelligent Development Operational Program 2014-2020 , Axis IV: Increasing the scientific and research potential, Measure 4.4: Increasing the human potential in the R&D sector.

Project leader: Dr. Eng. Paula Ratajczak

Acknowledgments

First and foremost, I would like to express my deepest gratitude to my scientific promoter, **Professor François Béguin**, for his unwavering support, dedication, and the countless hours he invested in guiding this research. His invaluable expertise and commitment have been instrumental to the success of this work and have greatly contributed to my professional growth throughout this journey. During my PhD studies, he set high standards for research excellence, provided meticulous guidance, offered continuous encouragement, and consistently motivated me to excel. He created an environment that allowed me to develop my strengths and expand my abilities. Moreover, he instilled in me a rigorous and practical approach to scientific research, imparting invaluable scholarly methods and problem-solving skills.

I would also like to extend my sincere thanks to my auxiliary promoter, **Dr. Paula Ratajczak**, for her valuable scientific guidance and support throughout my PhD studies. Her insights and contributions were crucial to my development as a researcher.

It is also a great pleasure to thank **Prof. Dr. hab Elżbieta Frąckowiak** for her role in helping me develop my skills in electrochemistry, which has been a vital part of this work.

I would like to extend my warm and sincere gratitude to all the members of the Power Sources Group for their support, camaraderie, and words of encouragement throughout this journey. Your collective assistance made this process all the more fulfilling.

Finally, I want to express my heartfelt thanks to my wife, Magdalena Szubińska-Parejo, for her unwavering support, boundless love, and being the driving force behind my personal growth. I am deeply grateful to her parents, Maria and Jarosław, and the rest of their family for embracing me as one of their own, welcoming me into their home, and making me feel truly at home, despite the language barrier. Your kindness and generosity have meant the world to me.

Table of Contents

Acknowledgments.....	5
Table of Contents	7
General introduction	11
Chapter I: Literature Review	19
Introduction.....	21
1. Electrical double-layer capacitors (EDLCs)	21
1.1. Electrical double-layer models (on a flat surface).....	21
1.2. Operation principle and properties of EDLCs.....	24
1.3. Carbons for EDLC electrodes.....	26
1.3.1. Type of carbons used as active materials of EDLC electrodes	26
1.3.2. Effect of the porous texture and structure of carbons on the capacitance of EDL electrodes.....	30
1.4. Electrolytes typically implemented in EDLCs	34
1.4.1. Aqueous electrolytes	35
1.4.1.1. Neutral aqueous electrolytes	36
1.4.1.2. “Water-in-Salt” electrolytes	37
1.4.2. Organic electrolytes.....	44
1.4.3. Ionic liquids as electrolytes	45
1.5. In-pore ion population changes during polarizing of EDL electrodes.....	47
2. Carbon-based Metal-ion Capacitors (MICs).....	51
2.1. Operational principles of MICs	51
2.2. Ion population changes in the positive carbon electrode of MICs	54
2.3. Carbons for the negative electrode of MICs and M ⁺ intercalation/insertion in these materials.....	56
2.3.1. Graphite.....	56

2.3.2. Reversible insertion mechanism in hard carbons	58
2.4. Organic electrolytes in MICs.....	62
2.4.1. Solvents	63
2.4.2. Salts	63
2.4.3. Additives	64
2.5. Solid-electrolyte interphase in the negative electrode of MICs	64
2.6. Pre-metalation methods for the preparation of MICs	66
3. Conclusion	69
Chapter II	73
1. Summary of the publication.....	75
Chapter III.....	79
1. Summary of the publication.....	81
Chapter IV.....	85
1. Summary of the publication.....	87
Chapter V	89
1. Summary of the publication.....	91
General conclusion.....	93
References.....	99
Scientific achievements	115
1. Publications.....	117
2. Oral Presentations	118
3. Poster presentations	118
4. Participation in scientific project	119
5. Awards	119
6. Grants.....	119
Abstract.....	121

Streszczenie.....	127
Co-authorship statements.....	133

General introduction

In the face of climate change and eventual depletion of fossil fuels, the humanity encounters an unprecedented situation that necessitates intensified search for new energy sources and development of non-combustion-based production methods. Combustion, the dominant source of energy for humanity, produces by-products that exacerbate environmental pollution, and the related greenhouse effect. While the combustion of fossil fuels has been a major driver of industrial and societal advancements, while improving the quality of life, it has also led to overpopulation and accumulation of harmful gases in the atmosphere, water, and soil, negatively impacting these environments. Furthermore, the increased production of chemicals and materials has accelerated resource depletion, adding to these environmental challenges. Renewable energy sources, such as solar and wind are already available, but present economic and political constraints as well as efficient exploitation challenges compared to combustion. The key issue is the instability of these renewable sources, as their output varies with weather conditions and geographic location, necessitating advanced energy storage solutions to adapt the energy supply to the demand.

At present, electrochemical systems, including secondary (rechargeable) batteries, are among the most suitable and adaptable devices for matching electricity delivery to demand. Storage batteries can convert electrical energy from sources such as solar cells or wind turbines into chemical energy, enabling non-spontaneous reactions. Rechargeable batteries, such as lead–acid, Ni-Cd, Ni-MH, and Li-ion, come in various shapes and sizes, making them useful for grid energy storage as well as for individual applications like automobile starters, powering of portable devices and light vehicles, etc. However, the chemical nature of the processes occurring in batteries imposes limitations, including restricted discharge rates, reduced cycle life and energy loss due to the internal resistance of cell components. Additionally, the high concentration of chemical energy in a compact form can lead to hazardous events, such as fires and explosions, particularly with Metal-ion batteries (MIBs) which utilize organic solvents. Therefore, it is essential to explore alternative energy storage solutions to circumvent few if not all these disadvantages, ensuring safer, more efficient, and versatile energy systems.

Among the various types of electrochemical energy storage systems, **symmetric electrical double-layer capacitors (EDLCs)** are distinguished by their simple construction and the electrostatic nature of energy storage, resulting in a rapid response time. Utilizing high surface area porous carbon electrodes immersed in an electrolytic solution, EDLCs can store several orders of magnitude greater energy than conventional dielectric capacitors. Moreover, the physical nature of the charge storage process, based on the attraction of a nanoscale layer of

ions from the electrolyte to the surface of a polarized electrode material, results in a remarkable power density of 15-30 kW kg⁻¹ and a long lifespan which surpasses one million charge/discharge cycles. Thus, EDLCs are highly suitable for high-power applications across various industries. They are employed in the automotive sector for functions such as operating emergency aircraft doors, regenerative braking, stop-start in vehicles, and power buffers in electrical drivetrains.

EDLCs at industrial scale often primarily utilize organic electrolytes, with 1 mol L⁻¹ tetraethylammonium tetrafluoroborate in acetonitrile (1 M TEABF₄/ACN) being the most prevalent choice. This electrolyte facilitates higher voltages (ranging from 2.85-3.0 V) and enables operation at very low temperatures (down to ca. -40 °C). However, EDLCs employing TEABF₄/ACN are environmentally unfriendly and hazardous due to the presence of acetonitrile, which has a low flash point of 5 °C. Moreover, organic electrolytes are highly hygroscopic and even a few parts per million of water can significantly diminish their electrochemical stability window (*ESW*). Consequently, EDLCs with organic electrolytes must be manufactured in controlled and moisture-free environments (including the removal of residual water from porous carbon electrodes before sealing the cells), which substantially increase the production costs. Conversely, conventional aqueous electrolytes such as H₂SO₄ and KOH used in batteries have been implemented to address a part of the aforementioned disadvantages of organic electrolytes. However, as the *ESW* and operating voltage are lower than 1 V, these electrolytes are not attractive for EDLCs. Recently, highly concentrated aqueous solutions of neutral salts, known as "Water-in-Salt" (WIS) electrolytes, have garnered considerable attention. These electrolytes, characterized by a salt-to-water mass and/or volume ratio greater than 1, effectively reduce the amount of free water at the surface of the electrodes, significantly enhancing the *ESW* beyond the thermodynamic stability limit of water. However, due to their high concentration, most WIS electrolytes are unsuitable for sub-ambient temperatures, where solute precipitation can reduce the electrolyte concentration and even block the porosity of activated carbon electrodes, deteriorating the device performance. Therefore, the design of WIS electrolytes that enable the cells to maintain performance down to sub-zero temperatures is crucial for advancing aqueous-based EDLCs.

While EDLCs offer high power density and rapid response times, **hybrid carbon-based metal-ion capacitors (MICs)** present another promising class of energy storage systems. Combining an electrical double-layer positive electrode with a battery-like negative electrode, MICs leverage these hybrid systems to achieve up to 4 times the output energy of EDLCs at

comparable power levels. Additionally, they exhibit a lower self-discharge rate owing to the presence of the battery-type negative electrode, providing a significant advantage over traditional EDLCs. Apart from that, carbon-based MICs demonstrate good cycling stability, achieving between 10,000-100,000 charge/discharge cycles. However, these hybrid cells face challenges in pre-metalation, which involves inserting metal ions into the negative electrode. This process is difficult to achieve in a single cell and typically requires an auxiliary electrode, complicating the assembly and potentially creating a dead mass, which reduces the specific energy and power output. Additionally, the use of alkali metal in auxiliary electrodes poses safety risks, such as thermal runaway or reactivity with moisture. To address these issues, there is growing interest in developing MICs with one electrode containing porous EDL carbon and a sacrificial metalated material, and the other electrode with the anodic host material. *In situ* formation of a solid electrolyte interphase (S.E.I.) and metalation of the anodic host is realized by irreversible oxidation of the sacrificial material (and associated metal transfer to the anode). For optimal performance, the sacrificial material must be fully utilized without producing solid residues or gases, and should have a low oxidation potential to prevent premature electrolyte decomposition. These factors are essential for forming an effective S.E.I. with good ionic conductivity and electronic insulation, enhancing MIC stability and performance. Hence, identifying and developing suitable cathodic sacrificial materials is a critical area of research, aiming to ensure safe and efficient operation of carbon-based MICs. Given the limited geographical availability, high cost, and geopolitical risks associated with lithium, research should also focus on more accessible materials like sodium, which is abundant and widely distributed, making it a promising alternative for mass production and enhancing political and economic stability. Therefore, exploring alternatives to lithium-ion capacitors (LICs), particularly sodium-ion capacitors (NICs), is important for the sustainable development of MIC technologies.

Noteworthy, the aforementioned higher specific energy of MICs compared to EDLCs is primarily related to their higher operative voltage and greater capacity/capacitance. The increased voltage, generally reaching around 3.8 V, is associated to the low potential at which the negative electrode operates. On the other hand, the high capacity/capacitance is linked to the broad potential range of the EDL positive electrode in MICs, which covers the typical potential of EDL positive electrode and partly that of the negative electrode in EDLCs. Given its operation within this extended potential range, the operative mechanism of the EDL positive electrode in MICs appears as an important area of study. While the ion population changes in

the porous electrodes of EDLCs are relatively well understood, there is a lack of similar fundamental studies for carbon-based MICs. In the existing research addressing the ion population changes in the pores of the positive electrode, faradaic signatures were observed, suggesting the formation of decomposition products that can interfere with the charge exchange processes. To minimize these interferences and to ensure reliable and efficient operation of MICs in energy storage applications, *operando* analyses should be conducted to track ion population changes in the EDL positive carbon electrode during charge and discharge cycles within the operating potential range of MICs.

In view of the presented context, this dissertation aims to address key challenges in EDLCs and MICs with the following objectives: **i) developing advanced WIS electrolyte for EDLCs to attain high voltage and stable operation, particularly in low-temperature environments, thereby enhancing energy density and extending cycle life; ii) refining the pre-metalation process in MICs by employing the irreversible oxidation of a carefully selected cathodic sacrificial material, enabling the S.E.I. formation and effective pre-metalation of the anodic host, without forming undesired by-products; and iii) developing an *operando* methodology for tracking ion population changes in the EDL positive electrode of MICs during charge and discharge cycles, providing critical insights into electrode processes to optimize performance and reliability.** The implementation of the introduced strategies and methodologies should enable overcoming the current limitations and advancing the performance of EDLCs and MICs, which is crucial for meeting the evolving energy storage needs of modern society, while providing environmentally friendly materials.

In order to address these issues, the dissertation is divided into 5 chapters, as follows:

Chapter I provides a comprehensive literature review that explores key advancements in EDLCs and MICs utilizing carbon-based electrodes. The first part delves into EDLCs, including their fundamental operational principles, common electrode materials, and the influence of texture/structure and electrolyte type on their performance. Special attention is given to the influence of porous texture and electrochemical stability window (*ESW*) on EDLCs efficiency, with a focus on organic, aqueous, and emerging WIS electrolytes. Additionally, the ion population dynamics within the EDLC electrodes during the charge and discharge cycles are explored, providing a detailed understanding of the electrostatic processes at play. In the second part, the chapter presents the operation principles of carbon-based metal-ion capacitors (MICs). It discusses the effects of pairing an EDL-type positive electrode with a battery-type

negative electrode and provides an overview of materials typically used for the negative electrode in these devices. Special attention is given to the formation of a solid electrolyte interphase (S.E.I.) on the negative electrode, which is crucial for ensuring the reliable operation of MICs. The chapter also reviews the various electrolytes used in MICs to facilitate S.E.I. formation and presents the latest techniques used for pre-metalating the negative electrode of this kind of device, aimed at optimizing MIC performance.

Chapter II presents the study *"The NaClO₄-Water Eutectic Electrolyte for Environmentally Friendly Electrical Double-Layer Capacitors Operating at Low Temperature"* realized to address the limitations of traditional electrolytes in low-temperature environments, such as solute precipitation and increased viscosity. In this context, the **NaClO₄-water eutectic solution** was examined to verify its transport properties between 25°C and -35°C. The research correlates molecular dynamics (MD) simulations with experimental data to show how hydrogen-bonded water channels enhance ionic diffusion, enabling the electrolyte to maintain high ionic conductivity at low temperatures. The electrochemical performance of activated carbon (AC) electrodes, combined with the use of this WIS electrolyte, demonstrates extended electrochemical stability windows (ESW) and significant energy output down to -35°C, providing a robust solution for environmentally friendly, low-temperature EDLCs.

In the pursuit of improving the pre-metalation process for sodium-ion capacitors (NICs), **Chapter III introduces the study** *"Ideally Realized Sodium-Ion Capacitor via Irreversible Oxidation of Sodium Azide to Pre-Metalate the Anodic Host"*. This research addresses the challenge of incomplete metal insertion and degraded electrode performance in traditional pre-metalation methods. By employing **sodium azide (NaN₃) as a sacrificial material**, the study demonstrates that NaN₃ undergoes complete and irreversible oxidation at 3.5 V vs Na/Na⁺, resulting in effective pre-metalation without compromising the porous structure of the activated carbon (AC) electrode. Utilizing nitrogen adsorption analysis and operando mass spectroscopy, the methodology confirms the preservation of AC porosity post-oxidation and efficient sodium transfer to the hard carbon mixture (HCM) in the negative electrode. This process yields a sodium-ion capacitor with high cycle stability and energy efficiency, making NaN₃ a promising zero-dead-mass sacrificial material.

To address the challenge of accurately assessing the distinct charge storage mechanisms in hybrid capacitors, **Chapter IV presents the publication titled** *"Comprehensive Potentiodynamic Analysis of Electrode Performance in Hybrid Capacitors"*. This study adapts

a calculation procedure previously used for EDLCs by **dynamically adjusting potential sweep rates for the positive and negative electrodes** according to their contribution to the voltage ramp. By employing cyclic voltammetry (CV) and comparing the performance of hybrid lithium-ion capacitor (LIC) to a symmetric EDLC, the methodology identifies differences in charge transfer dynamics of the battery-type and EDL-type electrodes. These insights provide a pathway to optimize the balance between energy density and power output by adjusting electrode composition and mass ratios, enhancing the overall performance of hybrid capacitors.

The ion exchange dynamics, critical to the performance of LICs, is addressed in **Chapter V, which summarizes the article titled "Operando Tracking of Ion Population Changes in the EDL Electrode of a Lithium-Ion Capacitor During Its Charge/Discharge"**. This study is focused on **tracking ion population changes** within the activated carbon (AC) electrode during charge/discharge cycles, revealing the perm-selective adsorption of partially solvated lithium ions and trapping of anions in less accessible pores at high potentials. By employing molecular dynamics (MD) simulations and *operando/in-situ* techniques such as electrochemical dilatometry (ECD), potentiostatic electrochemical impedance spectroscopy (PEIS), and Raman spectroscopy, the methodology sheds light on ion solvation/desolvation and transport within AC pores under electrode polarization. These findings emphasize the need to optimize the porous texture of AC materials to reduce ion trapping and improve the efficiency and lifespan of LICs.

The manuscript finishes with a general conclusion on the key findings and provides perspectives for future research based on the advancements discussed throughout this dissertation.

Chapter I: Literature Review

Introduction

This literature review explores the advancements in electrical double-layer capacitors (EDLCs) and carbon-based metal-ion capacitors (MICs). Both technologies offer high power density and rapid charge/discharge capabilities, making them promising for various applications. The first part provides a comprehensive overview of EDLCs, including their operational principles, electrode materials, and electrolytes. The effects of porous texture, structure, and electrolyte type on EDLC performance are discussed. The section also delves into in-pore ion population changes during electrode polarization.

The second part focuses on carbon-based MICs, outlining their operational principles, active materials for both positive and negative electrodes, and the role of electrolytes. The section discusses the challenges associated with using graphite and hard carbon in MICs and explores strategies for improving their performance, such as pre-metalation methods. Overall, this review aims to provide a thorough understanding of the current state-of-the-art in EDLC and MIC technologies and highlight the key challenges and opportunities for future research and development.

1. Electrical double-layer capacitors (EDLCs)

1.1. Electrical double-layer models (on a flat surface)

The electrical double-layer (EDL) is the structure which is formed at the interface of a charged electrode and an electrolytic solution, where the balancing counter charge accumulates to maintain electro-neutrality [1]. Numerous models of EDL formation have been developed over the last two centuries to understand/interpret a variety of interfacial processes in the context of energy storage, water desalination, actuation, drug delivery systems, electroplating, corrosion inhibition, and sensors, among others [2]. Various models of the EDL on a positively polarized electrode in an electrolyte with solvent are presented in **Figure 1**, where ϕ_E is the potential profile [3].

Figure 1a shows the model of EDL proposed by Hermann von Helmholtz in 1853 [4], in which the charge of the polarized solid electronic conductor is balanced by a monolayer of counter-ions (named compact layer [5]) dissolved in the solution: counter-ions are defined as charged atoms or molecules with opposite charge to the polarized electrode. In this model, the potential

decreases linearly with increasing the distance from the electrode. The capacitance of the Helmholtz double-layer (C_H) is given by **Equation (1)** [6]:

$$C_H = \frac{\varepsilon_r \varepsilon_0 S}{d} \quad (1)$$

where ε_r is the relative permittivity of the electrolyte, ε_0 the vacuum permittivity ($\varepsilon_0 = 8.854 \times 10^{-12} \text{ F m}^{-1}$), S the surface area of the electrode-electrolyte interface, and d the distance from the surface of the polarized electrode to the center of counter-ions forming the compact layer (**Figure 1a**). This model assuming the accumulation of counter-ions in a single plane along the electrode surface has two main defects: (i) it neglects interactions occurring further than the compact layer and (ii) it does not take into account the influence of electrolyte concentration in the EDL formation [5].

At the beginning of the 20th century, Gouy [7] and Chapman [8] developed independently an EDL model which includes a diffuse layer between the electrode and bulk electrolyte to take into account the thermal fluctuation according to the Poisson–Boltzmann equation [6]. According to Gouy-Chapman, the electrical double-layer is not as compact as in Helmholtz's description, but of variable thickness, with ions free to move (**Figure 1b**). This model considers that both the applied electrode potential and electrolyte concentration influence the value of the double-layer capacitance (C_D), as expressed by **Equation (2)** [9]:

$$C_D = \frac{\varepsilon_r \varepsilon_0}{\lambda_D} \cosh\left(\frac{z F \phi}{2 R T}\right) \quad (2)$$

where ϕ is the electrical potential applied to the electrode ($V_{vs \text{ Ref}}$), F the Faraday constant (96485 C mol^{-1}), R the ideal gas constant ($8.314 \text{ J (K mol}^{-1})$), T the temperature (K), ε_r the relative permittivity of the electrolyte, ε_0 the vacuum permittivity. The average thickness of the diffuse layer (also called Debye length, λ_D) for monovalent ions in the electrolyte is expressed by **Equation (3)** [9]:

$$\lambda_D = \sqrt{\frac{\varepsilon_r \varepsilon_0 R T}{2 F^2 C_0}} \quad (3)$$

where C_0 is the bulk electrolyte concentration (mol m^{-3}).

In this theory, one of the major flaws is to consider the ions as point charges, which can virtually approach the electrode's surface at zero distance, leading to an overestimation of the EDL capacitance [9]. The capacitance of two separated arrays of charges increases inversely with their separation distance as observed in **Equation (1)** [3].

More than twenty years later, Stern proposed a combination of Helmholtz and Gouy-Chapman models [10], where the closest counter-ions form a compact layer adsorbed on the polarized electrode surface, followed by a diffuse layer extending to the bulk electrolyte (**Figure 1c**). The two layers behave as two capacitors in series: the capacitance of the compact Helmholtz layer (C_H) and the capacitance of the diffuse Gouy-Chapman layer (C_D), hence, the electrical double layer capacitance (C_{EDL}) can be expressed as **Equation (4)** [9]:

$$\frac{1}{C_{EDL}} = \frac{1}{C_H} + \frac{1}{C_D} \quad (4)$$

The electric field at the electrode surface, the types of electrolyte ions, the solvent used, and the chemical affinity between the adsorbed ions and the electrode material all influence the electrical double-layer capacitance [3]. Noteworthy, the Stern model is indeed widely utilized for the interpretation of experimental results obtained with EDLCs [9].

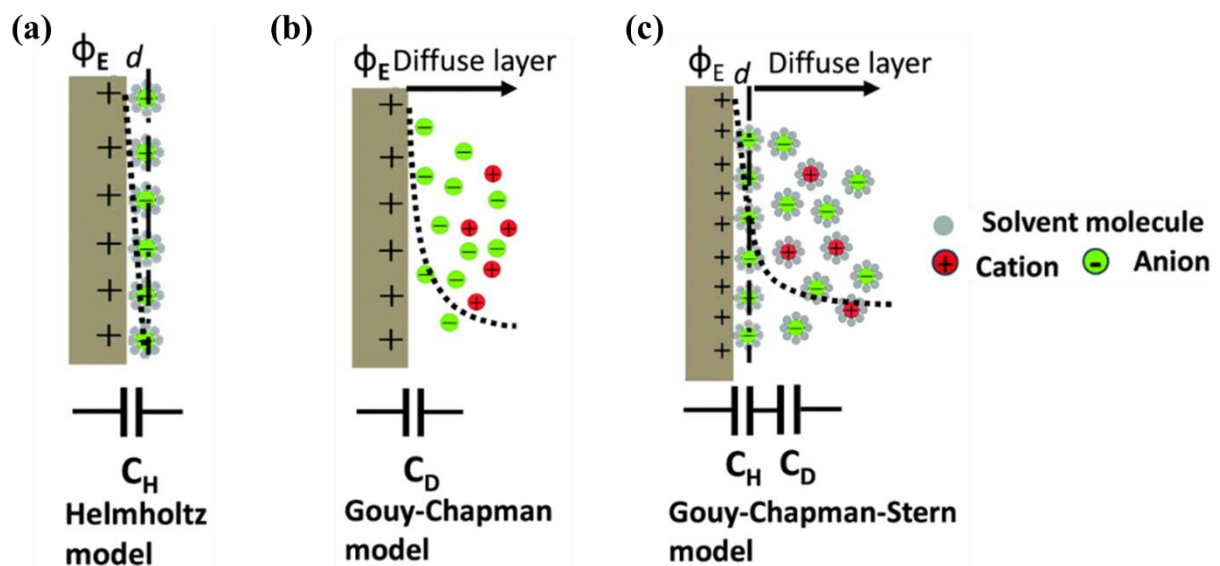


Figure 1. Schematic EDL models on the surface of a positively polarized electrode in an electrolyte with solvent: (a) Helmholtz model, (b) Gouy–Chapman model, and (c) Stern model. The dotted lines indicate for each model the potential profile (ϕ_E) in the solution. The bottom insets represent the simplified equivalent circuits. From [9].

1.2. Operation principle and properties of EDLCs

An electrical double-layer capacitor (EDLC) comprises two electrodes, typically made of porous carbon, in contact with an electrolyte (**Figure 2**). These electrodes are physically separated by a permeable membrane, which allows ions to freely pass between them. When a potential difference is applied between the electrodes, electrical double-layers form at the electrode/electrolyte interfaces. As shown in **paragraph 1.1**, these layers schematically represented in **Figure 2** include counter-ions balancing the charges (electrons or holes) injected into the electrodes. In the charged state (**Figure 2**, right), the device is equivalent to two capacitors of capacitance C_+ and C_- in series. The capacitance C [F] of the cell is given by **Equation (5)**:

$$\frac{1}{C} = \frac{1}{C_+} + \frac{1}{C_-} \therefore C = \frac{C_- * C_+}{C_- + C_+} \quad (5)$$

Noteworthy, even in a symmetric capacitor, the two electrodes may have different capacitance values due to the different sizes of ionic species in the electrolyte [11], leading according to **Equation (5)** the electrode with the smallest capacitance to determine the capacitance of the device.

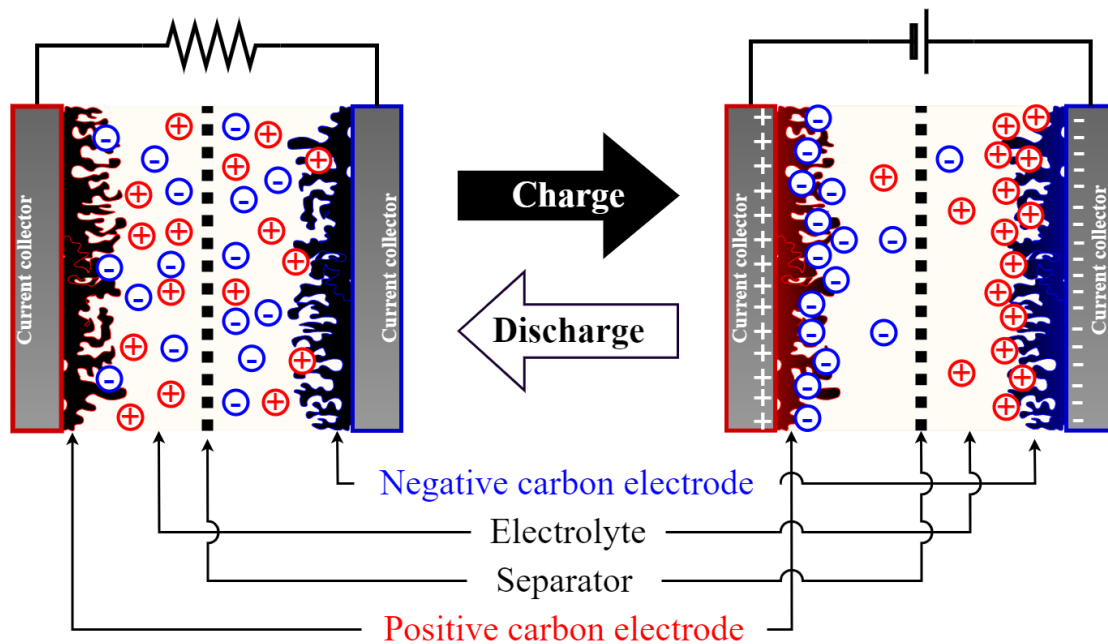


Figure 2. Schematic representation of a symmetric electrical double-layer capacitor depicting the distribution of charges when the device is discharged (left) and charged (right).

In reporting scientific results about electrode materials for EDLCs, it is a common practice to express the specific (gravimetric) capacitance, which refers to the capacitance of a single electrode, denoted as C_{SP} [F g⁻¹]. For a symmetric EDLC, where both electrodes are identical in mass, thickness, surface area, and material, **Equation 6** can be used [12]:

$$C_{SP} = \frac{2 * C}{0.5 * m_{AM}} \quad (6)$$

where C is the capacitance of the device referred to the total mass, m_{AM} , of active material in both electrodes.

To evaluate the practical applicability of EDLCs, their energy (E) and power (P) are the most important parameters to be determined and compared with other energy storage devices. They can be expressed per mass of the device, referred to as gravimetric or specific energy (E_s in Wh kg⁻¹) and power (P_s in W kg⁻¹) or per volume, referred to as volumetric energy (E_v in Wh L⁻¹) and power (P_v in W L⁻¹). The specific energy, E_s , stored in an EDLC depends on the capacitance of the device (C in F), cell voltage (U in V), and mass of the device (m in kg), as expressed in **Equation (7)** [12]:

$$E_s = \frac{C * U^2}{2 * m} \quad (7)$$

The power capability, P_s , expressed by **Equation (8)** depends on the nominal voltage of the EDLC and is inversely proportional to its equivalent series resistance (R_{ESR}) [12]:

$$P_s = \frac{U_{max}^2}{4 * R_{ESR} * m} \quad (8)$$

The ESR strongly depends on the ionic conductivity and viscosity of the electrolyte impregnated in the electrode, the electronic resistance of the electrodes, and the contact resistance between electrodes and respective current collectors [12]. Notably, normalizing energy and power of EDLCs to the masses of electrodes (or their active mass) is common practice in the scientific community, facilitating comparisons with other devices, particularly from an application perspective [13].

Typically, the performance of electrochemical energy storage systems (EES) is compared using the so-called Ragone plot, which shows the specific energy vs specific power (**Figure 3**). As

seen in this figure, EDLCs store more energy than conventional electrolytic capacitors, with keeping outstanding power rate. However, owing to the electrostatic nature of their operative mechanism, the specific energy is much lower than in the case of batteries. Noteworthy, hybrid capacitors, realized by the internal association of a battery-like anode with a positive EDL electrode, store more energy per mass than conventional EDLCs, while displaying good power capability [14, 15]. The diagonal dashed lines in **Figure 3** represent the energy/power ratio, called the time constant, τ , of the device expressed by **Equation (9)**:

$$\tau = R_{ESR} * C \quad (9)$$

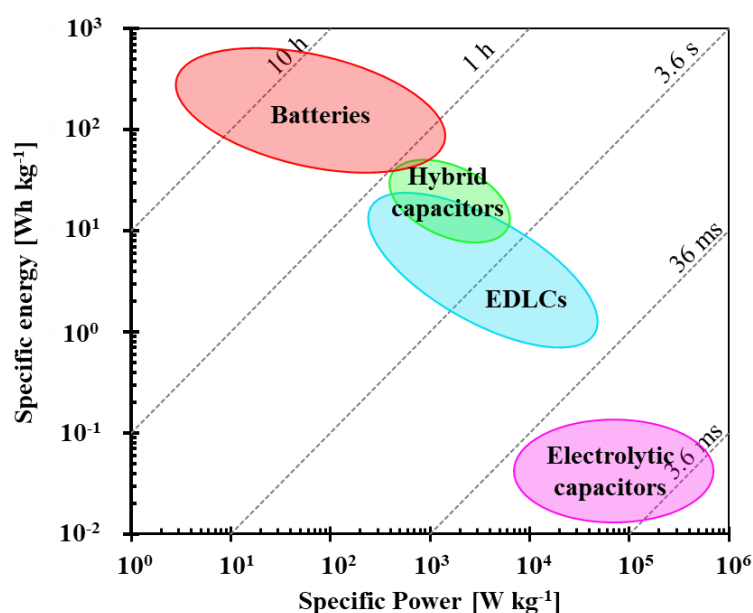


Figure 3. Ragone plot of various electrochemical energy storage systems. From [14].

1.3. Carbons for EDLC electrodes

1.3.1. Type of carbons used as active materials of EDLC electrodes

Nowadays, most of the commercially available electrical double-layer capacitors (EDLCs) utilize nanoporous carbon as the active material in their electrodes. The overall performance of these systems is closely linked to the porous texture, structure and surface functionality of carbon electrodes [9, 11, 16]. To achieve a high capacitance and an optimal balance between delivered energy and power, the following parameters must be considered in the selection of EDLC electrodes:

- **High electrical conductivity:** Ensures efficient charge transfer during electron or hole injection, reducing the internal resistance and improving performance. This facilitates rapid charge and discharge cycles, essential for high-power applications.
- **High specific surface area (SSA):** A greater surface area enhances the electrode/electrolyte contact and consequently capacitance. The specific surface area of porous carbons can be beyond $2000 \text{ m}^2 \text{ g}^{-1}$, thereby maximizing the EDL charge storage capacity [9]. Pore volume along with pore size distribution are key features for assessing the capacitive performance of electrodes.
- **Controlled porous texture:** A bimodal porosity featuring interconnected micropores and mesopores, known as hierarchical texture, is currently attractive for EDLC electrodes. The charge storage predominantly occurs in the smaller micropores, while the larger pores (preferably mesopores) facilitate the rapid transport of electrolyte ions to the micropores [16-18].
- **Structural disorder:** Recent investigations suggest that the capacitance of EDLC electrodes is significantly influenced by the degree of structural disorder in the carbon material [19].
- **Good corrosion resistance:** Extends the lifespan of EDLCs by withstanding the chemical environment within the device without degrading, thereby maintaining performance over many cycles.
- **Processability and compatibility in composite materials:** Ensures the mechanical stability and integration with the conductive additive and binder during manufacturing of the electrodes, enhancing the overall performance.
- **Low production cost:** Making EDLCs commercially viable requires keeping electrode production costs low, using cost-effective materials and efficient manufacturing processes without compromising quality.

Figure 4 shows the Transmission electron microscopy (TEM) images of carbons of various dimensionalities, which have been investigated for their application as active materials in EDLC electrodes. These include 0-dimensional onion-like carbons, 1-dimensional carbon nanotubes and carbon fibers, 2-dimensional graphene, and 3-dimensional porous carbons such as activated carbons, carbon black, templated carbons, and carbide-derived carbons.

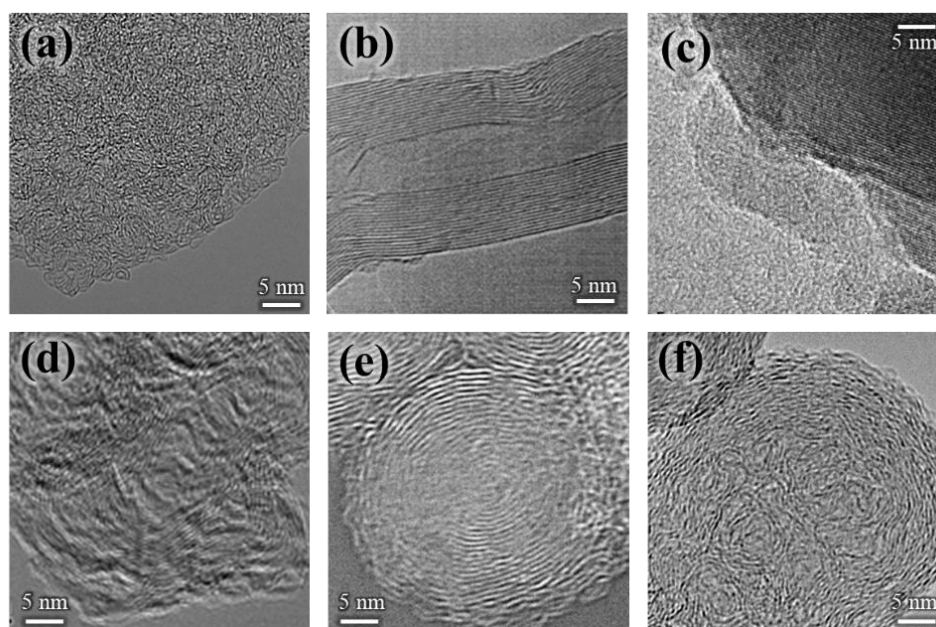


Figure 4. Transmission electron microscopy (TEM) images of carbons with various dimensionalities typically used for the construction of EDLC electrodes: (a) Activated carbon; (b) multi-walled carbon nanotube [20]; (c) few-layered graphene sheets [21] (d) Carbide-derived carbon (CDC) [22]; (e) Onion-like carbon [23] and (f) carbon black [24].

Activated carbons (ACs): Activated carbons are the most widely used/studied active materials for EDLC electrodes due to their attractive textural properties, facile preparation, and relatively low cost [12, 16, 25]. These porous materials primarily composed of sp^2 carbon atoms are generally prepared from natural or synthetic organic precursors, which are first pre-carbonized and then physically or chemically activated to open the porosity and create new pores [3, 9]. Physical activation involves heating the pre-carbonized precursor to high temperatures (700-1000 °C) in an oxidizing atmosphere as steam and CO_2 . Chemical activation, on the other hand, uses chemical reagents (such as KOH or $ZnCl_2$) at lower temperatures (400-700 °C) [26, 27]. The result of any activation process is the formation of a porous network within the carbon particles, significantly increasing their surface area. Precise measurement of this surface area by gas adsorption is challenging and can vary depending on the experimental conditions and calculation method [11]. While S_{BET} specific surface areas as high as ca. 3000 $m^2 g^{-1}$ have been reported [28], the usable surface area typically falls within the range of 1000-2000 $m^2 g^{-1}$ [25].

Recently, the electrochemical performance of AC-based electrodes has been significantly improved to reach 70 $F cm^{-3}$ or exceed 100 $F g^{-1}$ in nonaqueous-based electrolytes [14]. Most of the commercially available EDLCs are constructed with activated carbon electrodes and organic electrolytes.

Carbide-derived carbons (CDCs): are produced by selective etching of metals from various metal carbides, with titanium carbide (TiC) being the most used [29]. Leaching in supercritical water, high-temperature treatment in halogens, vacuum decomposition, and other methods can be used to remove metals from carbides, producing carbon coatings or bulk and powdered carbon [30]. The porous texture of CDCs can be tuned depending on the distribution of carbon atoms in the carbide precursor and synthesis temperature. For instance, titanium carbide-derived carbons (TiC-CDCs) exhibit a wider pore size distribution compared to silicon carbide-derived carbons (SiC-CDCs) when synthesized at the same temperature (1200 °C) [31]. CDCs are promising for EDLC electrodes due to their customizable porous network and better control of surface functionality compared to ACs [31]. TiC-CDCs electrodes were reported to have a high gravimetric capacitance, up to 220 F g⁻¹ in aqueous KOH solution and 120 F g⁻¹ in organic electrolyte, whereas SiC-CDCs have a relatively high volumetric capacitance up to 122 F cm⁻³ in aqueous KOH and 70 F cm⁻³ in organic electrolyte [25].

Templated carbons (TCs): these carbons are obtained by template-assisted carbonization of organic precursors and subsequent removal of the template. This method allows for precise control of the pore size distribution [32], an important parameter to consider in the selection of carbon materials for EDLC electrodes. Two types of templates can be employed: hard templates (like zeolites, mesoporous silicas, and metal oxides) and soft templates (such as metal-organic frameworks and block copolymer surfactants) [33]. In the literature, capacitance values ranging from 131 to 153 F g⁻¹ have been reported in 1.0 mol kg⁻¹ TEABF₄/propylene carbonate electrolyte for electrodes based on zeolite-templated carbon (ZTC) produced by chemical vapour deposition (CVD) [34].

Carbon onions (also known as onion-like carbons; OLCs): are spherical or polyhedral carbon nanoparticles composed of concentric, defective sp²-hybridized carbon multiple shells. These nanoparticles typically measure a few tens of nanometers in diameter [35]. The most commonly used synthesis method of carbon onions is the graphitization of nanodiamonds at high temperatures (>1700 °C) in an inert gas or vacuum [35, 36]. Unlike porous carbons, OLCs have a limited external surface area ranging between 300-600 m² g⁻¹. However, they exhibit a high interparticle pore volume of around 1 cm³ g⁻¹ [37]. Despite their non-porous nature, the entire surface of OLC particles is accessible to electrolyte ions, and due to that, OLC-based electrodes can deliver excellent power performance [38]. However, their limited capacitance of 50 F g⁻¹ makes them less suitable for increasing the overall capacitance of EDLC electrodes.

Carbon nanotubes (CNTs): are cylindrical carbon structures composed of a hexagonal arrangement of sp^2 carbon atoms. They are formed by rolling up a single layer of graphene (single-walled CNTs, SWCNTs) or multiple layers (multi-walled CNTs, MWCNTs) [39]. Common synthesis methods include arc discharge, laser ablation, and CVD [40]. CNTs generally have a surface area ranging from 100 to 1000 $m^2 g^{-1}$ [41]. Though exhibiting a narrow pore size distribution, the internal channel is unlikely to contribute significantly to the capacitive performance due to the limited accessibility of ions related to the absence of an internal electric field under typical operating conditions [9]. Similarly to OLCs, the external surface of CNTs can be used to form electrodes with a high external surface area displaying a moderate capacitance below 100 $F g^{-1}$ [41]. However, their highly accessible external surface and excellent electrical conductivity make CNTs ideal for high-power applications [42, 43].

1.3.2. Effect of the porous texture and structure of carbons on the capacitance of EDL electrodes

As previously mentioned, several parameters affect the capacitive performance of carbon electrodes in EDLCs. Notwithstanding, the most relevant are closely connected with the porous texture (specific surface area, pore volume, size and shape of pores, tortuosity). According to **Equation (1)**, a high specific surface area (pore volume) is desired for the EDL formation, yet the pores must be large enough to accommodate ions—at least in the desolvated state for electrolytes with solvents [44]. According to the International Union of Pure and Applied Chemistry (IUPAC) classification, there are three main kinds of pores: (i) micropores (with diameters <2 nm), mesopores (diameters from 2 to 50 nm) and macropores (diameters >50 nm) [45]. Since the macropores do not take part in the adsorption processes, their contribution to the total surface area is negligible. Ions are the most efficiently adsorbed in the micropores providing a high surface area, while the mesopores are intended to allow the ions to be transported to the micropores [16, 17, 18]. With ordered porous carbons containing both meso/macropores and micropores, it has been demonstrated that the capacitance contribution from meso/macropore surfaces is almost negligible and only the micropore surfaces near the openings are effective in contributing to capacitance [46]. Therefore, selecting an appropriate meso-/micro- pore volume ratio is essential for optimizing the capacitive performance of carbons.

The most popular and employed method for characterizing the textural properties of porous carbons is the physical adsorption of gases, which permits the determination of

adsorption/desorption isotherms. Various adsorbates, including N₂, CO₂, argon, helium, CH₄, benzene, and nonane, among others, can be employed [47]. However, N₂ adsorption at -196 °C is the most common owing to its ability to measure adsorption in both micropores and mesopores over a wide range of relative pressures starting from $P/P_0 = 10^{-7}$ [47]. In many studies, the specific surface area (*SSA*) is usually determined by analyzing the adsorption isotherm of porous carbons or carbon-based electrodes with the Brunauer-Emmett-Teller (BET) method [48]. Nevertheless, it is peremptory to note that, in highly porous carbons, physical adsorption may occur via a pore-filling mechanism instead of surface coverage exclusively, as is assumed by the BET method [49]. In such cases, the application of this method can lead to unrealistic estimations of surface area [50, 51]. Indeed, in a thorough investigation performed by Centeno and Stoeckli [50], the surface area determined by the BET method (S_{BET}) was compared with the average surface area (S_{av}) of 42 well-characterized microporous carbons having average pore size (L_0) values ranging from 0.66 to 1.65 nm. S_{av} was determined by averaging the *SSA* obtained by various methods: (i) the Dubinin-Radushkevich equation (S_{DR}) [52], (ii) the density functional theory (S_{DFT}) [53], (iii) the Kaneko's comparison plot on N₂ adsorption isotherms at -196 °C (S_{comp}) [54] and (iv) phenol immersion enthalpy (S_{phenol}) [55]; noteworthy, a good agreement was observed in the values of *SSA* determined with each method. The comparison revealed that S_{BET} and S_{av} closely align only for pores with a width of approximately 0.9 nm. For pores wider than 0.9 nm, the BET method overestimates the *SSA* of carbons. Conversely, it underestimates the surface area for pores narrower than 0.9 nm.

In the literature, various authors assumed that the surface area of the electrode-electrolyte interface during EDL formation is equivalent to S_{BET} measured for the carbon electrode [56, 57, 58], which induces inconsistencies in the value of surface-normalized capacitance (C/S in F m⁻²) in narrow pores [59]. In this context, García-Gómez et al. [60] conducted an interesting study elucidating the relationship between surface-normalized capacitance and L_0 for various carbon electrodes (and a few monolith binder-free electrodes) in a 1.0 mol L⁻¹ TEABF₄/ACN electrolyte. The surface-normalized capacitance of the electrodes is plotted vs S_{BET} in **Figure 5a** and vs $S_{>0.63} = S_{tot} - S_{<0.63}$ in **Figure 5b**, where S_{tot} is the average value of S_{DR} , S_{comp} , and S_{phenol} , and $S_{<0.63}$ is the surface inaccessible for the oblate spheroidal TEA⁺ desolvated cation with an equatorial diameter of 0.63 nm (to account that only pores larger than 0.63 nm can store TEA⁺ cations). When plotting C/S_{BET} vs. L_0 , **Figure 5a** shows a significant increase in C/S_{BET} for L_0 values lower than 0.9 nm, i.e., when the *SSA* is underestimated by the BET model

[50]. By contrast, when the capacitance is normalized to $S_{>0.63 \text{ nm}}$ (**Figure 5b**), there is not a significant dependence of $C/S_{>0.63}$ on L_0 in the whole range, and it is practically constant around 0.094 F m^{-2} ; a similar pattern is even shown up to 15 nm [61]. This is a notorious result because it demonstrates that the “anomalous” increase [62] in normalized capacitance, C/S_{BET} , claimed for TiC-CDC electrodes in 1.5 mol L^{-1} TEABF₄/ACN electrolyte when L_0 is smaller than 1 nm is likely attributable to the underestimated BET values [50].

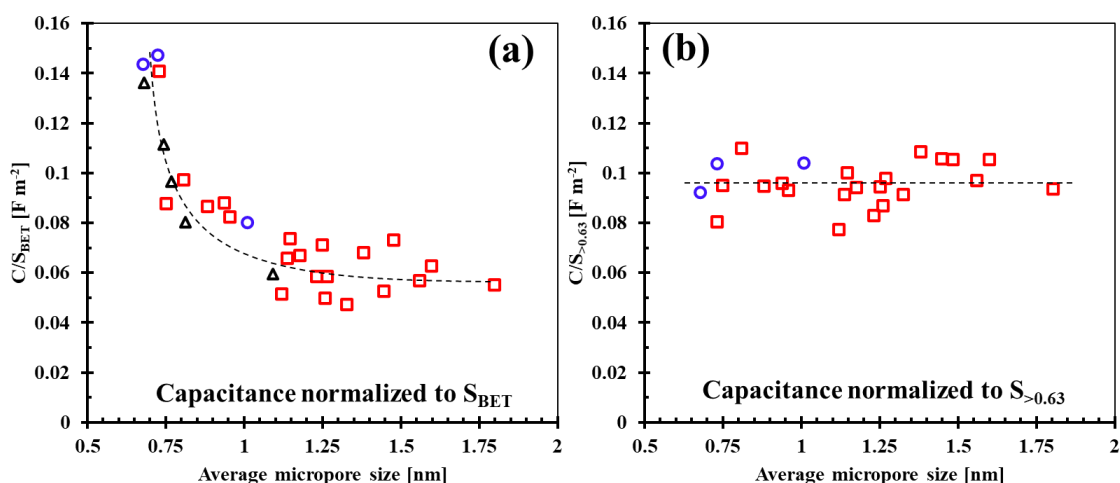


Figure 5. Variation of the capacitance in 1.0 mol L^{-1} TEABF₄/ACN normalized to (a) S_{BET} and (b) surface area related to pores larger than 0.63 nm ($S_{>0.63}$) vs average micropore size (L_0) of electrodes based on carbon monoliths (circles), a variety of porous carbons (squares), and carbide-derived carbons (triangles). Adapted from reference [60].

The lack of correlation between capacitance and pore size of EDL electrodes has prompted research into the influence of structural features of porous carbons. Very recently, Liu et al [19] correlated the gravimetric capacitance (F g^{-1}) of 23 carbon-based electrodes (including commercial and thermally annealed carbons) in 1.0 mol L^{-1} TEABF₄/ACN electrolyte with $\Delta\delta$ values determined by solid-state ^{19}F nuclear magnetic resonance (NMR) spectroscopy (**Equation (10)**). It should be noted that the ^{19}F NMR spectra of carbons soaked with the electrolyte show distinct resonances for ions within carbon nanopores ("in-pore") and those outside the pore network ("ex-pore"). The in-pore resonance appears at lower chemical shifts than the bulk electrolyte due to "ring currents" generated by the circulation of delocalized π -electrons in the aromatic carbon rings under the influence of the applied magnetic field [63]. Herein, this effect is quantified by the ^{19}F $\Delta\delta$ value (ppm) for the fluorine atom of the BF₄⁻ anion and expressed by **Equation (10)**:

$$\Delta\delta = \delta_{in-pore} - \delta_{neat\ electrolyte} \quad (10)$$

where $\delta_{neat\ electrolyte}$ is the chemical shift of bulk electrolyte and $\delta_{in-pore}$ is the chemical shift of the “in-pore” resonance. The magnitude of the $\Delta\delta$ value reflects the strength of the interaction between electrolyte anions and the carbon pore walls. As such, it serves as a probe for investigating the local structure of nanoporous carbon and the "ordered domain size", i.e., the average size of the graphene-like fragments which form the carbon pore walls. Noteworthy, porous carbons prepared at lower temperature exhibit smaller $\Delta\delta$ values owing to their more disordered local structure, i.e., smaller ordered domains [64]. In **Figure 6** showing the plot of specific capacitance vs $\Delta\delta$ values for the investigated carbon electrodes, it is seen that the carbons with the smallest $\Delta\delta$ values exhibit the highest gravimetric capacitance in the organic electrolyte. Interestingly, similar correlations of $\Delta\delta$ values with the structural disorder of carbons were found when tracking the nuclei of the TEA⁺ cation regardless of the nucleus probed [19].

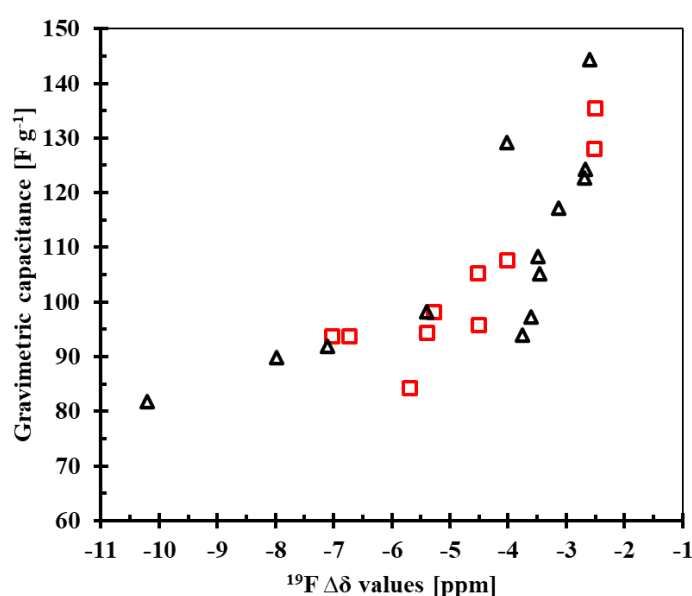


Figure 6. Gravimetric capacitance of carbon electrodes in the 1 mol L⁻¹ TEABF₄/ACN electrolyte vs $\Delta\delta$ values measured by ¹⁹F NMR (for the fluorine atom of the BF₄⁻ anion in the electrolyte). The electrodes included commercial (squares) and thermally annealed (triangles) carbons. Adapted from the reference [19].

In summary, the textural properties of carbon electrodes play a crucial role in their EDL performance. Whereas high porosity is beneficial, pore size must be sufficient to accommodate ions. However, it has been proved that there is no correlation between the capacitance and the pore size of the electrodes. Moreover, recent investigations revealed a possible correlation

between capacitance and structural disorder of carbons. Therefore, it is reasonable to conclude that the capacitance of carbon materials depends on a subtle combination of textural and structural properties. Further investigation is required to understand their impact on the capacitive performance of electrodes.

1.4. Electrolytes typically implemented in EDLCs

Electrolytes have been identified as an important component in the development of electrochemical capacitors (ECs). They strongly influence the operating voltage, equivalent series resistance, temperature limits, and the cycle life of the EDLCs (See **Figure 7**). As a result, the properties of the electrolyte have a large effect on the energy density and power capability which can be achieved using particular electrode materials. A number of reviews discussing the type of electrolytes, and their influence on the capacitive performance of EDLCs are available in the literature [65].

In order to expand the range of applications of EDLCs, current research is looking for strategies that improve their energy and power density. According to **Equation (7)**, the value of stored energy can be enhanced either by increasing the capacitance C or by extending the operating voltage U_{Max} , which is closely dependent on the electrochemical stability window (*ESW*) of the electrolyte with the electrode material of interest. Furthermore, as presented by **Equation (8)**, the power performance of the device is inversely proportional to R_{ESR} , which in turn depends strongly on the ionic conductivity of the electrolyte. Hence, the selection/design of the electrolyte plays a crucial role in the electrochemical performance of an EDLC [12]. Bearing this in mind, this section will be devoted to presenting various types of electrolytes with their advantages and disadvantages when implemented in EDLCs. The most commonly used electrolytes for EDLCs are aqueous, organic, and ionic liquid electrolytes.

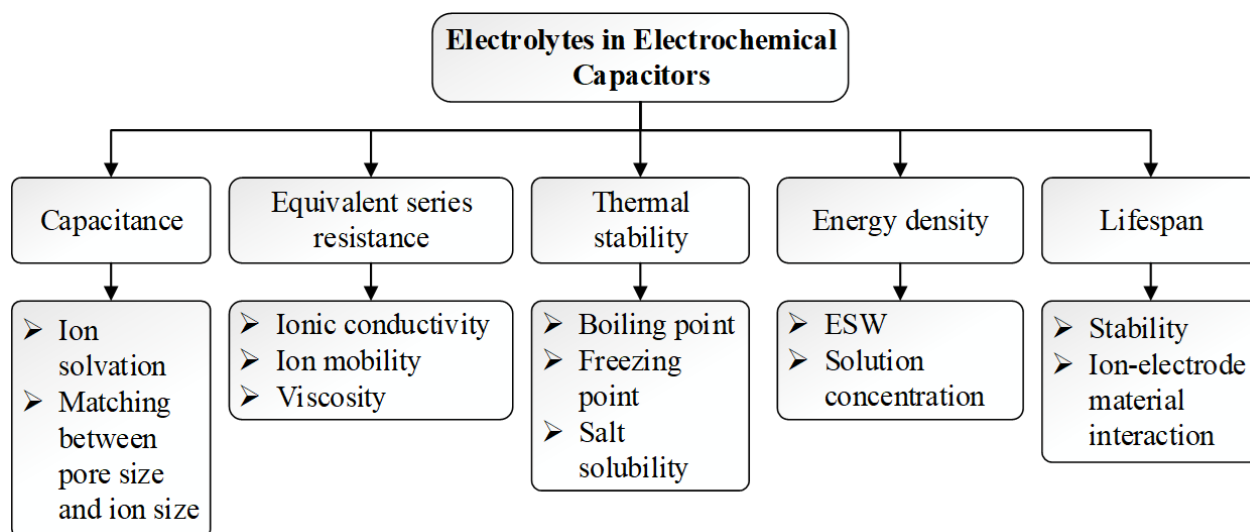


Figure 7. Effects of the electrolyte on the performance of electrochemical capacitors. Adapted from the reference [65].

1.4.1. Aqueous electrolytes

Aqueous electrolytes offer several distinct advantages that make them particularly attractive for EDLC applications. They typically exhibit higher ionic conductivity compared to their non-aqueous counterparts, which is crucial for ensuring efficient charge transport within the EDLC, leading to improved power density. This enhanced conductivity helps reduce internal resistance, minimizing energy losses and heat generation during operation [66].

Aqueous electrolytes, primarily composed of water and a dissolved solute, are generally non-toxic and non-flammable, contrasting sharply with many organic electrolytes where the solvent can be hazardous and pose significant safety risks, including flammability and chemical toxicity. The use of these solutions enhances the safety profile of EDLCs, making them more suitable for applications requiring stringent standards, such as in consumer electronics, automotive, and industrial settings. Additionally, the ecological nature of most water-based solutions aligns with the increasing emphasis on sustainable and green technologies. The materials used in aqueous solutions are typically more affordable and easier to source than those required for non-aqueous systems. Water is abundant and inexpensive, and the solutes used (such as potassium hydroxide or sulfuric acid) are generally inexpensive. These kinds of electrolytes are relatively easy to prepare and integrate into EDLC devices because there is no requirement for oxygen/moisture-free atmospheres as in the case of organic electrolytes [67]. Therefore, EDLCs with these solutions do not necessitate costly drying and pumping processes

for stacked electrodes before electrolyte introduction [68]. This simplicity also allows for better control over electrolyte composition and purity, ensuring consistent performance across different batches of EDLCs.

However, a significant disadvantage of aqueous electrolytes (with KOH or H₂SO₄ as solute) is their low thermodynamic stability window of 1.23 V, which limits the maximum voltage of the device [69]. In practice, the nominal voltage of symmetric EDLCs using 1 mol L⁻¹ H₂SO₄ or 6 mol L⁻¹ KOH aqueous electrolytes is lower than 1 V [70-72], whereas 2.7 V to 2.85 V can be reached with organic electrolytes [14, 73]. Therefore, researchers continue to seek/design aqueous electrolytes which provide high energy storage (with an extended operating voltage) and reduce assembly costs.

1.4.1.1. Neutral aqueous electrolytes

About a decade ago, research showed that practical voltage values of approximately 1.5-1.6 V could be achieved with activated carbon (AC) electrodes in neutral aqueous media such as Li₂SO₄, Na₂SO₄, and K₂SO₄ [71, 74, 75]. The significant increase in rated voltage, compared to EDLCs based on basic or acidic aqueous solutions, enables devices with neutral aqueous electrolytes to store and deliver more energy than aqueous electrolytes with KOH or H₂SO₄, as shown by the Ragone plot in **Figure 8**. These impressive voltage values can be attributed to the high overpotential of hydrogen evolution at the negative AC electrode (approximately 500 mV). Briefly, under negative polarization, water is reduced, leading to the formation of nascent hydrogen and hydroxide ions (OH⁻). These OH⁻ anions remain partly trapped into the porosity, which results in a higher pH and a shift of the Nernst potential to lower values [11]. However, the performance of symmetric EDLCs in Li₂SO₄ or Na₂SO₄ aqueous solutions deteriorates at voltage values higher than 1.5 V. This deterioration includes a drop in capacitance, an increase in resistance, and gas evolution, caused by the electrochemical oxidation of the positive electrode and hydrogen evolution at the negative electrode [2]. Despite the improvements in voltage and safety with neutral aqueous electrolytes, the operational voltage of these EDLCs is still insufficient for competing with organic electrolyte-based systems

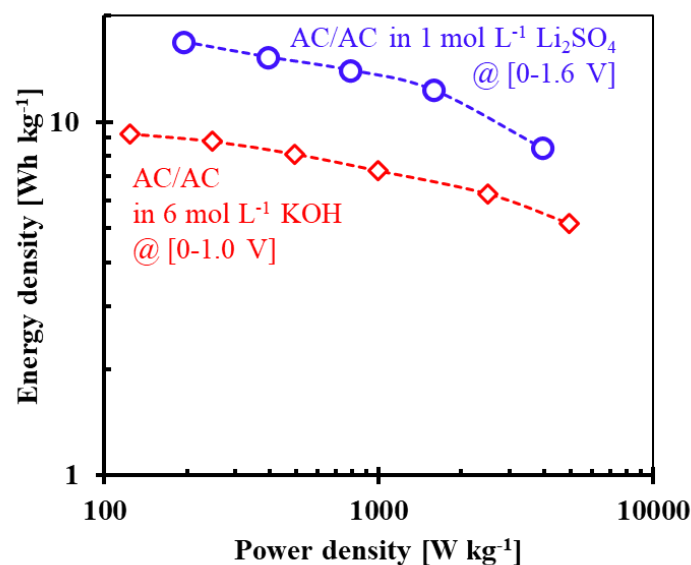


Figure 8. Ragone plots of EDLCs in 1 mol L⁻¹ Li₂SO₄ and 6 mol L⁻¹ KOH aqueous solutions. Values of specific energy and power are calculated for the total mass of active materials. From the reference [72].

1.4.1.2. “Water-in-Salt” electrolytes

Recently, highly concentrated aqueous solutions of neutral salts, known as “Water-in-Salt” (WIS) electrolytes, have gained significant attention. These electrolytes have a salt-to-water volume ratio (V_{salt}/V_{water}) or mass ratio (m_{salt}/m_{water}) greater than 1 [76, 77]. WIS electrolytes exhibit unique physicochemical properties and an extended electrochemical stability window (*ESW*) compared with diluted neutral salt solutions [78, 79]. A wide variety of WIS electrolytes has been investigated and implemented in EDLCs aiming to enhance their nominal voltage. These electrolytes include 20 mol kg⁻¹ lithium bis(trifluoromethanesulfonyl)imide (LiTFSI) [78], 8 mol kg⁻¹ sodium bis(trifluoromethanesulfonyl)imide (NaTFSI) [80], 22 mol L⁻¹ potassium acetate (KAc) [81], 17 mol kg⁻¹ sodium perchlorate (NaClO₄) [79, 82], among others.

The observed widened *ESW* in WIS electrolytes is closely linked to their local structure [76, 83]. **Figure 9** presents the results of various studies on LiTFSI aqueous solutions at different concentrations. The ¹⁷O NMR investigations (**Figure 9a**) showed two signals assigned to water (~0 ppm) and TFSI⁻ anions (~154 ppm) [76]. The chemical shift of the water signal gradually shifted to lower values as the salt concentration increased, which could be attributed to direct interactions between Li⁺ cations with the oxygen atom from water, indicating a progressive weakening of the water hydrogen-bonding network [84, 85]. Conversely, the signal of TFSI⁻ anions appears less sensitive to increasing the salt concentration, though it slightly shifts to

lower values, suggesting that the oxygen atom on the TFSI⁻ anion is not directly coordinated with Li⁺ for salt concentrations lower than 10 mol kg⁻¹.

A Raman spectroscopy study on LiTFSI aqueous solutions of increasing concentration (see **Figure 9b**) demonstrated a decrease in intensity of the symmetric ($\nu_s(\text{OH})$, ca 3200 cm⁻¹) and asymmetric ($\nu_a(\text{OH})$, ca 3400 cm⁻¹) stretching modes of water [86]. Simultaneously, a new peak attributed to the hydration of Li⁺ cations (near 3600 cm⁻¹) grew progressively from 9.5 mol kg⁻¹. This indicates that water molecules are essentially involved in Li⁺ solvation, while the amount of free water molecules decreases, aligning with observations from the aforementioned NMR study. Similar concentration dependence of Raman spectra has been disclosed on aqueous solutions of various salts, including NaClO₄ [83], lithium/sodium bis(fluorosulfonyl)imide (LiFSI, NaFSI) [87], lithium (nonafluorobutanesulfonyl)(trifluoromethanesulfonyl)imide (LiIM₁₄) [88], among others.

Further insights into the structure of LiTFSI solutions have been provided by molecular dynamics (MD) simulations [76]. **Figure 9c** illustrates the variation in average coordination numbers for Li⁺-O_w and Li⁺-O_{TFSI⁻} pairs of atoms, where O_w and O_{TFSI⁻} represent the oxygen atom of the water molecule and TFSI⁻ anion, respectively. Additionally, the fraction of free water was tracked across different solution concentrations. The number of water molecules in the first solvation shell of Li⁺ cations (Li⁺-O_w) decreased from 4 at 1 mol kg⁻¹ to ca. 2 at 21 mol kg⁻¹. Conversely, the number of TFSI⁻ ions increased from 0 at 1 mol kg⁻¹ to 2 at 21 mol kg⁻¹. These changes in coordination numbers indicate a strong ion association between Li⁺ and TFSI⁻ at high concentrations. It is noteworthy that pairs between Li⁺ and TFSI⁻ ions were not observed in dilute solutions, which is in good agreement with the aforementioned NMR data [76]. Interestingly, the fraction of free water molecules drops by almost 50% from 5 mol kg⁻¹ to 21 mol kg⁻¹, highlighting the involvement of water in the solvation of the Li⁺ cations as LiTFSI concentration increases. Based on the results of MD simulations, **Figure 9d** compares the Li⁺ solvation shell in highly diluted and highly concentrated solutions. Notably, the solvation shell in the WIS solution includes TFSI⁻ anions, while water molecules are scarce in comparison. Similar tendencies have been reported from computational simulations on aqueous solutions of NaClO₄ [83] and LiIM₁₄ [88].

This compendium of studies realized on a variety of WIS solutions allows the following observations to be drawn: (i) the high concentration of ionic pairs in WIS solutions could indicate that a significant proportion of water molecules are involved in ion solvation, leading

to an increase in contact ion pair (CIP) interactions; (ii) the decrease in the fraction of free water molecules within the solution is an important factor to consider in the structural changes of the WIS solutions [82].

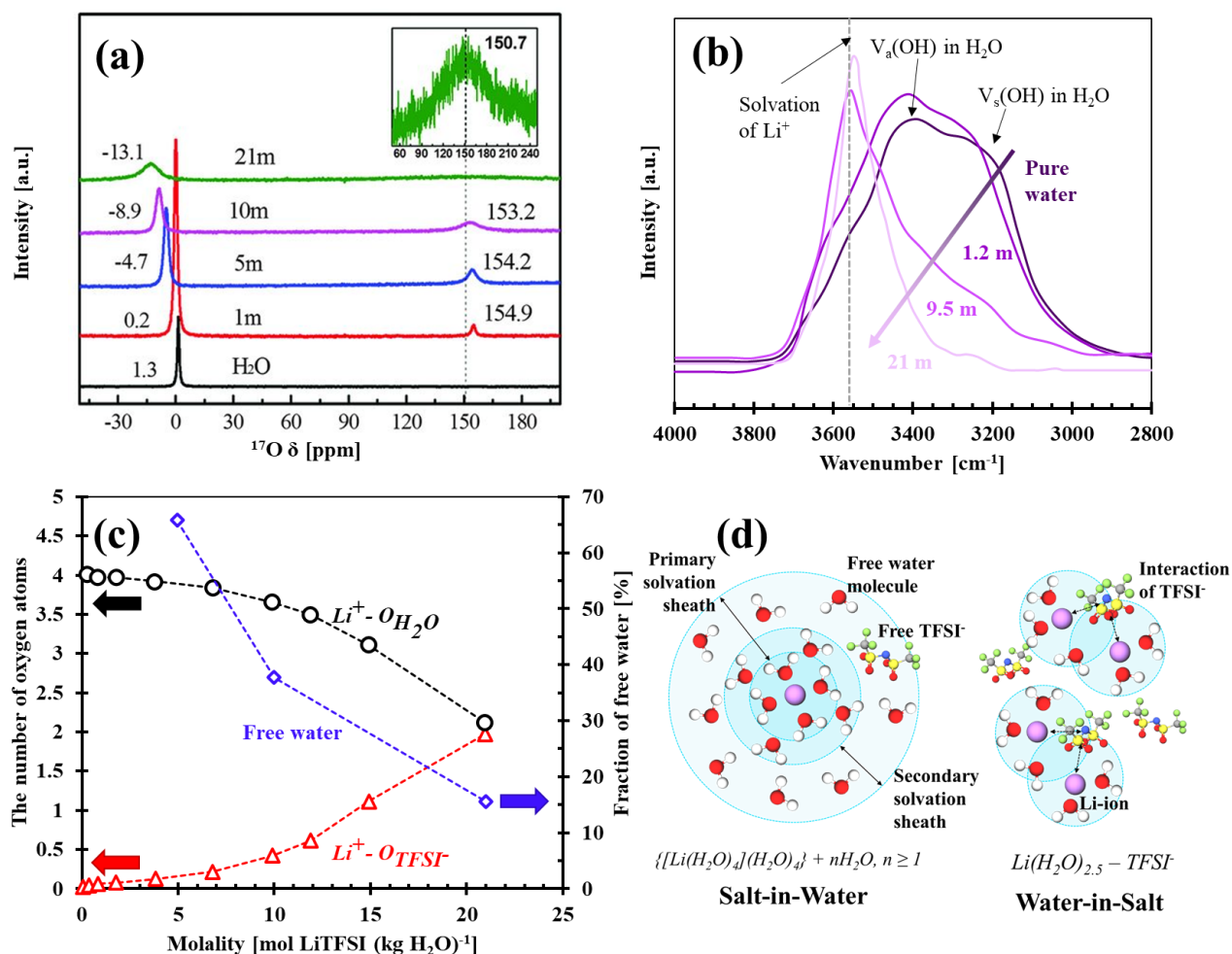


Figure 9. Local structural analysis of LiTFSI aqueous solutions at various concentrations: (a) Chemical shifts determined by ^{17}O NMR spectroscopy for the solvent (water) and anion (TFSI). The inset shows the TFSI peak in the 21 mol kg⁻¹ solution. From reference [76]. (b) Raman spectra in the region of the O-H stretching mode (2800–4000 cm⁻¹). Adapted from reference [86]. (c) Number of water and TFSI oxygen atoms within the primary solvation shell of Li⁺ (within a radius of 0.27 nm), along with the fraction of free water molecules not bound to any Li⁺, as determined from MD simulations. Adapted from references [76, 89]. (d) Illustration of the Li⁺ primary solvation shell in diluted and water-in-salt solutions. Adapted from reference [76].

WIS electrolytes, with near-saturation salt levels, are likely to exhibit dynamic viscosity and ionic conductivity distinct from those of dilute electrolytes. Generally, viscosity increases with salt concentration due to stronger electrostatic interactions and increased ionic friction [90].

Figure 10 illustrates for various aqueous solutions the increasing tendency of viscosity with concentration. Interestingly, when the molality of LiFSI and NaFSI in water increases from 1

to 20 mol kg⁻¹, the viscosity varies from approximately 2 to 14 and 19 mPa s at 25 °C (See **Figures 10c** and **d**), respectively [87]. These values are significantly lower than that of 20 mol kg⁻¹ LiTFSI (65.2 mPa s) (See **Figure 10a**), highlighting the importance of anion type and molecular size on the transport properties. At 30 mol kg⁻¹, both FSI salts exhibit higher viscosity, especially NaFSI (ca. 60 mPa s compared to LiFSI with ca. 45 mPa s) [87]. This particular property of 30 mol kg⁻¹ NaFSI may be attributed to the larger radius of Na⁺, causing more Coulombic friction between ions, and highlighting the cation's effect.

On the other hand, ionic conductivity typically peaks at intermediate values of concentration (**Figure 10**). According to refs. [91, 92], the highest ionic conductivity occurs at a specific concentration (denoted as C_{max}), where a shift in the conduction mechanism occurs. Noteworthy, two primary mechanisms govern ion transport: (i) the vehicular mechanism, where ions move with their solvation sheaths (common in electrolytes with strong cation-anion interactions); and (ii) ion hopping. Factors influencing this mechanism include ion-ion or ion-solvent interactions, salt aggregation, and electrolyte viscosity. At very low concentrations, the conductivity is governed by a vehicular mechanism. When the electrolyte concentration approaches C_{max} , it is suggested that ionic hopping occurs along the network structure composed of stable ion pairs and ionic clusters. Above C_{max} , ion transport shifts from vehicular mechanism to ion hopping [91].

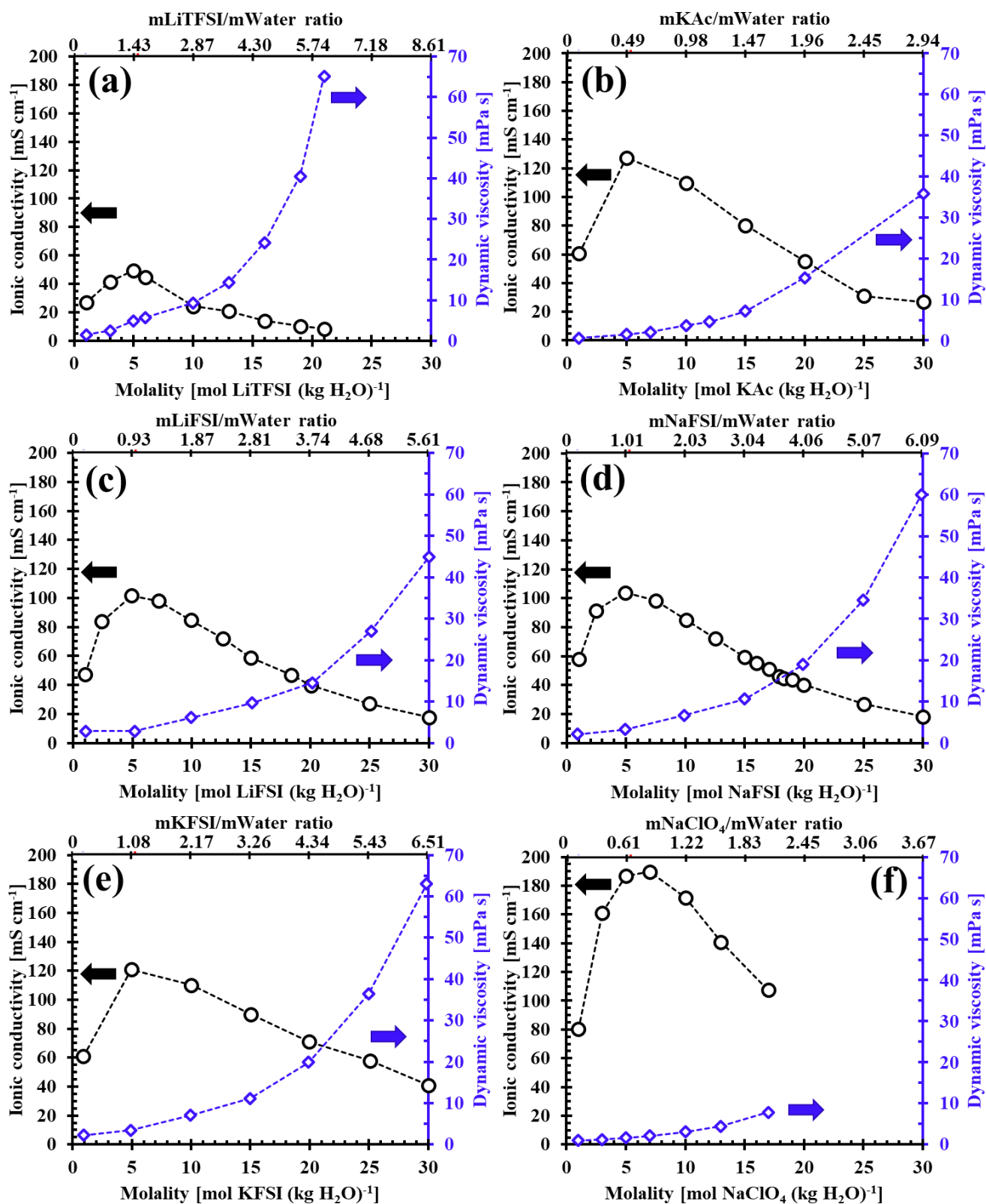


Figure 10. Ionic conductivity and dynamic viscosity measured at 25 °C on salt solutions of various concentrations: (a) LiTFSI [93]; (b) KAc [94]; (c) LiFSI [87]; (d) NaFSI [87]; (e) Potassium bis(trifluoromethanesulfonyl)imide (KFSI) [95]; and (f) NaClO₄[83].

The *ESW* of WIS electrolytes on AC electrodes significantly exceeds the thermodynamic stability limit of water. Extensive research has been conducted in this regard to understand the underlying effects and possible causes of this advantageous feature when WIS electrolytes are used. For example, **Figure 11** presents the effect of salt concentration in aqueous LiTFSI electrolytes on the potential limits and stability window (*ESW*) of EDL electrodes. The latter is determined by using the window opening method developed by Weingarth et al. [96], where cyclic voltammetry (CV) at 1 mV s^{-1} is conducted on separate electrodes under negative or positive polarizations. To accurately detect parasitic faradaic decomposition reactions, it is crucial to use low scan rates during the CV scans. Otherwise, the *ESW* on porous carbon electrodes can be unrealistically overestimated, as observed in various published investigations [97, 98]. The negative or positive vertex potential was gradually decreased or increased by 0.1 V steps until electrolyte decomposition was observed (**Figure 11a, b, and c**). The purely box-like CV loops (black voltammograms) represent the electrochemical stability region, while CVs with parasitic redox peaks (red lines) indicate electrolyte decomposition [99]. The S-values for positive and negative polarizations are calculated using **Equations (11) and (12)**, respectively.

$$S_{pos} = \frac{Q_+}{Q_-} - I \quad (11)$$

$$S_{neg} = \frac{Q_-}{Q_+} - I \quad (12)$$

where Q_+ and Q_- are the integrated charges during the anodic and cathodic scans. S-values were plotted against the corresponding vertex potentials (**Figure 11d, e, and f**). The *ESW* was determined by the condition that the difference between successive S-values should not exceed 0.005.

As shown in **Figure 11d, e, and f**, the negative potential limit of an AC electrode in the three electrolytes is -1.0 V vs AgQRE, i.e., 0.443 V lower than the thermodynamic reduction potential of water at $\text{pH} = 6.1$ ($E_H = -0.557 \text{ V vs AgQRE}$). To explain this similarity of overpotential, it is suggested that, during water reduction, OH^- anions accumulate at higher concentrations in the pore of electrodes than in the bulk electrolyte. Then, some of them diffuse out of the pores at a rate controlled by the AC's porous texture, i.e., independent of the $\text{H}_2\text{O}/\text{Li}^+$ molar ratio in the various LiTFSI aqueous solutions [78]. Under positive polarization, the

potential limit shifts from 0.6 V vs AgQRE in 1 mol kg⁻¹ LiTFSI to 1.0 V vs AgQRE in 20 mol kg⁻¹ LiTFSI (**Figure 11d, e, and f**). Interestingly, similar results were obtained in the case of AC electrodes in NaClO₄ aqueous solutions, in which the potential limit under positive polarization upshifts from 0.5 V vs AgQRE in 2 mol kg⁻¹ to 0.8 V vs AgQRE in 17 mol kg⁻¹ [79]. This shift in both electrolytes is likely due to the lower amount of free water in more concentrated solutions, leading to a significant presence of anions and a very small amount of water in the Stern layer, [100, 101].

Though the 20 mol kg⁻¹ LiTFSI solution is an interesting example of WIS widely studied in the literature, it exhibits an ionic conductivity of only 10 mS cm⁻¹ at room temperature, which is approximately 3 times lower than for 1 mol kg⁻¹ LiTFSI (27.8 mS cm⁻¹) or 1 mol L⁻¹ TEABF₄/ACN ($\sigma = 40.3 \text{ mS cm}^{-1}$ [102]). In this context, the 17 mol kg⁻¹ NaClO₄ solution emerged as a promising WIS electrolyte for EDLCs, owing to its high ionic conductivity $\sigma = 104 \text{ mS cm}^{-1}$ at room temperature (**Figure 10f**) [79, 83].

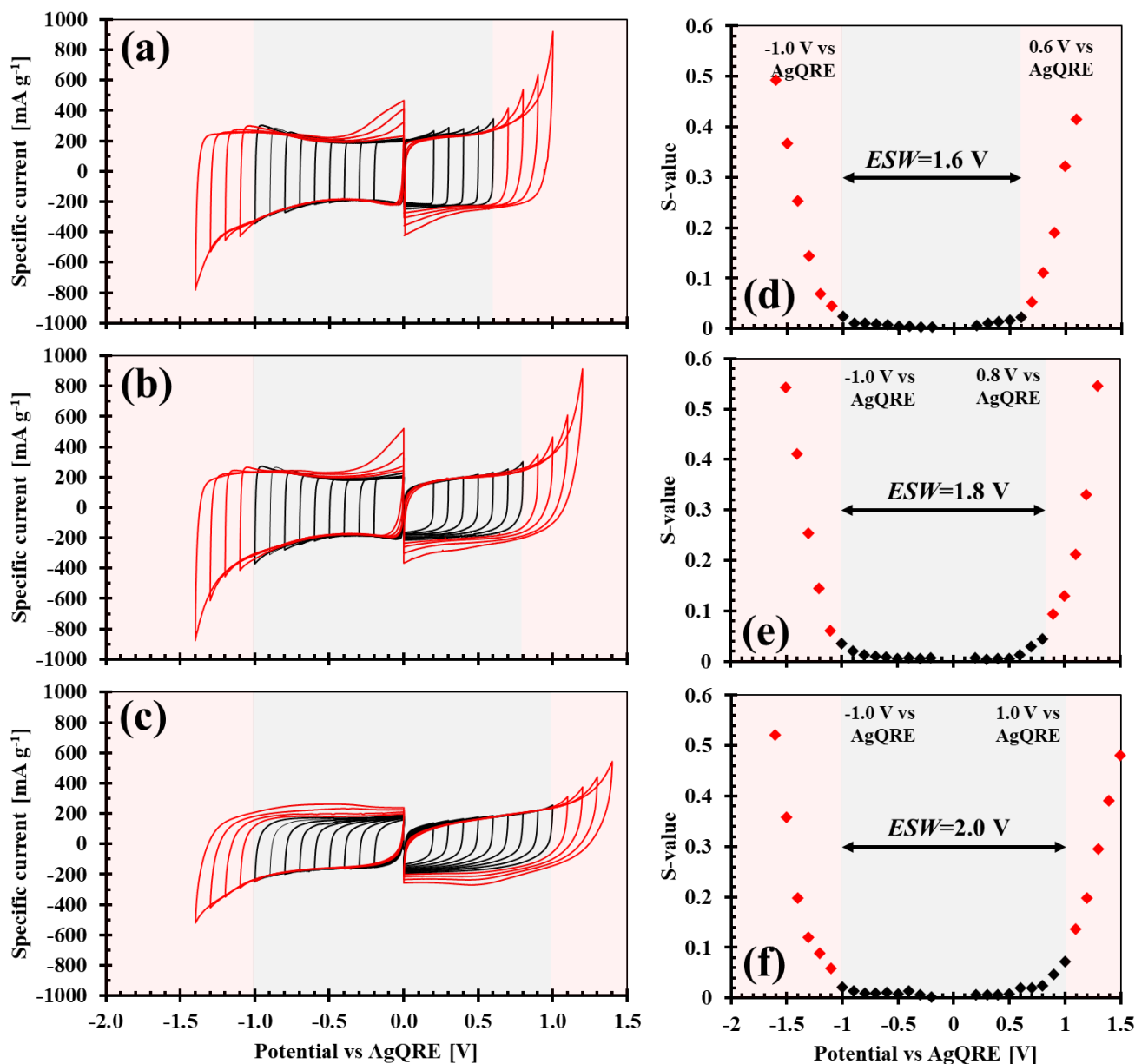


Figure 11. Cyclic voltammograms (1 mV s^{-1}) with potential window opening (by steps of 0.1 V) on AC electrodes in LiTFSI aqueous solution at different concentrations: (a) 1 mol kg^{-1} , (b) 7 mol kg^{-1} and (c) 20 mol kg^{-1} with black and red CVs representing the EDL stability and decomposition regions of the electrolyte, respectively. (d), (e) and (f) are the plots of S-values vs. vertex potential obtained from the data extracted from the CV plots of figures (a), (b), and (c), respectively. From the reference [78].

1.4.2. Organic electrolytes

Most industrial EDLCs on the market utilize organic electrolytes due to their wide ESW , allowing more energy to be stored in a given volume or mass. EDLCs implementing an organic electrolyte also operate efficiently over a broad temperature range (e.g. devices in 1 mol L^{-1} TEABF₄/ACN may operate from -40 to $65 \text{ }^\circ\text{C}$), making them suitable for applications in harsh environments like the automotive industry or aircraft. Notwithstanding, the rated voltage of

electrochemical capacitors with these organic media is significantly influenced by impurities in the components and functional groups on the carbon surfaces [103, 104]. Moreover, as organic electrolytes are highly hygroscopic (a few ppm of water in such electrolytes reduce considerably the ESW [67]), EDLCs in these media must be built under a controlled moisture-free atmosphere, which considerably increases the production cost. Compared to aqueous electrolytes, organic electrolytes typically exhibit lower ionic conductivity. As previously mentioned, this crucial factor affects the rate at which ions can move within the electrolyte, leading to higher internal resistance (R_{ESR}). This can reduce the power density during charge and discharge cycles. The production and disposal of organic electrolytes also have a greater environmental impact, as the chemicals involved can be more challenging to recycle and may pose pollution risks if not managed properly.

The most commonly used organic salt in EDLCs is $TEABF_4$, selected for its good solubility in organic solvents. Currently, the most popular solvent is acetonitrile (ACN), although propylene carbonate (PC) is also widely used. PC has a slightly higher dipole moment, higher density, viscosity, and dielectric constant than ACN [105]. However, ACN-based electrolytes offer higher conductivity and, consequently, lower electrical resistance than PC-based electrolytes when used in EDLCs [106]. Despite this advantage, EDLCs based on the use of $TEABF_4/ACN$ are often considered environmentally unfriendly/hazardous due to the presence of ACN with a low flash point (5.5 °C). Consequently, researchers have explored other solvents for organic electrolytes, such as dimethylsulfone, and ethyl methyl carbonate [107]. "Nitrile"-based electrolytes, such as adiponitrile (ADN), have been found suitable for high-voltage Li-ion batteries due to their high electrochemical stability [108, 109]. It has been shown that an EDLC with 0.7 mol L^{-1} $TEABF_4/ADN$ can be cycled up to 3.5-3.6 V, with a capacitance loss of less than 20% after 50,000 cycles [110].

1.4.3. Ionic liquids as electrolytes

Ionic liquids (ILs) are increasingly important as electrolytes in EDLCs due to their unique properties. These salts, liquid at room temperature, offer advantages and disadvantages that significantly influence EDLC performance and applications. ILs provide a wide electrochemical stability window, often exceeding 3.5 V, allowing EDLCs to operate at higher voltages compared to traditional aqueous and organic electrolytes. This increases energy density, enabling more energy storage in the same volume or weight, crucial for compact and efficient energy storage solutions. Additionally, ionic liquids have excellent thermal stability,

allowing EDLCs to function over a broad temperature range without degradation, making them suitable for extreme environments like aerospace and heavy industry. Their low volatility and non-flammability significantly enhance the safety of EDLCs, reducing fire risk and making them safer for consumer electronics and electric vehicles. The low vapor pressure of ionic liquids also reduces the risk of leakage and evaporation, contributing to the longevity and reliability of EDLCs.

Despite their benefits, ILs have drawbacks. They are relatively expensive to synthesize and purify, which can limit their use in cost-sensitive applications. Their higher viscosity compared to traditional electrolytes can result in lower ionic conductivity, increasing internal resistance and potentially reducing power density while increasing heat generation during operation. The availability of suitable ILs that meet all desired properties for EDLC applications is limited, necessitating ongoing research and development. While generally more environmentally friendly than some organic solvents, the environmental impact of ionic liquids depends on their specific composition, with some posing challenges in terms of biodegradability and toxicity.

The most commonly used ILs for EDLCs are imidazolium, pyrrolidinium, and ammonium salts, paired with anions such as tetrafluoroborate, trifluoromethanesulfonate, bis(trifluoromethanesulfonyl)imide, bis(fluorosulfonyl)imide, and hexafluorophosphate [111]. Galvanostatic cycling of an AC/AC electrochemical capacitor in N-methyl-N-butylpyrrolidinium bis(trifluoromethylsulfonyl)imide (Pyr₁₄TFSI) demonstrated 95% efficiency at 3.5 V and 60°C after 65,000 cycles [112]. Additionally, a constant voltage hold at 3.4 V revealed long-term operation (500 hours) of EDLCs based on 1-ethyl-3-methylimidazolium tetrafluoroborate (EMImBF₄) with mesoporous carbon black (BP 2000) [96].

In summary, each type of electrolyte offers distinct benefits and trade-offs, influencing the suitability of EDLCs for various applications based on factors such as cost, safety, environmental impact, and performance requirements. A comparison of the attributes of each type of electrolyte is presented in **Figure 12**.

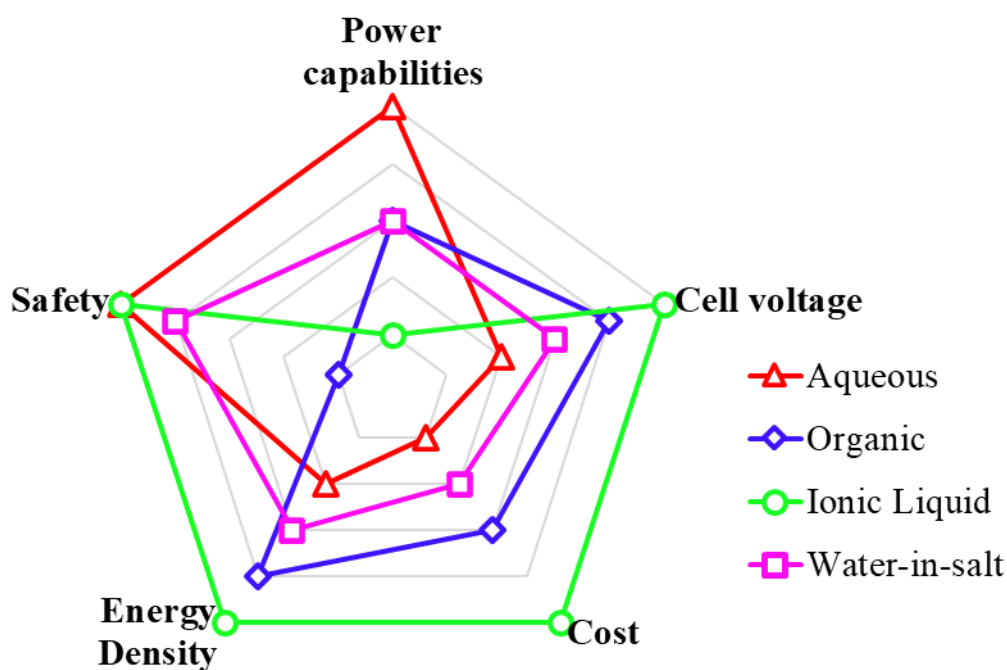


Figure 12. Comparison of the properties and performance of IL, aqueous, water-in-salt, and organic electrolytes when implemented in EDLCs. Adapted from ref [113].

1.5. In-pore ion population changes during polarizing of EDL electrodes

Extensive efforts within the research sphere on EDLCs have been devoted to the design/implementation of new carbons or electrolytes for storing and delivering more energy at high power rates. Nonetheless, the success of this approach relies upon understanding the interactions of ions from the electrolyte with the carbon electrodes, in other words, disclosing the ion population changes occurring in the electrodes of an EDLC during its charge and discharge.

Numerous studies have been performed using cutting-edge techniques such as NMR spectroscopy [114-117], electrochemical quartz crystal microbalance (EQCM) [118-121], electrochemical dilatometry (ECD) [122-124], aiming to improve the understanding of in-pore ion population changes during polarization of EDLC electrodes. For instance, Griffin et al. [114] conducted *in situ* NMR studies on EDLC electrodes (YP-50F) using tetraethylphosphonium tetrafluoroborate in acetonitrile (TEPBF₄/ACN) electrolyte at different concentrations. The electrodes were polarized at potentials lower and higher than the open circuit potential (OCP) by steps of 0.25 V. *In situ* ¹⁹F and ³¹P NMR spectra of in-pore anions

and cations, respectively, were recorded after the electrodes were held for 60 min (in 1.5 and 0.75 mol L⁻¹ electrolyte) or 90 min (in 0.5 mol L⁻¹ electrolyte) at each potential step. The results of this *in situ* NMR investigation are presented in **Figure 13**. When the AC electrodes are polarized at potentials higher than *OCP*, it is interesting to note that, for all electrolyte concentrations (**Figure 13a, b, and c**), the in-pore population of counter-ions (anions) increases with the potential, whereas the population of co-ions simultaneously diminishes, meaning that essentially ionic exchange occurs in this potential region. On the other hand, when AC electrodes are polarized negatively (from 0 to -1.5 V vs carbon), the population of co-ions inside the porosity remains practically unchanged, while the population of counter-ions increases, i.e., perm-selective cation adsorption occurs [114]. Notably, the charging mechanism remains consistent for the electrode-electrolyte system across all studied concentrations. However, the in-pore ion population at 0 V varies linearly with the electrolyte concentration. This suggests that the solvent content plays a significant role in determining the number of ions present within the pores in the absence of applied potential.

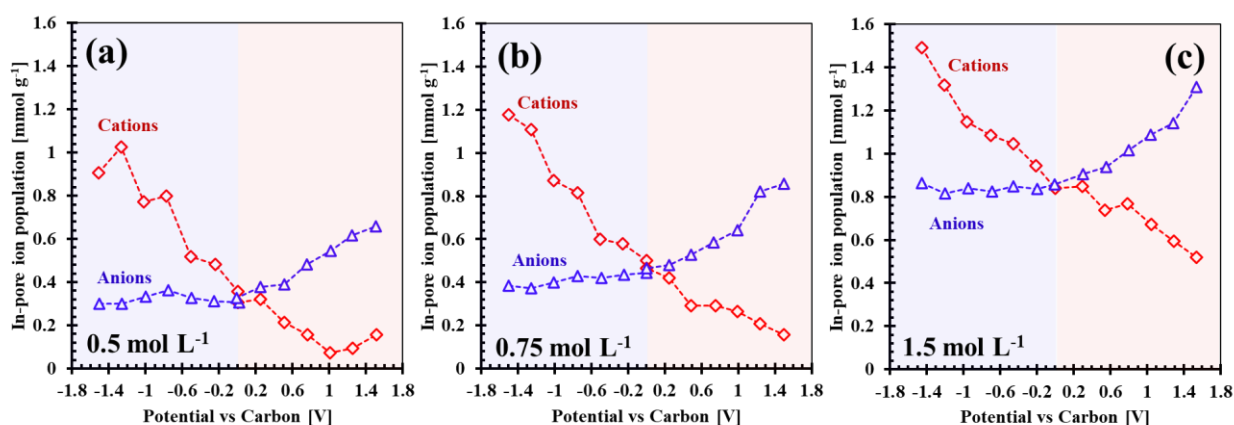


Figure 13. In-pore ion population changes determined by *in-situ* NMR for AC (YP-50F) electrodes polarized at various potentials vs Carbon in (a) 0.5 mol L⁻¹, (b) 0.75 mol L⁻¹ and (c) 1.5 mol L⁻¹ TEPPBF₄/ACN electrolytes. Adapted from reference [114].

In another study [118], the mass changes of CDC (with 1 nm average pore size) electrodes in 2 mol L⁻¹ 1-ethyl-3-methylimidazolium bis(trifluoromethanesulfonyl)imide in acetonitrile (EMImTFSI/ACN) electrolyte have been determined by *operando* EQCM while applying a constant potential sweep at positive or negative polarization vs the point of zero charge (*PZC*-the potential where the electrode net surface charge is zero ($Q = 0$) [125]). **Figure 14** compares the measured mass changes with the theoretical ones calculated from the Faraday's law when

neat counter-ions are adsorbed. At negative polarization relative to *PZC* ($Q < 0$), corresponding to the Domain I in **Figure 14**, the electrode mass increased linearly with charge. The calculated molar weight of the adsorbed species (265 g mol^{-1}) significantly exceeds the bare EMIm⁺ molecular weight (dashed pink line, **Figure 14**). Such a difference between the calculated and the experimental mass suggests that EMIm⁺ enters into the porosity partially solvated, therefore, the average solvation number of cations in-pore was estimated to be 3.7. Despite the presence of the solvation shell around the cations, the 1 nm micropores show a perm-selective behaviour since there is no visible ionic exchange in this region. For positive charge ($Q > 0$), in Domain II, the measured mass change is smaller than theoretically expected, indicating that the heavier solvated EMIm⁺ cations are expelled from the porosity and exchanged with neat TFSI⁻ anions. Finally, in Domain III, the mass change increases linearly and is almost parallel to the theoretical mass change, confirming that the counter-ion adsorption mechanism is dominant.

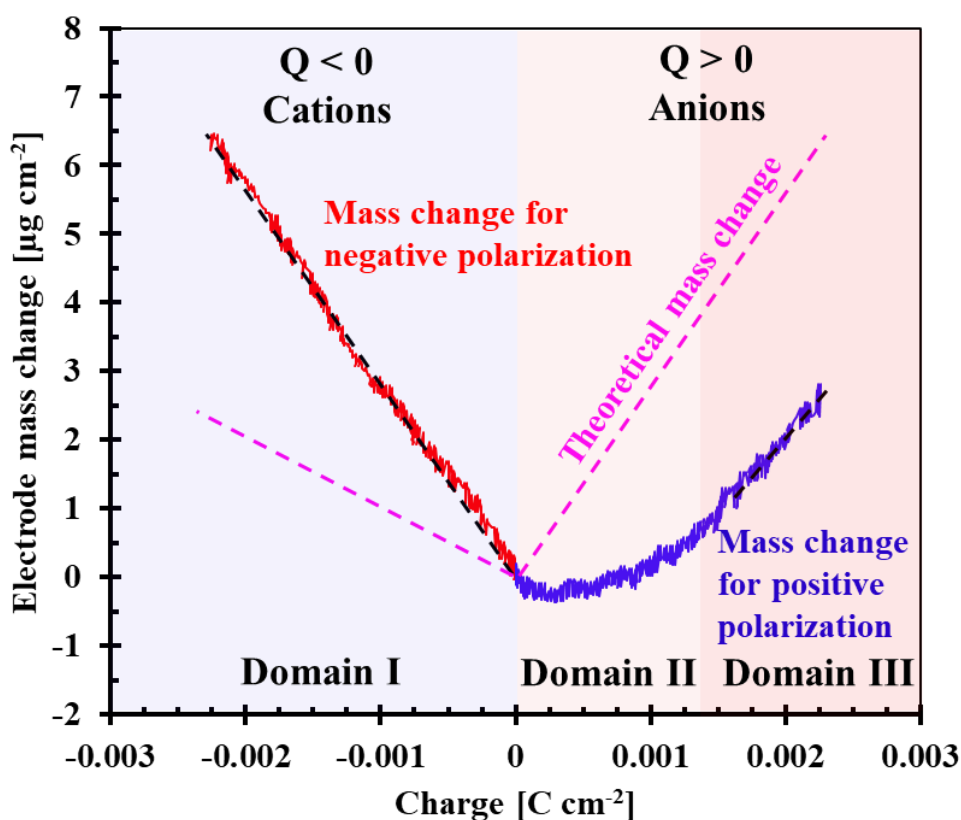


Figure 14. Electrode mass changes measured by EQCM during the polarization of CDC electrodes in 2 mol L^{-1} EMImTFSI/ACN electrolyte. Adapted from reference [118].

Operando ECD measurements were performed to study the ion population changes in porous carbon electrodes ($L_0 \approx 1.2$ nm) soaked in ionic liquids: 1-Ethyl-3-methylimidazolium bis(trifluoromethylsulfonyl)imide (EMImTFSI), 1-Ethyl-3-methylimidazolium tetrafluoroborate (EMImBF₄), and 1-Butyl-3-methylimidazolium hexafluorophosphate (BMImPF₆) [124]. The volumetric changes obtained from ECD during galvanostatic cycling (See **Figure 15a**) were used to deduce the composition of the IL-carbon interface, considering the volume of each ion as follows: EMIm⁺: 0.156 nm³, BMIm⁺: 0.196 nm³, BF₄⁻: 0.073 nm³, TFSI⁻: 0.232 nm³ and PF₆⁻: 0.109 nm³.

The ECD data showed that, under negative polarization of the electrodes relatively to the point of zero strain (*PZS*), the expansion behaviour differed in EMImBF₄ and EMImTFSI, despite both ILs including the same cation (**Figure 15a**). This discrepancy is attributed to strong ion-ion interactions and the involvement of a significant number of co-ions in the in-pore/ex-pore exchange processes. The spherical BF₄⁻ anions appear to cause less strain compared to the cylindrical TFSI⁻ anions, possibly due to lower freedom of movement and increased steric hindrance within the pores. **Figure 15b** presents a schematic representation of the changes in in-pore ion population when using EMIm⁺-containing electrolytes. In the case of EMImBF₄, when the electrode is positively polarized, perm-selective adsorption of BF₄⁻ anions occurs, leading to an increased population of anions within the pores, though some EMIm⁺ cations remain in the porosity. This behaviour differs from that of EMImTFSI, where the ionic exchange takes place, followed by the adsorption of TFSI⁻ anions. This highlights the influence of anion geometry in the charging mechanism of IL-carbon systems.

For EMImTFSI, the slope in the strain versus charge plot is smaller compared to BMImPF₆ (See **Figure 15a**). This difference in strain can be attributed to the larger size of the BMIm⁺ cation. The orientation of both co-ions and counterions likely affects the strain, especially in the case of nonspherical ions. A parabolic strain curve is generated by the spherical BF₄⁻ ion, whereas a more linear increase in strain is seen for TFSI⁻ and PF₆⁻ when paired with the BMIm⁺ cation. As a result, the two EMIm⁺-containing electrolytes show different strain levels at -300 C g⁻¹: 0.5% for EMImBF₄ and 0.7% for EMImTFSI.

Overall, this study permitted to conclude that the smaller ions, in this case, BF₄⁻ anions, are more likely to be involved in energy storage than the larger TFSI⁻ anions, resulting in either preferred co-ion expulsion or counter-ion adsorption.

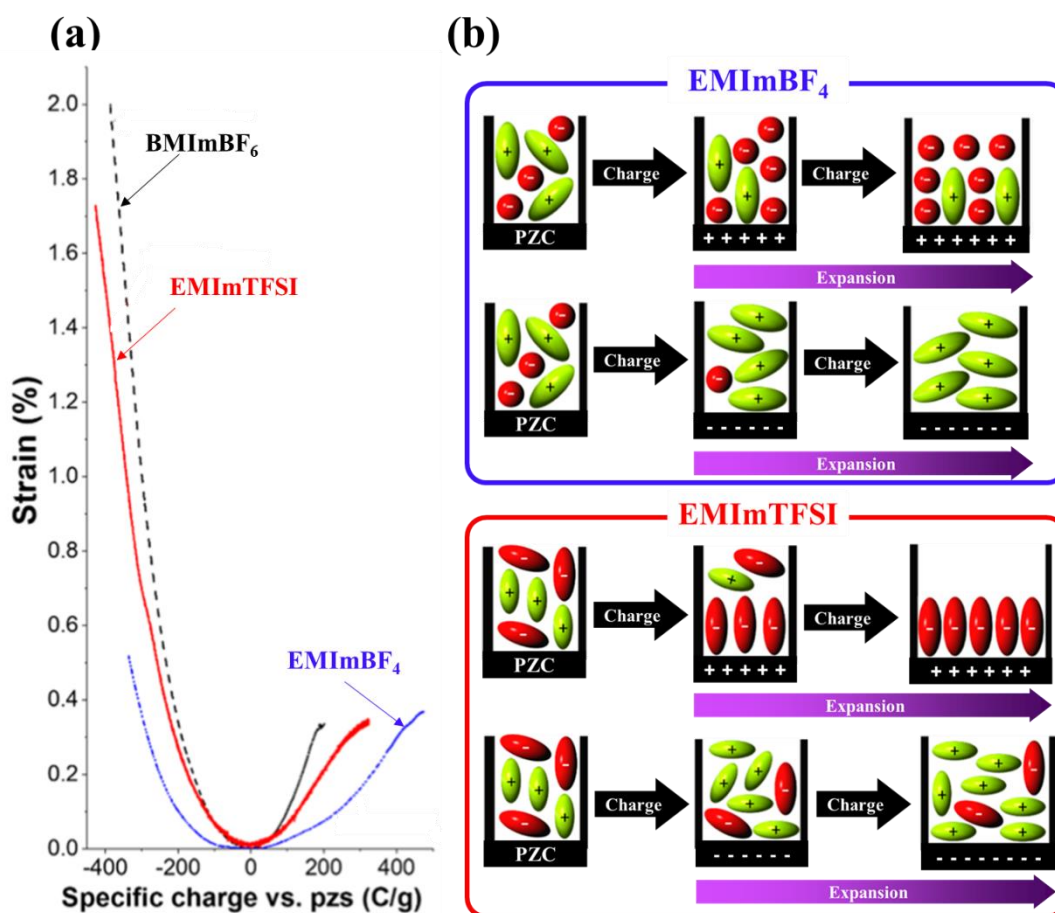


Figure 15. (a) Galvanostatic response of the porous carbon electrodes at a specific current of 0.1 A g^{-1} in three different ILs. The data are derived from the operando dilatometry results. The charge is normalized to the point of zero strain (PZS) and plotted versus the resulting strain of the working electrode. (b) The schematic drawings show the different in-pore ion population changes according to the shape of the adsorbed ions with spherical anions (BF_4^- and PF_6^-) and nonspherical ions (TFSI^-). The effect is exaggerated in the drawing to illustrate the trend but not to reproduce the amplitude shown in the ECD data. From reference [124].

2. Carbon-based Metal-ion Capacitors (MICs)

2.1. Operational principles of MICs

In the present era, metal-ion capacitors (MICs), a category of hybrid electrochemical energy storage devices, garner significant interest from both research and industrial sectors [126]. The attractive energy storage features of MICs arise from the combination of a battery-type negative electrode, where alkali cations (Li^+ , Na^+ , K^+ ...) are reversibly inserted or intercalated, and an electrical double-layer (EDL) positive electrode, typically made of porous activated carbon (AC), where ions from the electrolyte are electrosorbed [127, 128], as depicted in **Figure 16** for a Lithium-ion capacitor (LIC). This distinctive configuration offers two key advantages: (i) the EDL-positive electrode operates over a wider potential range in a MIC than an EDLC,

thereby increasing the device's capacity/capacitance compared to a conventional EDLC, and (ii) the negative electrode operates at a low and narrow potential range, close to 100 mV vs Li/Li⁺, enabling the maximum operative voltage of MICs to be significantly higher than that of an AC//AC capacitor, generally reaching 3.8 V [129, 130]. Owing to such features, the output energy of these devices is higher than for conventional EDLCs [129], while maintaining comparable power capabilities [14]. The most representative example of MIC is the lithium-ion capacitor (LIC), which has been reported in the literature to achieve between 10,000-100,000 charge/discharge cycles, which is one order of magnitude smaller than in the case of EDLC [14, 15].

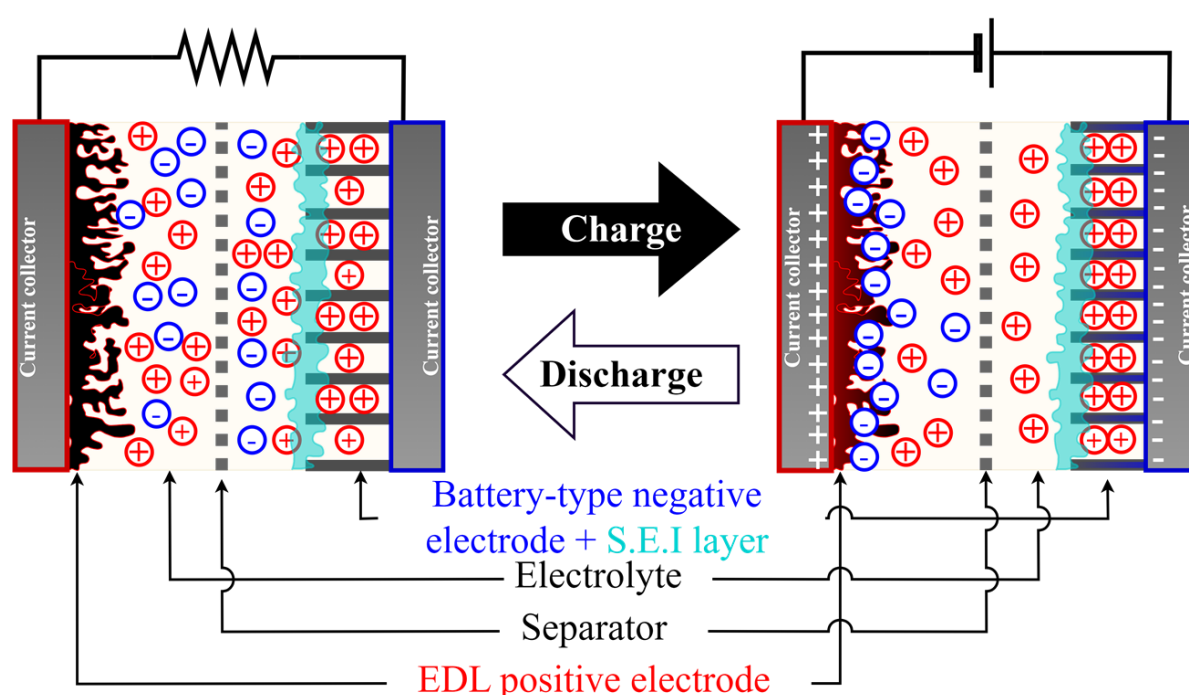


Figure 16. Schematic representation of a carbon-based Lithium-ion capacitor with a porous carbon positive electrode and the pre-lithiated graphite negative electrode. The figure depicts the distribution of charges when the device is discharged (Left) and charged (Right). Adapted from reference [131].

The superiority of MICs over EDLCs in terms of output energy can be understood by comparing their galvanostatic charge/discharge profiles (See **Figure 17**), following the demonstration presented in ref [129]. In the two systems, it is assumed that both the positive and negative electrodes have equal mass. In an EDLC, during galvanostatic charge/discharge, ions from the organic electrolyte are reversibly electrosorbed on the AC electrodes, as outlined in **Paragraph 1.5**. The potential of both electrodes varies linearly during this process, as shown in **Figure 17a**. As not all charges would be withdrawn when discharging the EDLC to 0 V, it is recommended to limit the discharge from U_{max} to $U_{max/2}$ (here, from 2.6 to 1.3 V) [13].

Considering that both electrodes exhibit similar capacitance and the oxidative potential limit of the positive electrode is around 4.1 V vs M/M^+ , the potential ranges for each electrode are illustrated in **Figure 17a**. In contrast, during charging a MIC, ions are electroadsorbed in the positive EDL electrode, while alkali metal ions are intercalated/inserted into the negative electrode. As a result, the positive electrode behaves in a wider potential range than in an EDLC, while the potential of the battery-type negative electrode remains almost constant, as shown in **Figure 17b**. In a MIC with a porous carbon positive electrode and a battery-type negative electrode, the voltage is capped at approximately 3.8 V to avoid electrolyte oxidation at the positive electrode (approximately 4.1 V vs M/M^+). Unlike EDLCs, the minimum voltage in an MIC is not fixed at $U_{max}/2$, yet at 2.2 V vs Li/Li^+ to avoid the risk of solid electrolyte interphase (S.E.I.) that might be formed on the AC electrode at lower potentials. Such S.E.I. development on an AC electrode would decrease the life span of the MIC and increase its internal resistance [132]. To prevent from such disagreements in the case of the example presented in **Figure 17b**, the minimum potential of the positive electrode was set at 2.5 V vs M/M^+ . Under these conditions, the discharge capacitance of an MIC is roughly twice higher than for an EDLC. Furthermore, as demonstrated in ref [129], the output energy of an MIC is approximately four times greater than for an EDLC.

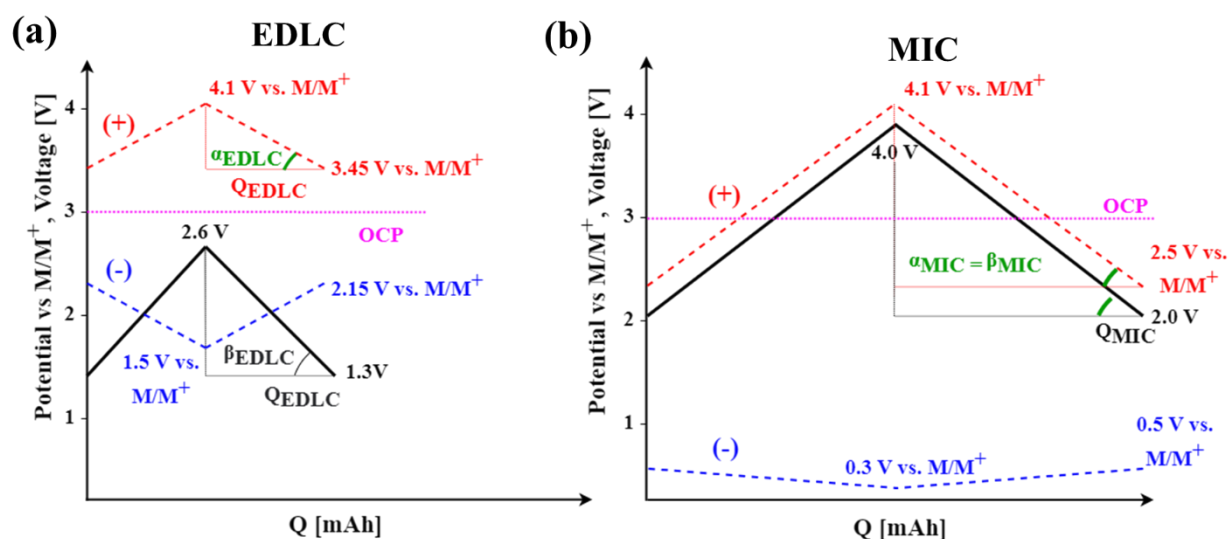


Figure 17. Galvanostatic charge/discharge profiles of a) EDLC (AC/AC capacitor) and b) MIC. The schematic representation of the MIC is based on the case of a Sodium-ion capacitor with a Sn_4P_3 -based negative electrode, where: red—positive electrode’s potential, blue—negative electrode’s potential, and black—cell voltage. From the reference [129]. Noteworthy, in the case of a LIC, the negative electrode would be from graphite and the electrolyte e.g., $LiPF_6$ in EC: DMC.

2.2. Ion population changes in the positive carbon electrode of MICs

As discussed in **Paragraph 2.1**, MICs employ a positive EDL electrode, where ions are reversibly electrosorbed during the charge and discharge of the device (See **Figure 16**). Therefore, the parameters for the selection of a positive electrode for MIC generally align with those outlined in **Paragraph 1.3**. Though the positive electrode of a MIC operates over a wider potential range than in typical EDLCs [129], little attention has been given to the charge exchange processes occurring in this electrode. **Figure 18** illustrates the four distinct regions empirically suggested by Zheng during a complete charge/discharge cycle of a LIC [132]:

1. **Region I:** During the initial charge of the LIC, the positive AC electrode is polarized above the point of zero charge (*PZC*) up to its maximum potential limit (E_{max}). Conversely, PF_6^- anions from the electrolyte are electrosorbed into the electrode's porosity.
2. **Region II:** As the LIC discharges, PF_6^- anions desorb from the AC electrode until it reaches the *PZC*.
3. **Region III:** Continuing the LIC discharge below the *PZC*, the Li^+ cations from the electrolyte are electrosorbed into the AC electrode until reaching the minimum potential limit (E_{min}).
4. **Region IV:** During the subsequent charging back to the *PZC*, Li^+ cations are desorbed from the electrode, returning to the electrolyte.

Noteworthy, similar charge exchange processes have been hypothesized by Dewar and Glushenko for the positive electrode of a pre-sodiated sodium-ion capacitor (NIC) [133]. Though such a sequence seems logical, it currently lacks experimental support.

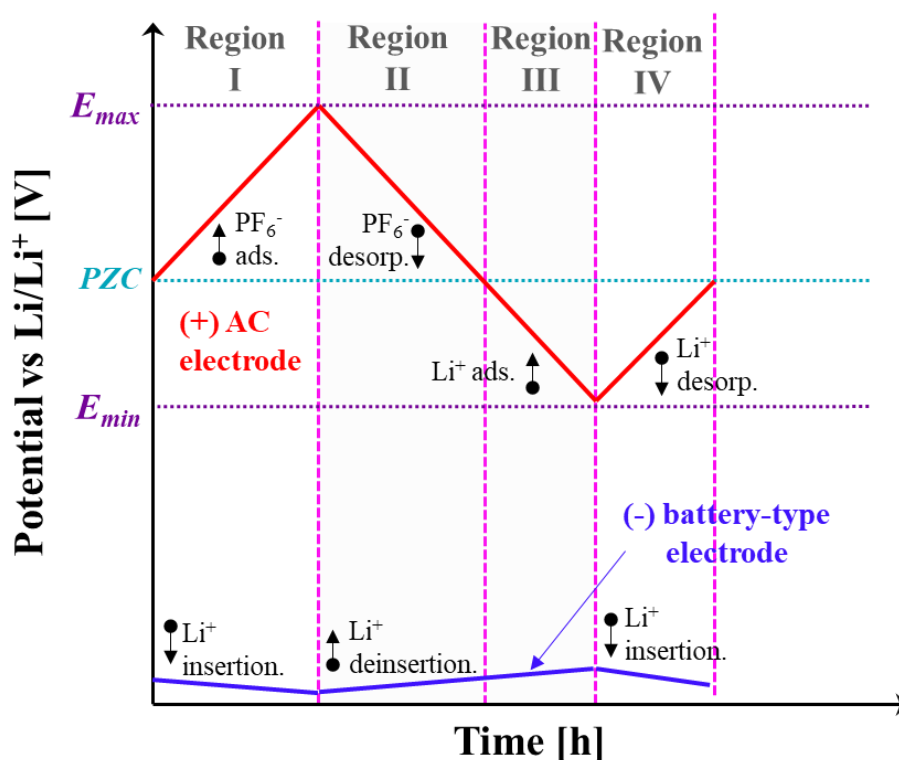


Figure 18. Schematic diagram illustrating galvanostatic profiles of the electrodes in the LiPF_6 -based electrolyte during the first charge/discharge sequences of the hybrid device after pre-lithiation of the negative electrode, where: red and blue lines represent the potential profile of positive and negative electrodes, respectively. Adapted from ref [132]

In this context, a significant contribution by Levi et al. [119] sheds light on the charge exchange processes occurring in an activated carbon (AC) electrode operating across an extended potential range, akin the positive electrode of a LIC during its charge/discharge. The study utilized *operando* electrochemical quartz crystal microbalance (EQCM) during cyclic voltammetry between 1.8 and 4.2 V vs Li/Li^+ to explore the compositional changes of a microporous AC electrode in contact with 0.1 mol L^{-1} lithium tetrafluoroborate (LiBF_4) in propylene carbonate (PC). The EQCM results, compared with the calculated mass changes of the AC electrode under negative polarization relatively to the *PZC*, revealed that lithium cations are not completely stripped of their solvation shell. They are accompanied by only three PC molecules within the electrode porosity, while they are surrounded by four PC molecules in the bulk electrolyte [134]. Conversely, under positive polarization relatively to the *PZC*, BF_4^- anions are found to be poorly solvated when electrosorbed. This finding is consistent with the observation that the energy required to strip $\text{BF}_4^-(\text{PC})_1$ anions from PC molecules is about ten times lower than for $\text{Li}^+(\text{PC})_4$ [135].

2.3. Carbons for the negative electrode of MICs and M^+ intercalation/insertion in these materials.

Among the various materials which have been explored for the construction of MICs, carbons have garnered significant attention for their excellent electrical conductivity. Several review articles discuss the various forms of carbons utilized in MICs, including graphite and hard carbons [136-138].

2.3.1. Graphite

Graphite was the first carbon material used to explore the reversible intercalation of lithium- [139, 140]. During negative polarization, lithium ions are intercalated between the graphene planes following a “staging” mechanism [141], as illustrated in **Figure 19**. Each 'nth stage compound' is defined by a periodic arrangement of intercalant layers within the graphite structure. Specifically, this means that layers containing the intercalated species are alternated with layers that do not incorporate any intercalant, with 'n' representing the number of graphene layers separating two consecutive intercalant layers (as illustrated in **Figure 19b**) [142]. As the concentration of the intercalant within the graphite host structure increases, the number of these empty, non-intercalated intervals (i.e., 'n-1') decreases, [143]. In its ultimate stage (stage 1), this process leads to a fully lithiated stoichiometry of LiC_6 , which provides a theoretical capacity of 372 mAh g^{-1} .

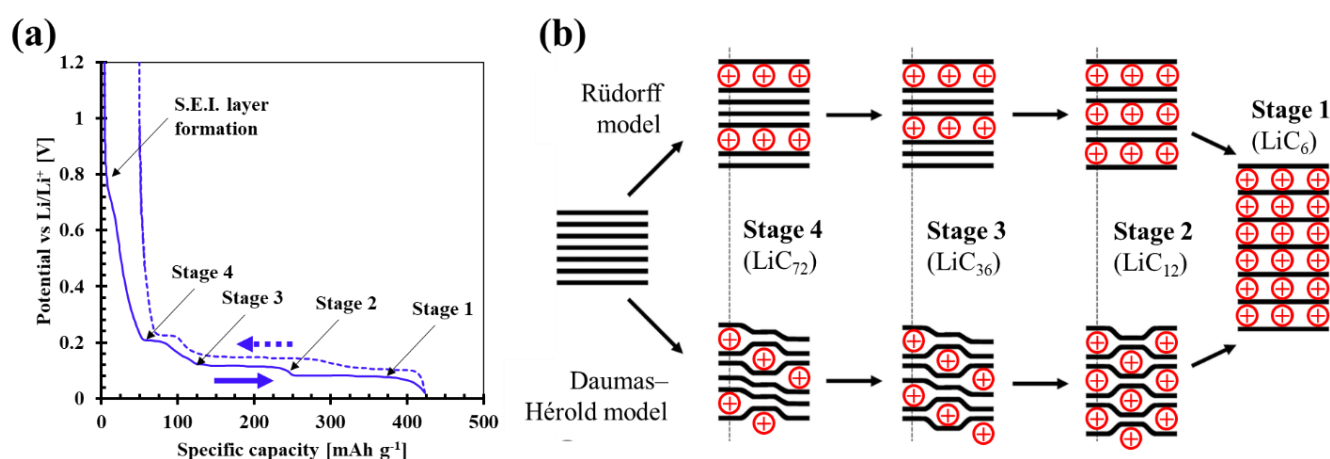


Figure 19. (a) Galvanostatic charge (continuous line)/discharge (dashed line) profile at C/20 (C theoretical capacity of graphite - 372 mAh g^{-1}) of graphite electrode in $1 \text{ mol L}^{-1} \text{ LiPF}_6/(\text{EC}:\text{DMC})$ electrolyte from ref [143] and (b) schematic models of lithium-ion intercalation into graphite as proposed by Rüdorff [142] (upper) and Daumas-Hérol [144] (lower). Adapted from reference [145].

Operando electrochemical dilatometry (ECD) during lithium-ion intercalation in a graphite anode demonstrated a volume expansion of 9.5% during the first cycle as the electrode composition varied from the C_6 state to a fully lithiated LiC_6 state [146], as illustrated in **Figure 20**. This expansion leads to strain within the graphene layers, particularly after repeated cycles of ion intercalation/deintercalation. Therefore, for the long-term stability of lithium-ion batteries (LIBs), it is recommended to limit the state-of-charge during cycling to preserve the integrity of the anode material and prevent excessive degradation [147].

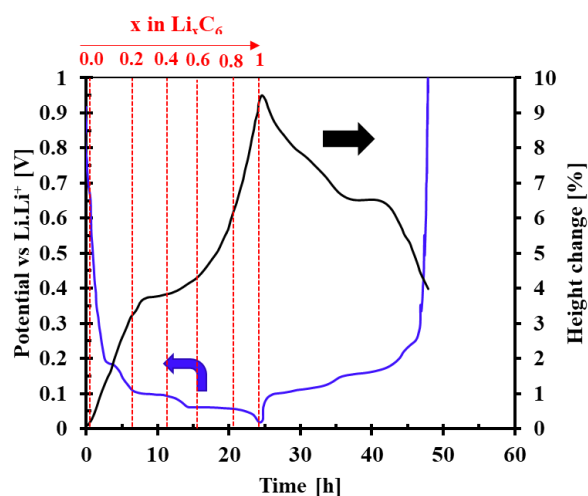


Figure 20. Electrochemical dilatometry during galvanostatic charge/discharge at $C/20$ ($C = 372 \text{ mAh g}^{-1}$) of a graphite electrode in $1 \text{ mol L}^{-1} \text{ LiPF}_6/(\text{EC} : \text{DMC})$ electrolyte. From reference [146].

Among alkali metals, sodium presents an important challenge in the formation of graphite intercalation compounds (GICs). Ge and Fouletier [148] were the first to report the reversible electrochemical intercalation of sodium into graphite, leading to the formation of the NaC_{64} compound with a theoretical capacity of 35 mAh g^{-1} . This finding was later confirmed by Doeff et al. [149]. This poor intercalation ability of sodium into graphite is generally attributed to a size mismatch between Na^+ and the graphite interlayer spacings. Detailed calculations performed on metal-graphite intercalation compounds (M^+ -GICs), with $M = \text{Li, Na, K, Rb}$ and Cs , revealed that the main reason is a change in chemical bonding between M^+ and C atoms [150]. It was demonstrated that the formation energy of MC_6 graphite intercalation compounds becomes progressively less negative (indicating lower stability) as the ion size decreases from Cs to Na . It results in progressively weaker ionic bonding, until NaC_6 exhibits a positive energy of formation, making it thermodynamically unstable. Noteworthy, Lithium, being much

smaller, is an exception to this trend because its bonds with carbon have a covalent character, leading to negative formation energy. These subtle differences in bonding explain why graphite is suitable for Li and K, but not for Na, in intercalation applications with graphite.

The electrochemical intercalation of K^+ into graphite has been investigated by Jian et al. [151], who confirmed the sequential formation of KC_{36} , KC_{24} , and KC_8 compounds. Using *ex situ* XRD, they found that KC_{36} is formed between 0.3 and 0.2 V vs K/K^+ , followed by KC_{24} and KC_8 at lower potentials. At a low current rate, a graphite electrode can achieve a discharge capacity of 273 mAh g^{-1} , which is very close to the theoretical value of 279 mAh g^{-1} when KC_8 is formed.

2.3.2. Reversible insertion mechanism in hard carbons

Hard carbons (HCs) are amorphous materials characterized by a three-dimensional (3D) cross-linked arrangement of graphene layers. During its synthesis, the sp^3 hybridization at the very early stage of carbonization hinders parallel growth of the graphite surface, and therefore, irrespective of pyrolyzing temperature, HC possesses a permanently disordered structure. This structural disorder promotes efficient ion and electron transport, making HCs highly suitable as anode materials for MIBs [152]. The storage mechanism in HCs is complex and involves the reversible insertion and extraction of metal cations within the carbon matrix through multiple processes. Factors such as the specific microstructure, surface chemistry, specific surface area (SSA), heteroatom doping, pore size distribution, electrolyte composition, and operating conditions significantly affect this storage mechanism [152].

Two main insertion mechanisms of Li^+ have been proposed to explain the high reversible capacity of HCs. Sato et al. [153] suggested that Li^+ ions occupy both ionic and covalent sites on the carbon layers, forming LiC_2 covalent molecules. Winter et al [154] suggested that lithium might be electrochemically stored not only in graphitic domains but also in the closed pores of the material. The electrochemical insertion of Li^+ cations into HC electrodes (made of HCs heat-treated at temperatures between 700°C and 1600°C) has been monitored by *ex situ* 7Li NMR, using 1 mol L^{-1} $LiPF_6/EC: DEC$ electrolyte [155]. Depending on the heat treatment temperature, two or three distinct signals were detected and attributed to:

- Lithium irreversibly stored in the disorganized carbon structure, due to the S.E.I. layer formation;
- Lithium reversibly inserted into stacks of disordered layers;

- Lithium inserted into nanopores of the carbon matrix.

These findings align well with the 'house of cards' model (**Figure 21a**) proposed by Dahn to explain lithium/sodium storage in hard carbon [156]. In the particular case of sodium insertion/deinsertion in hard carbon, the galvanostatic characteristics (**Figure 21b**) can be divided into i) a sloping region at high potentials ($\sim 0.1\text{--}2.0$ V vs Na/Na⁺) attributed to sodium accommodation between nearly parallel graphene layers and ii) a plateau region at low potentials ($\sim 0\text{--}0.1$ V vs Na/Na⁺) linked to metal insertion into nanopores between randomly stacked layers, a process akin to adsorption [156]. Hence, the relatively high reversible capacity of HCs (approximately 300 mAh g⁻¹) can be easily justified by the occupation of these two sites by sodium.

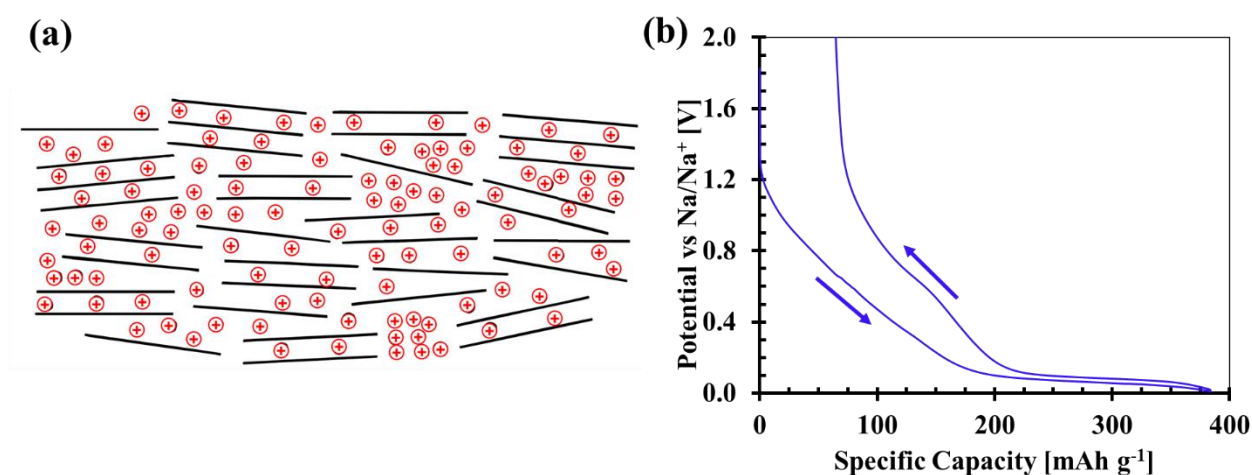


Figure 21. (a) "House of cards" model for sodium/lithium insertion in hard carbon (HC) and (b) galvanostatic charge/discharge profile at C/20 ($C = 300$ mAh g⁻¹) of an HC electrode in 1 mol L⁻¹ NaPF₆/EC:PC electrolyte. From the reference [156]

Operando ⁷Li solid-state NMR measurements on analogous HC electrode materials revealed a low-potential peak shifting from 18 to 114 ppm during the insertion of the alkali metal [157, 158]. This significant shift, compared to the peak for the stage 1 GIC, suggests the presence of quasi-metallic lithium within the pores.

The mechanism hypothesized in ref. [156] was confirmed by *operando* ²³Na NMR, which identified two distinct steps during the sodiation process (**Figure 22**) [159]. In the first step, which corresponds to the sloping region from the open circuit potential down to 180 mV vs. Na/Na⁺, a NMR signal close to 0 ppm was observed. This signal is consistent with either the formation of diamagnetic species within the bulk of the electrode or the formation of the S.E.I. layer due to electrolyte decomposition. In the second step, occurring below 180 mV vs. Na/Na⁺,

a new signal gradually shifting up to 760 ppm appears; it corresponds to the formation of metallic sodium clusters (**Figure 22**).

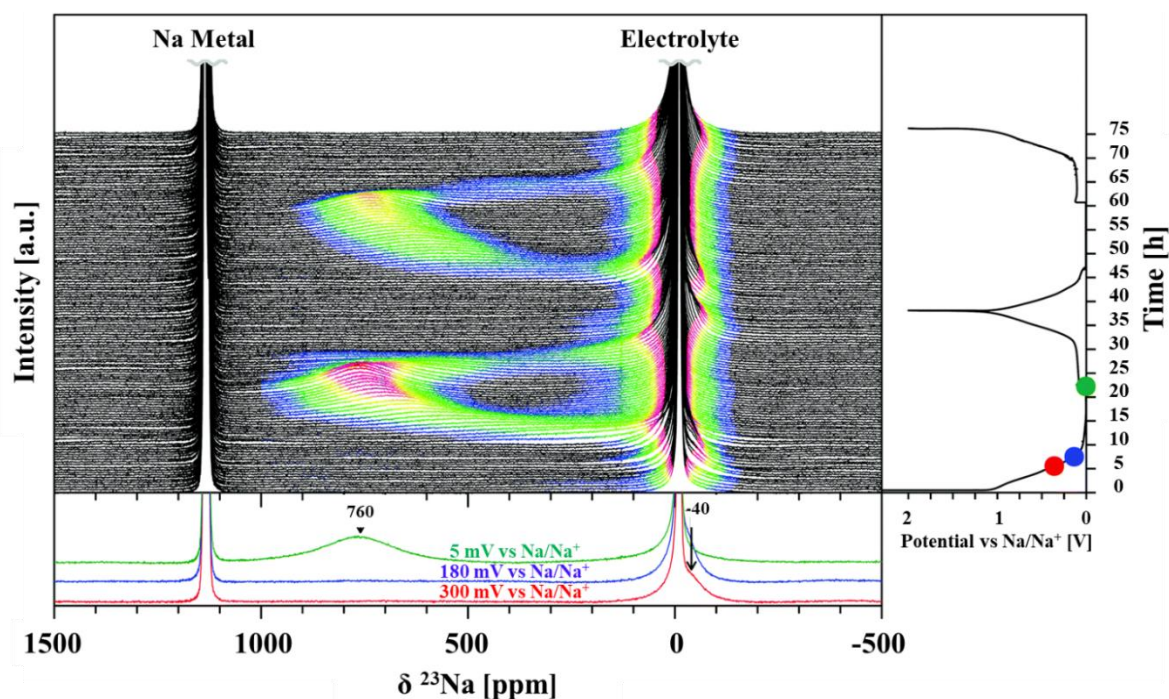


Figure 22. Result of two galvanostatic cycles (shown on the right side) for operando ^{23}Na NMR spectra on a half cell with a hard carbon working electrode and a sodium disc counter/reference electrode in NaPF_6 electrolyte. The cell was cycled at $C/20$ ($C = 300 \text{ mAh g}^{-1}$) between 2 V and 5 mV vs. Na/Na^+ and held at 5 mV vs. Na/Na^+ until the applied current dropped to $C/100$. From reference [159]

Ab initio calculations revealed that, while larger interlayer spacing compared with graphite in hard carbon facilitates sodium embedding, it is not the sole contributing factor. Vacancy defects within the hard carbon structure also significantly enhance sodium insertion due to the strong ionic bonds formed between these defects and the sodium. It underscores the importance of structural defects in optimizing the electrochemical performance of hard carbon electrodes for sodium-ion storage [160].

Sodium insertion in hard carbon was investigated by *operando* electrochemical dilatometry (ECD), which demonstrated an electrode expansion of only 2.3 % (**Figure 23**) [161]. Interestingly, this expansion is approximately four times smaller than that observed in graphite intercalation compounds with lithium (**Figure 20**) despite the difference in cation sizes, further emphasizing the mechanical advantages of hard carbon over graphite to reduce the risk of mechanical degradation during long term cycling. **Figure 23** shows also that the sloping region of the galvanostatic profile (blue line) gives rises to a greater electrode expansion than the plateau region (yellow line). This is an additional confirmation that sodium ion insertion

between graphene layers with suitable spacing is the primary mechanism contributing to the capacity in the slopy region. In contrast, pore filling becomes the dominant mechanism for sodium ion storage during the plateau region.

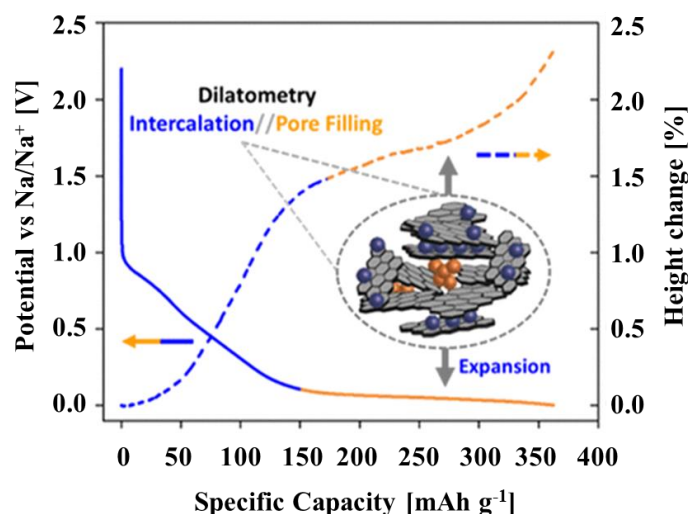


Figure 23. Galvanostatic profile at $C/20$ ($C = 300 \text{ mAh g}^{-1}$) during the first sodium insertion of a Hard carbon electrode in $1 \text{ mol L}^{-1} \text{ NaPF}_6/\text{EC}:\text{DMC}$ electrolyte and simultaneous height change recorded using operando ECD. From reference [161]

The ability to effectively store potassium in hard carbons (HCs) is a key to advancing potassium-ion capacitors (KICs). The performance of KICs is influenced by the structure and surface chemistry diversity among different carbon materials, such as graphite, graphene, and HC. In this context, Lin et al. [162] have investigated the correlation between the microstructure of carbon materials and their potassium storage electrochemical performance. To explore the correlation between the carbon microstructure and K ion storage in $1 \text{ mol L}^{-1} \text{ KPF}_6/\text{EC}:\text{DMC}$ electrolyte, three annealing temperatures, i.e., 650, 1250, and 2800 °C were selected to produce carbons with disordered structure, partially ordered structure, and ordered structure, respectively. By combining *in-situ* characterization by Raman spectroscopy and Ab initio calculations aiming to obtain additional information about adsorption energy of K^+ cations, three mechanisms for K^+ cation storage in hard carbon were identified: (i) adsorption on defect sites; (ii) adsorption on isolated graphene sheets in partially disordered carbon; and (iii) intercalation between graphene layers in highly graphitized carbon. Noteworthy, the different carbon structures exhibited a similar reversible capacity of approximately 280 mAh g^{-1} . The non-graphitic carbon demonstrated superior rate capability and reduced temperature dependence, attributed to faster ion diffusion.

2.4. Organic electrolytes in MICs

In MICs, the electrolyte design/selection is crucial because, in addition to meeting the requirements typical for electrolytes used in electric double-layer capacitors, mentioned in **Paragraph 1.4**, it must also support successively the formation of a solid electrolyte interphase (S.E.I.) on the negative electrode and its pre-metalation. This preliminary step is essential for properly preparing the hybrid device [163]. Notably, the electrolytes used in MIBs are typically implemented in MICs because they are designed to form a stable S.E.I.

Selecting electrolytes for MIBs or MICs, including lithium-ion, sodium-ion, and potassium-ion batteries, involves several key requirements to ensure optimal performance and stability:

- **High ionic conductivity:** The electrolyte must exhibit high ionic conductivity to facilitate efficient ion transport between the electrodes. This is crucial for the battery's overall energy and power performance.
- **Electrochemical stability:** The electrolyte should be stable within the operating voltage range of the battery. It must resist decomposition and side reactions at the electrode interfaces to ensure long-term stability and cycle life.
- **Compatibility with Electrode Materials:** The electrolyte must be chemically and electrochemically compatible with both the positive and negative electrodes. It should not react adversely with electrode materials or degrade their performance.
- **Formation of Stable S.E.I.:** For certain metal-ion batteries, especially those with graphitic anodes, the electrolyte should form a stable and protective S.E.I. layer to enhance cycling stability and prevent excessive capacity loss.
- **Low Viscosity:** The electrolyte should have low viscosity to ensure good wetting of the electrode materials and efficient ion transport, which contributes to better battery performance.
- **Thermal Stability:** The electrolyte needs to remain stable at various operating temperatures to avoid risks of leakage, evaporation, or degradation under different thermal conditions.
- **Safety:** The electrolyte should be non-toxic, non-flammable, and environmentally friendly to ensure safe handling and operation. It should also have a low propensity for hazardous reactions in case of battery damage or failure.

- **Cost and Availability:** The components of the electrolyte should be cost-effective and readily available to ensure the economic feasibility and scalability of battery production.

2.4.1. Solvents

Key components of electrolytes include metal-based (Li^+ , Na^+ , K^+ ...) salts, solvents, and additives. Solvents like ethers, ethylene carbonate, diethyl carbonate, dimethyl carbonate, propylmethyl carbonate, and ethyl methyl carbonate can dissolve metal-based salts and facilitate ionic transport. However, these solvents can significantly influence the formation and structure of the S.E.I. Currently, the carbonate esters used are either cyclic, such as propylene carbonate (PC) and ethylene carbonate (EC), or linear, like ethyl methyl carbonate (EMC), dimethyl carbonate (DMC), and diethyl carbonate (DEC) [164]. Among these, PC and EC are attractive for MICs due to their high dielectric constant and stable chemical and electrochemical properties. However, no single solvent can meet all the requirements of metal-ion capacitors. For instance, sodium-ion cells with PC-based electrolytes experience significant capacity decay over time, mainly due to the continuous decomposition of PC and the growth of the S.E.I. layer [165, 166]. Though pure EC is unsuitable as a solvent at ambient temperature, due to its high melting point (36.4 °C), it is an excellent co-solvent, especially when paired with PC in optimized proportions, as it effectively contributes to forming a protective S.E.I. layer [167]. Besides, linear carbonate esters such as EMC, DMC, and DEC have lower viscosity and melting points compared to cyclic carbonate esters. They are often used as co-solvents with cyclic carbonates (EC or PC) to enhance the overall performance of the electrolyte.

2.4.2. Salts

An ideal electrolyte solute for MICs should meet several key requirements: (i) it must be completely dissolved and dissociated, allowing the solvated ions, particularly the lithium cation, to move with high mobility; (ii) the anion should be stable against oxidative decomposition at the positive electrode and must remain inert to electrolyte solvents; (iii) both the anion and cation should be chemically inert toward other cell components, such as the separator, electrode substrate, and cell packaging materials; (iv) the anion should be non-toxic and remain stable under thermally induced reactions with electrolyte solvents and other cell components [164].

In lithium-ion devices, lithium hexafluorophosphate (LiPF_6) is the most commonly used salt due to its favourable solubility and stability. LiPF_6 features a complex anion structure, where the fluoride ion (F^-) is stabilized by the Lewis acid PF_5 , forming a superacid anion [168]. The formal negative charge is distributed across the strongly electron-withdrawing ligands of PF_5 , enhancing the salt's solubility in low dielectric media and contributing to its relatively low melting point [168]. These characteristics make LiPF_6 highly suitable for lithium-ion devices compared to other lithium salts [164]. However, LiPF_6 is both expensive and highly hygroscopic; it reacts with absorbed moisture to form hydrofluoric acid (HF), which can be highly corrosive and harmful to the system's components [169].

The most commonly used salt in sodium-ion devices is sodium perchlorate (NaClO_4). However, a significant issue with NaClO_4 is its notoriously difficult drying process, which poses safety concerns [170]. Although the water content in electrolytes is rarely reported in the literature, NaClO_4 -based electrolytes typically exhibit higher water content (>40 ppm) compared to those based on NaPF_6 (<10 ppm), even after drying the powder at 80°C under vacuum overnight [171]. The second most popular salt is NaPF_6 , which allows for direct comparison with many studies on lithium-ion devices.

2.4.3. Additives

Another important component often required to create a functional electrolyte for MICs is the additive, typically used at concentrations of less than 5 wt%. Additives are essential for forming a stable S.E.I. on the surface of the negative electrode during the pre-metalation process [133]. The S.E.I. layer plays a critical role in MIC performance and safety by ensuring long-term stability and efficiency. It helps protect the electrolyte from degradation, which in turn prolongs lifespan and enhances cycling stability. Additionally, a well-formed S.E.I. contributes to safety by reducing the risk of flammability and preventing overcharging, thereby mitigating potential hazards during battery operation [172, 173].

2.5. Solid-electrolyte interphase in the negative electrode of MICs

The solid electrolyte interphase (S.E.I.) plays a crucial role in the performance and durability of metal-ion capacitors (MICs). Formed on the negative electrode during the insertion/intercalation of M^+ cations in the anodic host, the S.E.I. arises from the decomposition of the electrolyte and consists of a variety of organic and inorganic compounds [133, 174, 175] as depicted in **Figure 24**. This layer serves as a protective barrier, shielding the anode surface

from further reactions with the electrolyte, which is essential for maintaining the integrity of the electrode material and ensuring the long-term stability of the capacitor. A good S.E.I. should meet the following criteria: (i) protect the electrode surface from direct contact with the electrolyte, and (ii) allow the diffusion of desolvated ions and prevent the transport of electrons (the S.E.I. is a pure cationic conductor).

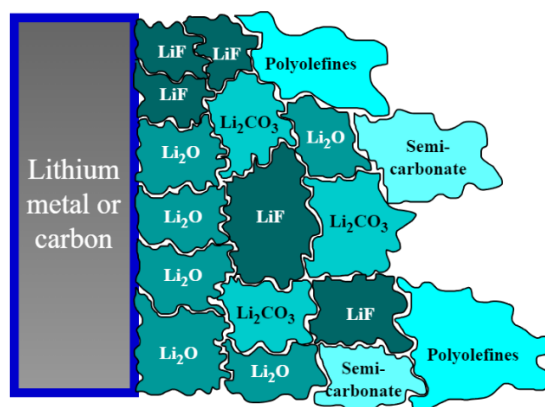


Figure 24. Mosaic model of the SEI according to Peled et al. From reference [165]

In metal-ion capacitors, the S.E.I. controls the transport of metal alkali cations to the bulk of the negative electrode by being selectively permeable. It allows metal ions, such as lithium or sodium, to move through it while blocking electrons, a critical function that supports the rapid ion transport needed for the high-power applications typical of MICs [133]. This selective ion passage is a key to minimizing energy loss and maintaining the efficiency of the capacitor. The S.E.I. also enhances the stability of metal-ion capacitors by stabilizing the anode during the fast charge-discharge cycles that characterize these devices. Doing so helps prevent capacity fade, ensuring that the capacitor can repeatedly deliver quick bursts of energy without significant degradation over time [176]. Moreover, the S.E.I. reduces unwanted side reactions between the electrolyte and the anode, such as gas formation and electrolyte breakdown, which can otherwise increase the internal resistance and lower the power output [163]. Additionally, a well-formed S.E.I. contributes to the safety and longevity of MICs by preventing the growth of dendrites, which could cause short circuits, and by mitigating the risk of thermal runaway through a stable and controlled interface [165]. An overly thick or resistive S.E.I. can impede ion transport and reduce the power performance of the capacitor, whereas a thin or unstable S.E.I. might fail to protect the anode, leading to rapid degradation or safety issues.

2.6. Pre-metalation methods for the preparation of MICs

Despite the outstanding characteristics of MICs, a significant challenge in their conceptualization, design, and optimization is the pre-metalation step [133]. This critical phase involves the formation of an S.E.I. and doping of the negative electrode. Proper execution of these processes is essential for the successful preparation and performance of MICs [133, 177].

The first widely implemented method in the research field is known as the two-step assembling process. In this method, the negative electrode of a MIC is prepared by assembling an electrochemical cell where the working electrode is the desired anodic material, and a metal disc serves as both the counter/reference electrode and the primary source for pre-metalation. After electrochemically reducing/doping the anodic material, the cell is transferred to an oxygen- and moisture-free environment, where the doped anode is introduced into a new cell and combined with an activated carbon (AC)-based positive electrode to complete the MIC [127, 133]. While effective, this method is cumbersome and expensive due to the multiple steps involved.

An alternative approach consolidates the two operations into a single cell, including an AC-based EDL electrode, an anodic material electrode for metal insertion/intercalation, and an auxiliary alkali metal electrode. In this method, the anodic host electrode is first connected with the auxiliary metal electrode and negatively polarized for doping. Once pre-metalation is complete, the auxiliary electrode is disconnected, and the MIC is assembled by connecting the AC-based EDL electrode with the pre-metalated negative electrode [133]. This streamlined approach simplifies the process and reduces manufacturing costs.

Another pre-metalation method involves the use of a highly concentrated electrolyte which plays the role of a metal-ion reservoir [178]. This approach eliminates the need for alkali metals and the associated safety concerns. However, despite the abundance of metal cations in the electrolyte, the pre-metalation process results in a noticeable depletion of electrolyte concentration. This reduction in concentration reduces the ionic conductivity of the electrolyte, and consequently the power of the system. Recently, redox-active electrolytes containing thiocyanate-based salts have been proposed for the one-step assembly of metal-ion capacitors [179]. Nonetheless, this approach requires more investigation, since the life span of MICs prepared by this method does not exceed 1000 cycles.

The most promising method is based on creating a cell where the porous EDL carbon electrode includes a sacrificial material, and the other electrode is constituted by the anodic host material.

The sacrificial material is irreversibly oxidized, releasing metal for S.E.I. formation and doping of the anodic host, thus forming the metal-ion capacitor [180] as depicted in **Figure 25**. For optimal MIC operation, the mass of the sacrificial material must be precisely adjusted to ensure its complete utilization [129]. This method is the most practical, as the doping of the negative electrode can be performed *in situ* within the intended MIC electrochemical cell. Additionally, it avoids the use of alkali metals, mitigating associated safety risks during preparation and operation. However, there are potential drawbacks to consider. The decomposition of the sacrificial material in the positive electrode could lead to issues such as (i) residual solid remaining in the positive electrode, which might reduce the pore volume and capacitance [181, 182, 183] or (ii) the appearance of oxidation products in the electrolyte [184, 185]. These reaction products might be detrimental to the MIC operation; for example, due to the solid residues in the positive EDL electrode, the pore volume and consequently the capacitance might decrease.

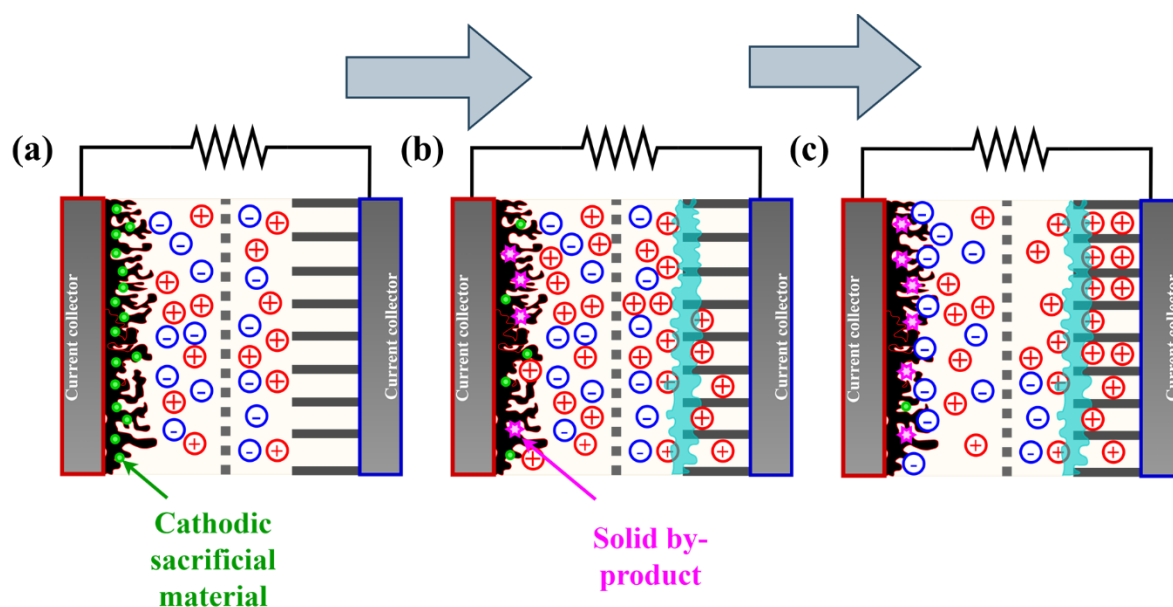


Figure 25. Illustration of using a sacrificial material (green circles) incorporated in the positive AC electrode for the preparation of a MIC. The sacrificial material is irreversibly oxidized to release M^+ and solid by-product remaining on the AC electrode (pink stars) during the first metal extraction, conversely, the S.E.I. layer (turquoise) is formed and the metal is inserted/intercalation into the negative electrode: (a) Precursor cell; (b) cell during pre-metalation and (c) metal-ion capacitor. Adapted from reference [186]

The sacrificial material chosen for realizing a MIC should ideally meet the following criteria [177]:

- **Low Oxidation Potential:** the pre-metalation agent introduced in the formulation of the positive electrode should be irreversibly oxidized at potential lower than the

oxidation potential limit of the electrolyte on the considered porous carbon electrodes, e.g., 4.1-4.2 V vs Na/Na⁺ for the classical 1 mol L⁻¹ NaClO₄/EC:PC (with equal volume ratio of ethylene carbonate and propylene carbonate) electrolyte on porous carbon electrodes based on Maxsorb, BP2000 or YP80F carbons [187, 188].

- **High Irreversible Capacity:** high first cycle irreversible capacity is desired to minimize the amount of sacrificial in the positive EDL electrode and thereof diminish the mechanical impact on the electrode integrity.
- **Stability in Ambient Atmosphere:** For easy electrode fabrication, without the need for a costly protective neutral atmosphere, the material should be stable in ambient conditions.
- **Non-Detrimental By-products:** Upon oxidation, the material should produce non-detrimental by-products (such as solid residues) to ensure optimal performance of the final device.
- **Cost-Effectiveness:** Given the cost disadvantages of the MIC technology compared to other technologies, the synthesis of these materials should be cost-effective, relying on low-cost precursors and soft synthesis conditions to avoid significantly increasing the final product's price.

These criteria ensure that the sacrificial material not only enhances the performance of the MIC but also contributes to its practicality and economic viability for large-scale applications. In this context, **Table 2** presents a recollection of various sacrificial cathodic materials used for the preparation of MICs by pre-metalation. Examples include sodium amide (NaNH₂), sodium sulfide (Na₂S), and sodium borohydride (NaBH₄), which all exhibit high irreversible capacity and oxidation potential values within the *ESW* of the classical 1 mol L⁻¹ NaClO₄/EC:PC electrolyte in (AC) electrodes. However, a significant drawback during the electrochemical oxidation of these compounds is the generation of by-products that remain mixed with the cell components, potentially affecting the performance of the hybrid capacitor. Additionally, all three salts require moisture- and oxygen-free conditions during electrode manufacturing to prevent premature oxidation and the formation of undesired products. Materials like Li₅FeO₄, Li₆CoO₄, and Li₅ReO₆ also show high irreversible capacity, but their oxidation potential is very high, possibly exceeding the oxidative limit of the electrolyte. This could lead to the decomposition of the electrolyte during the pre-lithiation process, further complicating the performance and reliability of the MIC.

Table 1. Properties of sacrificial cathodic materials which have been utilized for the pre-metalation step aimed to prepare MICs. Adapted from reference [163].

Sacrificial material	Oxidation potential	Irreversible capacity [mAh g ⁻¹]	By-products	Stable in air	Ref
Li ₂ MoO ₃	4.7 V vs Li/Li ⁺	250	Li _{2-x} MoO ₃ (0 < x < 1.7) (solid)	No	[189]
Li ₅ FeO ₄	4.7 V vs Li/Li ⁺	700	LiFeO ₃ (solid); O ₂ (gas)	No	[181]
Li ₆ CoO ₄	4.3 V vs Li/Li ⁺	600	LiCoO _{2.5} (solid); O ₂ (gas)	No	[182]
Li ₅ ReO ₆	4.3 V vs Li/Li ⁺	410	α-ReO _{3.5} (solid); O ₂ (gas)	No	[183]
Li _{0.65} Ni _{1.35} O ₂	4.1-4.3 V vs Li/Li ⁺	120	Li _{1-x} Ni _{1.35} O ₂ (solid)	No	[190]
Li ₂ CuO ₂	3.6 V vs Li/Li ⁺	342	CuO (solid); O ₂ (gas)	Yes	[191]
Li ₃ N	4.0-4.3 V vs Li/Li ⁺	1379	N ₂ (gas)	No	[192]
Li ₂ DBHN	3.2 V vs Li/Li ⁺	365	3,4-dioxobenzonitrile (liquid)	No	[184]
Li ₂ C ₄ O ₄	3.9-4.2 V vs Li/Li ⁺	425	C (solid) ; CO ₂ (gas)	Yes	[193]
NaNH ₂	3.8 V vs Na/Na ⁺	680	N ₂ H ₄ (liquid), H ₂ (gas), N ₂ (gas)	No	[185]
Na ₂ S	3.8 V vs Na/Na ⁺	687	Polysulfides (liquid); Sulfur (solid)	No	[188]
NaBH ₄	2.4 V vs Na/Na ⁺	700	B (solid), H ₂ (gas)	No	[194]
Na ₂ C ₂ O ₄	4.4 V vs Na/Na ⁺	400	CO ₂ (gas)	Yes	[195]
NaCrO ₂	4.16 V vs Na/Na ⁺	230	Na _{1-x} CrO ₂ (solid)	Yes	[196]
Na ₂ C ₄ O ₄	3.6 V vs Na/Na ⁺	339	C (solid) ; CO ₂ (gas); CO (gas)	Yes	[187]

3. Conclusion

In this chapter, the state-of-the-art on electrochemical capacitors has been presented and discussed. As highlighted in the review, Electrical Double-Layer Capacitors (EDLCs) are classified as high-power energy storage devices due to their charge/discharge mechanism, which relies on the electrostatic accumulation of ions at the electrode-electrolyte interface. Since this process does not involve electron transfer, EDLCs offer significantly higher power than conventional lithium-ion batteries, although their energy density is lower. As a result, much of the research focuses on improving energy density by optimizing capacitance and voltage.

To enhance capacitance, EDLCs are typically constructed using nanoporous carbon electrodes with high surface areas and significant micro-/mesopore volumes. A variety of carbon materials have been extensively investigated, with a focus on their textural and structural properties, which are critical for capacitive performance. Among these, activated carbon is particularly notable due to its high electrical conductivity, chemical and thermal stability, diverse morphologies, and the ability to fine-tune its porous features. The design/selection of electrolytic solutions is equally important for EDLC performance. Electrolytes should have high ionic conductivity to enhance specific power and the widest possible electrochemical stability window (*ESW*) to maximize energy storage and extend the device's lifespan. Organic electrolytes are commonly used because they offer relatively high ionic conductivity, a broad operating temperature range, and a wide *ESW*. However, organic electrolytes are highly hygroscopic and even trace amounts of water can drastically reduce the *ESW*, necessitating the construction of EDLCs in controlled, moisture-free environments. In this context, highly-concentrated aqueous solutions of neutral salts called "Water-in-Salt" (WIS) electrolytes, have attracted significant attention in recent years due to the involvement of most water molecules in solvating ions, leading to an important increase of *ESW* compared with diluted aqueous solutions. However, whereas most of the highly concentrated WIS electrolyte offers significant benefits in terms of ionic conductivity and extended *ESW*, it should be noted that most examples presented in the literature for EDLCs concern concentrations close to saturation at room temperature (RT). This makes them unsuitable for use at low temperatures in EDLCs, unlike the traditional 1 mol L⁻¹ TEABF₄/ACN electrolyte. Hence, to apply profitably WIS electrolytes in environmentally friendly EDLCs, it is necessary to circumvent the obstacle of operation at low temperatures.

In the present era, metal-ion capacitors (MICs) are emerging as a promising category of hybrid electrochemical energy storage devices, garnering significant attention in both research and industrial sectors. MICs offer the potential to store approximately four times the specific energy of electrical double-layer capacitors (EDLCs) while maintaining comparable power capabilities. They achieve this by integrating a battery-type negative electrode, where alkali cations are reversibly inserted or intercalated within a narrow potential range, with an electrical double-layer (EDL) positive electrode that operates across a broader potential range than conventional EDLC electrodes.

However, there is still limited knowledge about the synergy between these electrodes in hybrid capacitors. Understanding the individual performance of electrodes during MIC operation is

vital for optimizing these systems. Moreover, despite the promising characteristics of MICs, little research has been conducted to understand the changes in ion populations within the positive electrode during charge/discharge cycles. This lack of experimental data is crucial, as it could reveal the factors responsible for the shorter lifespan of MICs compared to EDLCs. Closing this knowledge gap is essential for enhancing the performance and durability of MICs moving forward.

Another significant challenge in developing metal-ion capacitors (MICs) is the formation of a solid electrolyte interphase (S.E.I.) that provides both good ionic conductivity and electronic insulation on the anodic material, as well as addressing the issue of pre-metalation due to the lack of inserted or intercalated metal in the anodic material. One promising approach to pre-metalate the negative electrode involves incorporating a sacrificial material in the positive electrode of the MIC. The ideal sacrificial material should exhibit a low extraction potential, a high irreversible capacity to minimize inactive mass, be stable in the air to facilitate electrode manufacturing, and ideally leave behind an inert gas as residue. Currently, no single material reported in the literature meets all these criteria perfectly, highlighting a crucial gap in the field. To advance the development of MICs, it is essential to explore and identify new sacrificial materials that can meet these requirements and enhance the performance and practicality of MICs.

Chapter II

The NaClO₄-water eutectic electrolyte for environmentally friendly electrical double-layer capacitors operating at low temperature

1. Summary of the publication

Advancements aiming at increasing the energy density of electrical double-layer capacitors (EDLC) in aqueous electrolytes have focused recently on highly concentrated solutions of neutral salts, commonly known as "Water-in-Salt" (WIS) [76]. Though WIS electrolytes offer extended electrochemical stability window (*ESW*) on activated carbon (AC) electrodes compared to traditional diluted neutral aqueous electrolytes, most reports indicate that they are near saturation at room temperature (RT, 25 °C) [78-81]. This limits their practical applicability, especially in sub-ambient environments, due to potential solute precipitation and electrode porosity blockage. The publication titled "*The NaClO₄-Water Eutectic Electrolyte for Environmentally Friendly Electrical Double-Layer Capacitors Operating at Low Temperature*" addresses this issue. According to the literature, an eutectic melting at -35 °C is observed at 8.84 mol kg⁻¹ NaClO₄ in the NaClO₄-water binary diagram; this relatively concentrated solution displays the characteristics of a WIS electrolyte.

Interestingly, the eutectic electrolyte demonstrated a high ionic conductivity of 180 mS cm⁻¹ and a low dynamic viscosity of 2.48 mPa s at room temperature (RT). At lower temperatures, the ionic conductivity remained relatively high, reaching 23.7 mS cm⁻¹ even at -30 °C, while the dynamic viscosity increased to 24.8 mPa s. The transport properties of the NaClO₄-water eutectic solution did not follow Arrhenius-type dependence with temperature. This behaviour characterizes "fragile" liquids, which lack directional bonding and undergo significant structural changes as they approach the glass transition temperature [197]. Instead, the Vogel-Tammann-Fulcher (VTF) equations were applied to model the temperature dependence of these transport properties, and the results aligned well with the experimental data. These liquids can be readily rearranged by minor disturbances, indicating weak molecular interactions and high molecular mobility, which is consistent with their elevated ionic conductivity. MD simulations on the 8.84 mol kg⁻¹ NaClO₄ solution revealed that the solvation shell of Na⁺ consists of ca. 4 water molecules and 2 ClO₄⁻ anions at -35 °C, being very similar to the solvation shell at RT [82, 83]. Distinct channel-like domains formed by hydrogen-bonded water molecules were observed, which aid in facilitating ionic diffusion throughout the bulk electrolyte [198].

The *ESW* of the NaClO₄-water eutectic electrolyte on an AC electrode was found to increase from 1.8 V at RT to 2.1 V at -35 °C. These high *ESW* values for an aqueous solution were attributed to several factors: *i*) the quasi-neutral pH of the electrolyte, which favors a high overpotential of water reduction on porous AC electrodes [11]; *ii*) the WIS characteristics,

which reduce the amount of free water in the Stern layer of the positively polarized AC electrode [78]; and *iii*) the higher oxidation potential at lower temperatures due to improved immobilization of ClO_4^- anions and reduced kinetic of water oxidation. It is important to note that the *ESWs* of AC electrodes in the eutectic electrolyte could not be directly translated into operating voltage of EDLCs, because the differences in cation and anion sizes affect the potential ranges of the positive and negative electrodes differently [79]. Considering this, nominal voltages of 1.7, 2.0, and 2.1 V were determined on AC//AC laminate capacitors in the 8.84 mol kg^{-1} NaClO_4 electrolyte at RT, $-30 \text{ }^\circ\text{C}$, and $-35 \text{ }^\circ\text{C}$.

Electrochemical impedance spectroscopy measurements on EDLCs showed that their resistive components are relatively low down to $-30 \text{ }^\circ\text{C}$, indicating that this temperature represents the lowest practical limit for efficient operation of these devices. To establish a comparison, Ragone plots were generated under constant discharge power at various temperatures on AC//AC cells using the NaClO_4 -water eutectic electrolyte and the 1 mol L^{-1} $\text{TEABF}_4/\text{ACN}$ organic electrolyte (taken as a reference). For the cell in the eutectic solution, the maximum voltage was set at the above-determined values of 1.7 V for RT and 2.0 V for $-30 \text{ }^\circ\text{C}$. In the case of the 1 mol L^{-1} $\text{TEABF}_4/\text{ACN}$ organic electrolyte, 2.7 V was selected as the maximum voltage [14]. The results indicated that the cell with the eutectic electrolyte delivered slightly higher energy at $-30 \text{ }^\circ\text{C}$ (12.7 Wh kg^{-1} up to ca. 3 kW kg^{-1}) than at RT (10.5 Wh kg^{-1} up to ca. 10 kW kg^{-1}). Notably, at $-30 \text{ }^\circ\text{C}$ and high power levels, the output energy of the cell with eutectic electrolyte surpassed that of the cell with organic electrolyte.

Figure 26 underscores the significant potential of environmentally friendly EDLCs utilizing the NaClO_4 -water eutectic electrolyte to compete with conventional devices employing organic electrolytes, particularly in sub-ambient temperature conditions. This advancement does not only demonstrate the feasibility of sustainable energy storage solutions, yet also suggests that these novel systems could play a pivotal role in enhancing the performance of electrochemical capacitors in diverse applications, especially under extreme climatic conditions.

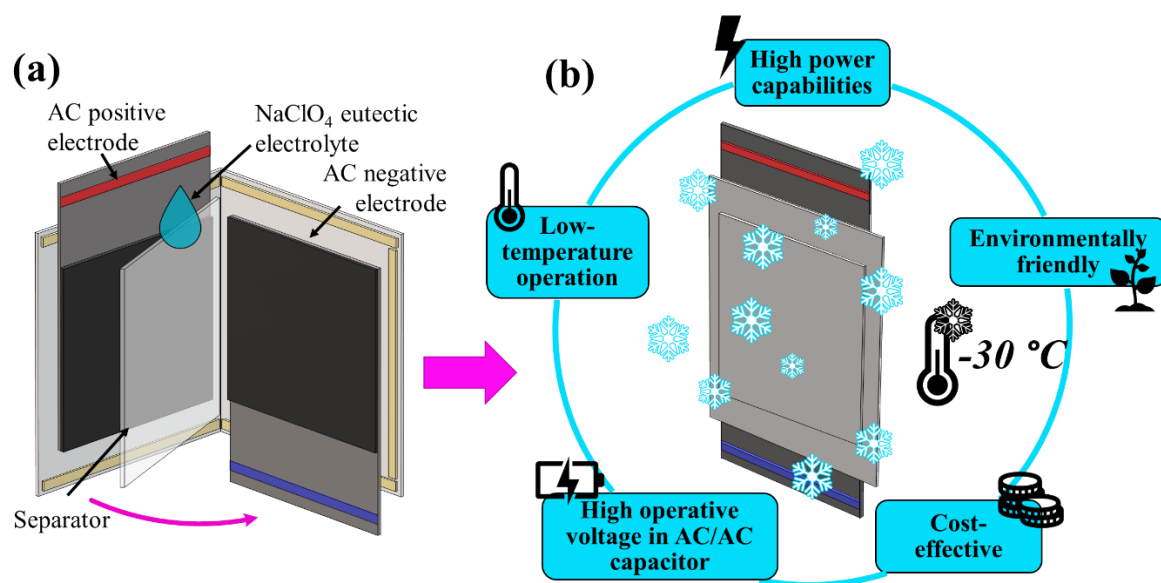


Figure 26. Schematic representation of the laminate AC//AC capacitor using $8.84 \text{ mol kg}^{-1} \text{ NaClO}_4/\text{H}_2\text{O}$ as electrolyte: (a) Components of the cell before closing and (b) Sealed cell with a brief presentation of the benefits of using NaClO₄-water eutectic electrolyte.

Chapter III

Ideally realized sodium-ion capacitor via irreversible oxidation of sodium azide to pre-metalate the anodic host

1. Summary of the publication

Recently, MICs have garnered significant attention in both academic and industrial fields due to their hybrid design, which enables them to achieve up to approximately four times the output energy of EDLCs, while maintaining comparable power levels [129]. A major challenge in their design and optimization is the pre-metalation of the anodic material in the negative electrode. **Chapter I** highlights that the most promising method involves incorporating sacrificial material into the EDL positive electrode [180]. However, the success of this method relies on a sacrificial material exhibiting high irreversible capacity at low oxidation potential, producing no harmful by-products, and being both air-stable and cost-effective. In this context, **Chapter III** presents a study titled “*Ideally Realized Sodium-Ion Capacitor via Irreversible Oxidation of Sodium Azide to Pre-Metalate the Anodic Host*”. This study explored the use of sodium azide (NaN_3) as a sacrificial cathodic material to address metal deficiency in the anodic host, aiming to effectively prepare sodium-ion capacitors (NICs) without producing any residual solid product.

To address this, the study first elucidated the irreversible capacity and oxidation potential of sodium azide. The nature and quantity of gas released during the electrochemical oxidation of NaN_3 electrodes percolated by conductive carbon ($\text{NaN}_3\text{-C65}$) was analyzed. Subsequently, similar experiments were conducted on electrodes composed of NaN_3 and activated carbon ($\text{NaN}_3\text{-AC}$) to specifically investigate the impact of NaN_3 oxidation on the porous texture of the EDL-positive electrode. The selected anodic host for the NIC was a mixture of hard carbons (HCM), whose mass composition was adjusted to minimize the ohmic drop during cycling. Finally, a precursor $\text{NaN}_3\text{-AC//HCM}$ laminate cell was constructed with a reference electrode to monitor the electrode potentials throughout the pre-metalation of the negative electrode, till forming an $\text{AC//Na}_x\text{HCM}$ sodium-ion capacitor.

Galvanostatic cycling at $C/40$ (C of $\text{NaN}_3 = 412 \text{ mAh g}^{-1}$) coupled with *operando* electrochemical mass spectroscopy on a $\text{NaN}_3\text{-C65}$ electrode in $1 \text{ mol L}^{-1} \text{ NaClO}_4/\text{EC:PC}$ electrolyte, demonstrated the complete and irreversible oxidation of NaN_3 at 3.5 V vs Na/Na^+ , which is below the oxidative potential limit of 4.1 V vs Na/Na^+ for typical activated carbon (AC) materials used in EDL electrodes [187, 188]. It was experimentally demonstrated that N_2 is the sole by-product of the oxidation, which can be readily extracted from the cell. When $\text{NaN}_3\text{-AC}$ electrodes were subjected to the same galvanostatic cycling conditions, complete oxidation of NaN_3 was achieved after 5 cycles, yielding a total irreversible capacity of 411

mAh g⁻¹. The incomplete oxidation observed during the first cycle was attributed to the lower amount of conductive additive, which may have hindered uniform charge distribution throughout the bulk electrode, preventing full access to all NaN₃ particles. Therefore, to successfully implement the NIC in subsequent steps, a few additional cycles were deemed necessary to ensure full oxidation of the sacrificial material.

To confirm the complete oxidation of NaN₃, nitrogen adsorption analysis at 77 K was conducted on three types of electrodes: (i) pristine NaN₃-AC electrodes, (ii) oxidized NaN₃-AC electrodes, and (iii) NaN₃-free electrodes, which contained the same relative proportions of components as the NaN₃-AC electrodes, yet excluding sodium azide. The analysis revealed that the textural properties of the oxidized NaN₃-AC electrodes were very similar to those of the NaN₃-free electrodes, with comparable pore volumes of 0.51 and 0.58 cm³ g⁻¹, respectively. This indicates significant regeneration of AC porosity after NaN₃ oxidation, further supporting the suitability of sodium azide as an effective sacrificial material.

Three types of hard carbon electrodes were compared as potential candidates for the anodic host in the negative electrode of NICs: (i) Carbotron®P-J (HC-J), (ii) glucose-derived hydrothermal carbon (HCG), and (iii) a mixture of both. During the first galvanostatic charge/discharge cycle from open-circuit potential (*OCP*) down to 30 mV vs Na/Na⁺ at low current, the HC-J electrode showed a relatively high reversible capacity of 247 mAh g⁻¹ and a low irreversible capacity of 36 mAh g⁻¹ but suffered from a significant ohmic drop of 25 mV [185, 194], attributed to loose particle packing. In contrast, the HCG electrode exhibited a minimal ohmic drop of 2.3 mV, though, its irreversible capacity was relatively high (101 mAh g⁻¹), likely due to the more developed external surface compared to HC-J. To balance the respective advantages of HC-J and HCG, several mixtures of these hard carbons were formulated, with an optimized blend of 70 wt.% HC-J and 30 wt.% HCG (referred to as HCM) being identified. The HCM electrode demonstrated a small ohmic drop of 6 mV, a low irreversible capacity of 63 mAh g⁻¹, and a high reversible capacity of 270 mAh g⁻¹. This attractive electrochemical performance was attributed to tight particle packing, where small HCG aggregates filled the spaces between HC-J particles, potentially enhancing interparticle contact. Further electrochemical testing of the HCM electrode at various low potential limits revealed that 30 mV vs Na/Na⁺ should be imposed as the low potential limit of the HCM anode to avoid sodium plating during NIC cycling.

In the fabrication of the laminated $\text{NaN}_3\text{-AC//HCM}$ precursor cell, the mass balance of electrodes was crucial for effective sodium ion transfer between electrodes. Indeed, NaN_3 can release a capacity of ca. 412 mAh g^{-1} during oxidation, while the HCM anode requires approximately 350 mAh g^{-1} for complete sodiation down to 30 mV vs Na/Na^+ . To achieve this, the mass ratio of NaN_3 to HCM should be about 0.85, calculated using their respective capacities. Additionally, to optimize the balance between energy and power, the mass of AC in the positive electrode should match the mass of HCM in the anode [199], maintaining the same 0.85 ratio. Under these conditions, the HCM electrode of the $\text{NaN}_3\text{-AC//HCM}$ cell was pre-sodiated by electrochemical oxidation of the $\text{NaN}_3\text{-AC}$ electrode at $C/40$ ($C = 412 \text{ mAh g}^{-1}$) to transfer sodium to the negative electrode, thereby realizing an $\text{AC//Na}_x\text{HCM}$ sodium-ion capacitor (See **Figure 27**). This NIC demonstrated impressive capacitance retention of 90% and energy efficiency of 95% after 15,000 galvanostatic cycles over a voltage range of 2.0 V to 3.8 V . In terms of energy and power performance, it exhibited output energy of 38 Wh kg^{-1} up to 4 kW kg^{-1} .

These results demonstrate that sodium azide serves as an exceptional "zero dead mass" sacrificial material, paving the way for the cost-effective development of NICs with highly attractive electrochemical performance.

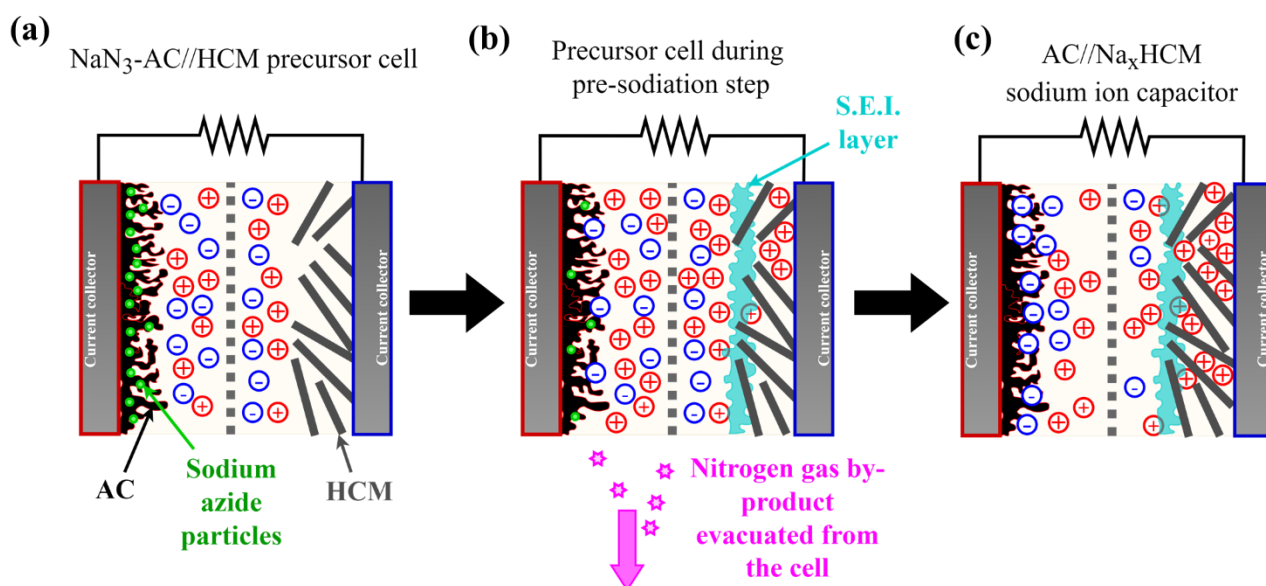


Figure 27. Scheme of the realization of a sodium-ion capacitor through the irreversible oxidation of sodium azide (NaN_3 - green balls) as a sacrificial cathodic material for pre-metalation of the anodic host: (a) $\text{NaN}_3\text{-AC//HCM}$ precursor cell, (b) precursor cell during the pre-sodiation process, and (c) final sodium-ion capacitor after pre-sodiation. The active materials of the positive and negative electrodes are AC and HCM, respectively. The electrolyte is $1 \text{ mol L}^{-1} \text{ NaClO}_4/\text{EC:PC}$

Chapter IV

Comprehensive potentiodynamic analysis of electrode performance in hybrid capacitors

1. Summary of the publication

The combination of the high energy density of the battery-type electrode with the high-power capabilities of the capacitive electrode makes hybrid capacitors promising for advanced energy storage. However, the distinct charge storage mechanisms in the two electrodes - electrostatic double-layer formation in the positive electrode and metal-ion intercalation/insertion in the negative one - require specific methodologies to evaluate their performance. The commonly applied techniques, such as cyclic voltammetry (CV), galvanostatic cycling with potential limitation (GCPL), electrochemical impedance spectroscopy (EIS), and chronoamperometry (CA), often fail to capture the unique behaviours of electrodes in hybrid systems. For example, in CV studies, a typically applied approach where one electrode is designated as the "working" electrode and the other as the "auxiliary" one, with a constant potential scan rate ($\frac{dE}{dt}$) assumed for both electrodes can lead to inaccurate performance characterization, particularly in symmetric electrical double-layer capacitors (EDLCs) [200], highlighting the need for a more accurate method for hybrid capacitors.

In this context, **Chapter IV** presents a study titled “*Comprehensive Potentiodynamic Analysis of Electrodes Performance in Hybrid Capacitors*”, which introduces a methodology for accurately assessing the characteristics of individual electrodes in hybrid capacitors. The calculation procedure was adapted from the one previously used for EDLCs [200], where the potential sweep rates for the positive and negative electrodes ($\frac{dE^+}{dt}$ and $\frac{dE^-}{dt}$, respectively) were dynamically assigned based on their contribution to the voltage ramp ($\frac{dU}{dt}$) [200]. To validate this approach for hybrid cells, an (+)AC//Li_xC₆(-) lithium-ion capacitor (LIC) in 1 mol L⁻¹ LiPF₆/EC: DMC equipped with a reference electrode was analyzed by CV, and the electrodes' contributions in the LIC were compared to the characteristics of a symmetric (+)AC//AC(-) EDLC in 1 mol L⁻¹ LiPF₆/EC: DMC. For the LIC, the voltage scan rate $\frac{dU}{dt}$ was reduced from 5 mV s⁻¹ (applied for EDLCs) to 1 mV s⁻¹ to account for the kinetic limitations of lithium intercalation/deintercalation into the negative electrode.

During the charge/discharge cycles of the symmetric EDLC, both AC electrodes maintained a scan rate close to $\frac{1}{2} \frac{dU}{dt}$, viz. 2.5 mV s⁻¹, with minimal variation, although the negative electrode required a slightly higher rate to compensate for its broader potential range. In contrast, for the LIC, the scan rate of the positive (AC) electrode began near zero, while the negative electrode's scan rate started at its maximum (1 mV s⁻¹). The scan rate of the negative electrode gradually

approached zero (0.01 mV s^{-1}) after 380 s as it reached its redox equilibrium, whereas the potential scan rate of the positive electrode increased to almost 1 mV s^{-1} . Increasing the graphite(negative electrode)-to-AC(positive electrode) mass ratio from 1:1 to 2:1 resulted in a reduced stabilization period of the negative electrode to 150 seconds, indicating faster charge transfer. Conversely, reducing the ratio to 0.5:1 extended the stabilization period to 600 seconds, highlighting the impact of negative electrode material utilization on LIC performance. Apart from that, the current (i_{eff}^+) passing the LIC's positive electrode (calculated at each point of the measurement from the capacitive response of the electrode) reached almost 120 mA g^{-1} within a few seconds of charging, confirming rapid charge accumulation due to electric double layer (EDL) formation. In contrast, the negative electrode (Li_xC_6), dominated by lithium-ion intercalation, showed a much slower rise in i_{eff}^- of ca. 500 s, disclosing that it cannot accommodate with the speed of the electrostatic charging of its counterpart. When the cell was discharged, the current evolution was the same as during the charging process, yet with the reversed sign.

For verification of the proposed methodology, CVs for the negative and positive electrodes in a LIC at a constant voltage scan rate of 1 mV s^{-1} were compared with curves recorded separately for each electrode at constant potential scan rates (0.99 mV s^{-1} set for the positive electrode and 0.01 mV s^{-1} for the negative one, to correspond with the values after stabilization). It was found that the battery-type electrode's characteristics varied significantly depending on whether the potential scan rate was dynamically adapted (constant $\frac{dU}{dt}$) or fixed (constant $\frac{dE}{dt}$). In contrast, the EDL-type electrode exhibited consistent characteristics in both conditions. This demonstrates that applying an equal potential scan rate ($\frac{1}{2} \frac{dU}{dt}$) to both electrodes fails to reflect their true contributions in a hybrid cell.

Overall, an accurate representation of the electrode CVs during real cell operation can be obtained by dynamically adjusting the potential sweep rates (calculating the electrode potential scan rate over time). This approach provides essential information on any imbalance in the contribution of the electrodes during device operation.

Chapter V

Operando tracking of ion population changes in the EDL electrode of a lithium-ion capacitor during its charge/discharge

1. Summary of the publication

As discussed in the literature review (**Chapter I**), limited research has been conducted to understand the charge exchange processes at the positive electrode of MICs, which operates over a broader potential range than conventional EDLC electrodes. This broader range influences ion exchange dynamics, potentially affecting the performance and lifespan of MICs. Previous studies, while offering some hypotheses on ion adsorption/desorption processes, lack direct experimental validation. To address this gap, **Chapter V** of this dissertation summarizes the publication titled "*Operando tracking of ion population changes in the EDL electrode of a lithium-ion capacitor during its charge/discharge*," which aims to elucidate the in-pore/ex-pore exchange processes in an activated carbon (AC) electrode operating within an extended potential range, akin to the positive electrode of a lithium-ion capacitor (LIC) during its charge/discharge.

The first step involved studying the electrochemical properties of the 1 mol L⁻¹ LiPF₆/EC:DMC electrolyte in presence of a porous AC electrode. The stability domain of this electrolyte, determined by the window opening method [96], was found to range from 2.2 V to 4.5 V vs Li/Li⁺. Therefore, the experiments related to the analysis of the charging mechanism were further restricted to this potential range to eliminate the occurrence of any parasitic reactions that might disrupt in-pore/ex-pore exchange. Molecular dynamics (MD) simulations applied to the battery-type electrolyte, both in bulk and adsorbed within a model porous carbon, revealed that the solvation shell of Li⁺ consists of 3 EC molecules, 2 DMC molecules, and 1 PF₆⁻ anion in the bulk electrolyte, whereas 1 EC molecule is lost from this shell inside the porosity of the model carbon. Notably, the PF₆⁻ anions are not accompanied by any solvent molecule, either in the bulk solution or inside the porosity of the model carbon.

Operando electrochemical dilatometry (ECD), *in-situ* potentiostatic electrochemical impedance spectroscopy (PEIS), and *operando* Raman spectroscopy were realized on an AC electrode in the 1 mol L⁻¹ LiPF₆/EC:DMC electrolyte within the potential range from 2.2 V to 4.5 V vs Li/Li⁺. General changes observed in the literature on AC electrodes in organic electrolytes were identified together with new features:

- i) During the initial anodic sweep above the point of zero charge (PZC = 2.9 V vs. Li/Li⁺), ionic exchange followed by anion adsorption was observed, evidenced by an increase in electrode height and capacitive current. The significant decrease in ionic resistance, observed by PEIS during this phase, indicates more rapid diffusion

of PF_6^- anions which are smaller than the solvated Li^+ cations previously occupying the pores before polarization

- ii) The subsequent cathodic polarization down to the point of minimum height (*PMH*, ca. 3.1 V vs. Li/Li^+) resulted in anion desorption, with a small amount of trapped anions being released near the *PMH*. As this trapping, revealed by a peak in the cyclic voltammograms (CVs), occurred when the AC electrode was polarized above 3.8 V vs. Li/Li^+ during the anodic scan, it supports anions trapping in less accessible pores at anodic potentials higher than 3.8 V vs. Li/Li^+ .
- iii) Continuing the cathodic polarization below the *PMH* resulted in perm-selective adsorption of partially solvated Li^+ cations. This observation is supported by the much smaller capacitive current observed in this potential region compared to that recorded above the *PZC*, indicating limited access of the partially solvated Li^+ cations to the electrode porosity.
- iv) During the subsequent anodic scan, Li^+ ions are desorbed up to the *PMH*. Above the *PMH*, the same ionic exchange followed by anion adsorption as in step (i) occurred. However, a peak at approximately 3.8 V vs. Li/Li^+ was observed in the CVs, attributed to desorption of lithium cations, which were trapped in the poorly accessible pores of the AC electrode during the cathodic scan down to 2.2 V vs. Li/Li^+ .

Raman spectroscopy on the AC electrode during cycling confirmed these findings by identifying structural defects induced during the liberation of trapped Li^+ cations. This was evidenced by the increasing I_{D1}/I_{G1} ratio in this domain. The high polarization required to extract the trapped lithium ions from the AC porosity suggests that, during cycling of a LIC, the repeated desorption of Li^+ cations from narrow pores leads to a progressive degradation of the electrode material, thereby shortening the lifespan of the device.

In conclusion, this study highlights the complex interplay between ionic exchange, anion adsorption/desorption, and cation trapping, which are critical factors affecting the performance and lifespan of LICs. The findings suggest that optimizing the porous texture of AC materials to reduce ion trapping should be a key focus for improving LIC performance in further research.

General conclusion

This dissertation addresses several important challenges in advancing the performance of symmetric and hybrid electrochemical capacitors, hence, offers significant insights into the development of more efficient energy storage systems (ESSs). Key contributions include the identification and optimization of Water-in-Salt (WIS) electrolytes for Electrical Double Layer Capacitors (EDLCs), the innovative use of sacrificial materials for pre-metalation in Metal-Ion Capacitors (MICs), and an improved understanding of ion dynamics within electrodes during operation. Through these studies, the research highlights the role of electrolyte composition, electrode textural and structural properties, and ion population behavior in determining the overall performance and lifespan of electrochemical capacitors (ECs).

The assessment of the NaClO₄-water eutectic solution as electrolyte for EDLCs demonstrated its potential for high energy output in sub-ambient conditions. The work discloses that the electrolyte's viscosity increase at lower temperatures (from 2.48 mPa·s at RT to 24.8 mPa·s at -30°C) does not significantly affect its ionic conductivity, which allows EDLCs using the NaClO₄-water eutectic electrolyte to outperform traditional organic electrolytes at sub-ambient temperatures, particularly in terms of energy output under high-power conditions. It also reveals that the NaClO₄-water eutectic electrolyte maintains high ionic conductivity (23.7 mS cm⁻¹ at -30°C) due to weak molecular interactions and channel-like domains formed by hydrogen-bonded water molecules, resulting in efficient ion transport even at low temperatures. Furthermore, the quasi-neutral pH of the electrolyte, combined with the reduced free water content in the Stern layer, leads to an extended electrochemical stability window (*ESW*) from 1.8 V at RT to 2.1 V at -35°C which is critical for enhancing energy density in extreme conditions.

In the area of sodium-ion capacitors (NICs), it has been revealed that the pre-metalation of carbon-based electrodes is successfully facilitated by utilizing sodium azide as sacrificial material. NaN₃ demonstrates a complete and irreversible oxidation at 3.5 V vs Na/Na⁺, below the oxidative limit of current electrolytes on activated carbon (4.1 V vs Na/Na⁺). Furthermore, sodium azide oxidation does not compromise the porous texture of the activated carbon (AC) electrode, as demonstrated by nitrogen adsorption analysis. Next, the optimized blend of hard carbons (70 wt.% HC-J and 30 wt.% HCG) in the negative electrode reduces the ohmic drop (by 6 mV) and enhances the reversible capacity (270 mAh g⁻¹), ensuring better charge distribution and energy output. This highlights the dependence of performance on particle packing and material composition. What is more, the mass ratio of NaN₃ to hard carbon (0.78)

ensures efficient sodium transfer for pre-sodiation, achieving high cycle stability (90% capacitance retention after 15,000 cycles) and energy efficiency (95%).

By applying a potentiodynamic analysis methodology, precise evaluation of electrode behavior during charge/discharge cycles is provided. Indeed, the dynamically adjusted potential sweep rates for each electrode in hybrid capacitors better reflect real operating conditions compared to fixed potential sweep rates. For example, the positive electrode's (AC) scan rate increases gradually, while the negative electrode (Li_xC_6) scan rate decreases, revealing the need for allowing the charge/discharge rate adjustment individually for each electrode. Moreover, as confirmed, the capacitive positive electrode exhibits a rapid current response (withing few seconds), while the battery-type negative electrode responds more slowly (~200 s) due to lithium-ion intercalation, demonstrating the inherent differences in the occurring charge storage mechanisms. Moreover, changing the mass ratio of graphite (negative electrode) to AC (positive electrode) affects the charge transfer rate; a higher mass ratio (2:1) leads to faster stabilization of the negative electrode (150 s vs. 600 s for 0.5:1), illustrating how electrode composition impacts the current passing the electrodes in hybrid capacitors.

The combination of *operando* electrochemical dilatometry (ECD), *in situ* potentiostatic electrochemical impedance spectroscopy (PEIS), and *operando* Raman spectroscopy on AC electrodes in a 1 mol L^{-1} $\text{LiPF}_6/\text{EC}:\text{DMC}$ electrolyte provided valuable insights into ion dynamics:

- i) During the initial anodic sweep above the point of zero charge ($PZC = 2.9 \text{ V vs. Li/Li}^+$), ionic exchange followed by PF_6^- anion adsorption increased electrode height and capacitive current; PEIS showed decreased ionic resistance, indicating faster PF_6^- diffusion compared to partially solvated Li^+ cations.
- ii) The subsequent cathodic polarization down to the point of minimum height (PMH , ca. $3.1 \text{ V vs. Li/Li}^+$), anion desorption occurred, with trapped anions released near PMH . A peak in CVs above 3.8 V vs Li/Li^+ suggested anions trapped in less accessible pores.
- iii) Continuing the cathodic polarization below the PMH resulted in perm-selective adsorption of partially solvated Li^+ which was supported by smaller capacitive current in this potential region compared to that recorded above the PMH , showing limited Li^+ access to pores.
- iv) During the subsequent anodic scan, Li^+ desorption occurred up to PMH , followed by anion adsorption. A peak observed at approximately $3.8 \text{ V vs. Li/Li}^+$ in the CVs was attributed to desorption of lithium cations, which were trapped in the poorly accessible pores of the AC electrode during the cathodic scan down to $2.2 \text{ V vs. Li/Li}^+$.

Apart from these observations, Raman spectroscopy confirmed structural defects caused by trapped Li^+ cations, shown by the increasing I_{D1}/I_{G1} ratio. High polarization needed to extract Li^+ ions suggests that repeated cycling leads to degradation of the AC electrode and reduced LIC lifespan. In summary, the interplay between ionic exchange, anion adsorption/desorption, and Li^+ trapping critically impacts LIC performance and optimizing AC porosity to reduce ion trapping is key to improving LIC longevity and efficiency.

Overall, the outcomes of this dissertation underscore the necessity for continued research into several critical areas. Investigating the self-discharge rates and operational limits of EDLCs at elevated temperatures in NaClO_4 -water electrolytes is needed for further enhancing their applicability. Furthermore, understanding the impact of sacrificial material oxidation on ion dynamics in MICs should help optimize electrode design. Furthermore, a deeper exploration of ion desorption mechanisms by addressing ion trapping through carbon material pore size optimization could enhance the capacitive performance of MICs. By advancing these points, this research initiates the groundwork for the development of next-generation ECs.

References

- [1] A. Gonzalez, E. B. J. Goikolea and R. Mysyk, "Review on supercapacitors: Technologies and materials," *Renew. Sustain. Energy Rev.*, 58 (2016) 1189-1206
- [2] P. Ratajczak, K. Jurewicz, P. Skowron, Q. Abbas and P. Béguin, "Effect of accelerated ageing on the performance of high voltage carbon/carbon electrochemical capacitors in salt aqueous electrolyte," *Electrochim. Acta*, 130 (2014) 344-350
- [3] L. L. Zhang and X. S. Zhao, "Carbon-based materials as supercapacitor electrodes," *Chem. Soc. Rev.*, 38 (2009) 2520-2531
- [4] H. Helmholtz, "Ueber einige Gesetze der Vertheilung elektrischer Ströme in körperlichen Leitern mit Anwendung auf die thierisch-elektrischen Versuche," *Ann. Phys.*, vol. 165, pp. 211-233, 1853.
- [5] M. Endo, T. Takeda, Y. Kim, K. Koshiba and K. Ishii, "High Power Electric Double Layer Capacitor (EDLC's); from Operating Principle to Pore Size Control in Advanced Activated Carbons," *Carbon Sci.*, 1 (2001) 117-128
- [6] B. Conway, "Behavior of Dielectrics in Capacitors and Theories of Dielectric Polarization," in *Electrochemical Supercapacitors: Scientific fundamental and Technological Applications*, New York, Kluwer Academic/Plenum Publishers, (1999) 87-105.
- [7] M. Gouy, "Sur la constitution de la charge électrique à la surface d'un électrolyte," *J. Phys. Theor. Appl.*, 9 (1910) 457-468
- [8] D. Chapman, "A contribution to the theory of electrocapillarity," *London Edinburgh Philos. Mag. & J. Sci.*, 225 (1913) 475-481
- [9] H. Shao, Y. Wu, Z. Lin, P. Taberna and P. Simon, "Nanoporous carbon for electrochemical capacitive energy storage," *Chem. Soc. Rev.*, 49 (2020) 3005-3039
- [10] H. Stern, "Zur Theorie Der Elektrolytischen Doppelschicht," *Z. Elektrochem.*, 30 (1924) 508-516
- [11] P. Ratajczak, M. Suss, F. Kaasik and F. Béguin, "Carbon electrodes for capacitive technologies," *Energy Stor. Mater.*, 16 (2017) 126-145
- [12] F. Béguin, V. Presser, A. Balducci and E. Frąckowiak, "Carbons and Electrolytes for Advanced Supercapacitors," *Adv Mater*, 26 (2014) 2219-2251
- [13] A. Burke and M. Miller, "Testing of electrochemical capacitors: Capacitance, resistance, energy density, and power capability," *Electrochim. Acta*, 55 (2010) 7538-7548
- [14] A. Burke and J. Zhao, "Past, present and future of electrochemical capacitors: Technologies, performance and applications," *J. Energy Storage*, 35 (2021) 102310-102323
- [15] B. Babu, P. Simon and A. Balducci, "Fast Charging Materials for High Power Applications," *Adv. Energy Mater.*, 10 (2020) 2001128-2001161
- [16] E. Frąckowiak and F. Béguin, "Carbon materials for the electrochemical storage of energy in capacitors," *Carbon*, 39 (2001) 937-950
- [17] A. Pandolfo and A. Hollenkamp, "Carbon properties and their role in supercapacitors," *J. Power Sources*, 157 (2006) 11-27

- [18] M. Suss, T. Baumann, M. Worsley, K. Rose, T. Jaramillo, M. Stadermann and Santiago, "Impedance-based study of capacitive porous carbon electrodes with hierarchical and bimodal porosity," *J. Power Sources*, 241 (2013) 266-273
- [19] X. Liu, D. Lyu, C. Merlet, M. Leesmith, X. Hua, Z. Xu, C. Grey and A. Forse, "Structural disorder determines capacitance in nanoporous carbons," *Science*, 384 (2024) 321-325
- [20] J. Bitter, "Nanostructured carbons in catalysis a Janus material—industrial applicability and fundamental insights," *J. Mater. Chem.*, 20 (2010) 7312-7321
- [21] P. Anagbonu, M. Ghali and A. Allam, "Low-temperature green synthesis of few-layered graphene sheets from pomegranate peels for supercapacitor applications," *Sci. Rep.*, 13 (2023) 1-12
- [22] A. Tamayo, M. A. Rodriguez, F. Rubio and J. Rubio, "Cobalt-catalyzed tunable carbon microstructures from halogenated SiC preceramic precursors," *J Am Ceram Soc.*, 106 (2023) 53-67
- [23] M. Matsumoto, H. Kinoshita, J. Choi and T. Kato, "Formation of large area closely packed carbon onions film by plasma-based ion implantation," *Sci. Rep.*, 10 (2020) 1-9
- [24] R. Vander Wal, A. Tomasek, K. Street, D. Hull and W. Thompson, "Carbon Nanostructure Examined by Lattice Fringe Analysis of High-Resolution Transmission Electron Microscopy Images," *Appl. Spectrosc.*, 58 (2004) 230-237
- [25] P. Simon and A. Burke, "Nanostructured Carbons: Double-Layer Capacitance and More," *Electrochem. Soc. Interface*, 17 (2008) 1-6
- [26] F. Caturla, M. Molina-Sabio and F. Rodriguez-Reinoso, "Preparation of activated carbon by chemical activation with ZnCl₂," *Carbon*, 29 (1991) 999-1007
- [27] D. Lozano-Castelló, M. Lillo-Cardenas, D. Cazorla-Amoros and A. Linares-Solano, "Preparation of activated carbons from Spanish anthracite: I. Activation by KOH," *Carbon*, 39 (2001) 741-749
- [28] L. Wei, M. Sevilla, A. Fuertes, R. Mokaya and G. Yushin, "Hydrothermal Carbonization of Abundant Renewable Natural Organic Chemicals for High-Performance Supercapacitor Electrodes," *Adv. Energy Mater.*, 1 (2001) 356-361
- [29] Y. Gogotsi, A. Nikitin, H. Ye, W. Zhou, J. Fischer, B. Yi, H. Foley and M. Barsoum, "Nanoporous carbide-derived carbon with tunable pore size," *Nature Mater.*, 2 (2003) 591-594
- [30] D. Stout, N. Durmus and T. Webster, "Synthesis of carbon based nanomaterials for tissue engineering applications," in *Nanomaterials in Tissue Engineering*, Nashville, Woodhead Publishing Series in Biomaterials, (2013) 119-157.
- [31] G. Yushin, A. Nikitin and Y. Gogotsi, "Carbide derived carbon," in *Nanomaterials handbook*, Boca Raton, CRC Press, (2006) 237-280.
- [32] H. Nishihara and T. Kyotani, "Templated Nanocarbons for Energy Storage," *Adv. Mater.*, 24 (2012) 4473-4498
- [33] Y. Zhai, Y. Dou, D. Zhao, P. Fulvio, R. Mayes and S. Dai, "Carbon Materials for Chemical Capacitive Energy Storage," *Adv. Mater.*, 23 (2011) 4828-4850

- [34] H. Nishihara, H. Itoi, T. Kogure, P.-X. Hou, H. Touhara, F. Okino and T. Kyotani, "Investigation of the Ion Storage/Transfer Behavior in an Electrical Double-Layer Capacitor by Using Ordered Microporous Carbons as Model Materials," *Chem. – Eur. J.*, 15 (2009) 5355-5363
- [35] M. Zeiger, N. Jäckel, V. Mochalin and V. Presser, "Review: carbon onions for electrochemical energy storage," *J. Mater. Chem. A*, 4 (2016) 3172-3196
- [36] V. Kuznetsov, A. Chuvilin, Y. Butenko, I. Mal'kov and V. Titov, "Onion-like carbon from ultra-disperse diamond," *Chem. Phys. Lett.*, 222 (1994) 343-348
- [37] M. Zeiger, N. Jäckel, M. Aslan, D. Weingarth and V. Presser, "Understanding structure and porosity of nanodiamond-derived carbon onions," *Carbon*, 84 (2015) 584-598
- [38] C. Portet, G. Yushin and Y. Gogotsi, "Electrochemical performance of carbon onions, nanodiamonds, carbon black and multiwalled nanotubes in electrical double layer capacitors," *Carbon*, 45 (2007) 2511-2518
- [39] R. Baughman, A. Zakhidov and W. De Heer, "Carbon Nanotubes--the Route Toward Applications," *Science*, 297 (2002) 787-792
- [40] Z. Yang, J. Tian, Z. Yin, C. Cui, W. Qian and F. Wei, "Carbon nanotube- and graphene-based nanomaterials and applications in high-voltage supercapacitor: A review," *Carbon*, 141 (2019) 467-480
- [41] A. Peigney, C. Laurent, E. Flahaut, R. Bacsa and A. Rousset, "Specific surface area of carbon nanotubes and bundles of carbon nanotubes," *Carbon*, 39 (2001) 507-514
- [42] E. Frackowiak, K. Méténier, R. Pellenq, S. Bonnamy and F. Béguin, "Capacitance properties of carbon nanotubes," *AIP Conf. Proc.*, 486 (1999) 429-432
- [43] P. Simon and Y. Gogotsi, "Capacitive Energy Storage in Nanostructured Carbon–Electrolyte Systems," *Acc. Chem. Res.*, 46 (2013) 1094-1103
- [44] E. Raymundo-Piñero, K. Kierzek, J. Machnikowski and F. Béguin, "Relationship between the nanoporous texture of activated carbons and their capacitance properties in different electrolytes," *Carbon*, 44 (2006) 2489-2507
- [45] K. Sing, "Reporting physisorption data for gas/solid systems with special reference to the determination of surface area and porosity," *Pure & Appl. Chem.*, 57 (1985) 603-619
- [46] H. Yamada, H. Nakamura, I. Nakahara and T. Kudo, "Electrochemical Study of High Electrochemical Double Layer Capacitance of Ordered Porous Carbons with Both Meso/Macropores and Micropores," *J. Phys. Chem. C*, 111 (2007) 227-233
- [47] M. Kwiatkowski, V. Fierro and A. Celzard, "Confrontation of various adsorption models for assessing the porous structure of activated carbons," *Adsorption*, 25 (2019) 1673-1682
- [48] S. Brunauer, P. Emmett and E. Teller, "Adsorption of gases in multimolecular layers," *J. Am. Chem. Soc.*, 60 (1938) 309-319
- [49] J. Rouquerol, F. Rouquerol and K. Sing, "Assessment of Surface Area," in *Adsorption by Powders and Porous Solids: Principles, Methodology and Applications*, vol. 97, Massachusetts, Academic Press, (1999) 165-189
- [50] T. Centeno and F. Stoeckli, "The assessment of surface areas in porous carbons by two model-independent techniques, the DR equation and DFT," *Carbon*, 48 (2010) 2478-2486

- [51] F. Stoeckli and T. Centeno, "Optimization of the characterization of porous carbons for supercapacitors," *J. Mater. Chem. A*, 1 (2013) 6865-6873
- [52] M. Dubinin, "The Potential Theory of Adsorption of Gases and Vapors for Adsorbents with Energetically Nonuniform Surfaces," *Chem. Rev.*, 60 (1960) 235-241
- [53] J. Olivier, W. Conklin and M. Von Szombathely, "Determination of pore size distribution from density functional theory: a comparison of nitrogen and argon results," *Stud. Surf. Sci. Catal.*, 84 (1994) 81-89
- [54] N. Setoyama, M. Ruike, T. Kasu, T. Susuki and K. Kaneko, "Surface Characterization of Microporous Solids with He Adsorption and Small Angle X-ray Scattering," *Langmuir*, 9 (1993) 2612-2617
- [55] P. C. P. Mourão and M. Ribiero-Carrott, "Application of different equations to adsorption isotherms of phenolic compounds on activated carbons prepared from cork," *Carbon*, 44 (2006) 2422-2429
- [56] C. Largeot, C. Portet, J. Chmiola, P. Taberna, Y. Gogotsi and P. Simon, "Relation between the Ion Size and Pore Size for an Electric Double-Layer Capacitor," *J. Am. Chem. Soc.*, 130 (2008) 2730-2731
- [57] G. Feng and P. Cummings, "Supercapacitor Capacitance Exhibits Oscillatory Behavior as a Function of Nanopore Size," *J. Phys. Chem. Lett.*, 2 (2011) 2859-2864
- [58] D. Jiang, Z. Jin and J. Wu, "Oscillation of Capacitance inside Nanopores," *Nano Lett.*, 11 (2011) 5373-5377
- [59] B. Lobato, L. Suarez, L. Guardia and T. Centeno, "Capacitance and surface of carbons in supercapacitors," *Carbon*, 122 (2017) 434-445
- [60] A. García-Gómez, G. Moreno-Fernandez, B. Lobato and T. Centeno, "Constant capacitance in nanopores of carbon monoliths," *Phys.Chem.Chem.Phys.*, 17 (2015) 15687-15690
- [61] A. Centeno, O. Sereda and F. Stoeckli, "Capacitance in carbon pores of 0.7 to 15 nm: a regular pattern," *Phys. Chem. Chem. Phys.*, 13 (2011) 12403-12406
- [62] J. Chmiola, G. Yushin, Y. Gogotsi, C. Portet, P. Simon and P. Taberna, "Anomalous Increase in Carbon Capacitance at Pore Sizes Less Than 1 Nanometer," *Science*, 313 (2006) 1760-1763
- [63] R. Harris, T. Thompson, P. Norman and C. Pottage, "Phosphorus-31 NMR studies of adsorption onto activated carbon," *Carbon*, 37 (1999) 1425-1430
- [64] A. Forse, C. Merlet, P. Allan, E. Humphreys, J. Griffin, M. Aslan, M. Zeiger, V. Presser, Y. Gogotsi and C. Grey, "New Insights into the Structure of Nanoporous Carbons from NMR, Raman, and Pair Distribution Function Analysis," *Chem. Mater.*, 27 (2015) 6848-6857
- [65] C. Zhong, Y. Deng, W. Hu, J. Qiao, L. Zhang and J. Zhang, "A review of electrolyte materials and compositions for electrochemical supercapacitors," *Chem. Soc. Rev.*, 44 (2015) 7484-7539
- [66] J. Zhao and A. Burke, "Electrochemical Capacitors: Performance Metrics and Evaluation by Testing and Analysis," *J. Energy Storage*, 35 (2021) 102310-102338
- [67] F. Béguin, E. Raymundo-Piñero and E. Frackowiak, "Electrical Double Layer Capacitors and Pseudocapacitors," in *Carbons for electrochemical energy storage and conversion systems*, Boca Raton, CRC Press, (2010) 329-376

- [68] P. Azais, "Manufacturing Industrial Supercapacitors," in *Supercapacitors Materials, Systems and Applications*, Edited by Béguin François and Frackowiak Elzbieta, Weinheim, Wiley-VCH Verlag GmbH & Co, (2013) 307-363
- [69] E. Calvo, F. Lufrano, P. Staiti, A. Brigandi, A. Arenillas and J. Menéndez, "Optimizing the electrochemical performance of aqueous symmetric supercapacitors based on an activated carbon xerogel," *J. Power Sources*, 241 (2013) 776-782
- [70] V. Ruiz, R. Santamaria, M. Granda and C. Blanco, "Long-term cycling of carbon-based supercapacitors in aqueous media," *Electrochim. Acta*, 54 (2009) 4481-4486
- [71] L. Demarconnay, E. Raymundo-Piñero and F. Béguin, "A symmetric carbon/carbon supercapacitor operating at 1.6 V by using a neutral aqueous solution," *Electrochem. Commun.*, 12 (2010) 1275-1278
- [72] X. Sun, X. Zhang, H. Zhang, D. Zhang and Y. Ma, "A comparative study of activated carbon-based symmetric supercapacitors in Li₂SO₄ and KOH aqueous electrolytes," *J. Solid State Electrochem*, 16 (2012) 2597-2603
- [73] Skeleton Technologies, "Skeleton," 2024. [Online]. Available: <https://www.skeletontech.com/en/skelcap-supercapacitors>. [Accessed 19 January 2024].
- [74] M. Bichat, P. Raymundo-Piñero and F. Béguin, "High voltage supercapacitor built with seaweed carbons in neutral aqueous electrolyte," *Carbon*, 48 (2010) 4351-4361
- [75] Q. Gao, L. Demarconnay, E. Raymundo-Piñero and F. Béguin, "Exploring the large voltage range of carbon/carbon supercapacitors in aqueous lithium sulfate electrolyte," *Energy Environ. Sci.*, 5 (2012) 9611-9617
- [76] L. Suo, O. Boridin, T. Gao, M. Olguin, J. Ho, X. L. C. Fan, C. Wang and K. Xu, "'Water-in-salt' electrolyte enables high-voltage aqueous lithium-ion chemistries," *Science*, 350 (2015) 938-943
- [77] J. Park, J. Lee and W. Kim, "Water-in-Salt Electrolyte Enables Ultrafast Supercapacitors for AC Line Filtering," *ACS Energy Lett.*, 6 (2021) 769-777
- [78] E. Pamete and F. Béguin, "Effect of salt concentration in aqueous LiTFSI electrolytes on the performance of carbon-based electrochemical capacitors," *Electrochim*, 389 (2021) 138687-138696
- [79] S. Gharouel and F. Béguin, "Revisiting the performance of electrical double-layer capacitors implementing a sodium perchlorate water-in-salt electrolyte," *Electrochim. Acta*, 450 (2023) 142212-142221
- [80] D. Reber, R. Kühnel and C. Battaglia, "High-voltage aqueous supercapacitors based on NaTFSI," *Sustain. Energy Fuels*, 1 (2017) 2155-2161
- [81] X. Liao, L. Zhong, H. Zeng, Y. Xiao, B. Cheng and S. Lei, "A dual-acetate synchronous catalysis-activation strategy towards regulable porous graphitic carbon for high-energy supercapacitor with acetate water-in-salt electrolyte," *Carbon*, 213 (2023) 118305-118318
- [82] D. Da Silva, M. Pinzon, A. Messias, E. Fileti, A. Pascon, D. Franco, L. Da Silva and H. Zanin, "Effect of conductivity, viscosity, and density of water-in-salt electrolytes on the electrochemical behavior of supercapacitors: molecular dynamics simulations and in situ characterization studies," *Mater. Adv.*, 3 (2022) 611-623

- [83] R. Sakamoto, M. Yamashita, K. Nakamoto, Y. Zhou, N. Yoshimoto, K. Fujii, T. Yamaguchi, A. Kitajou and S. Okada, "Correction: Local structure of a highly concentrated NaClO₄ aqueous solution-type electrolyte for sodium ion batteries," *Phys. Chem. Chem. Phys.*, 22 (2020) 26452-26458
- [84] H.-I. Kim, E. Shin, S.-H. Kim, K. M. Lee, J. Park, S. J. Kang, S. So, K. C. Roh, S. K. Kwak and S.-Y. Lee, "Aqueous eutectic lithium-ion electrolytes for wide-temperature operation," *Energy Stor. Mater.*, 36 (2021) 222-228
- [85] A. Serva, N. Dubouis, A. Grimaud and M. Salanne, "Confining Water in Ionic and Organic Solvents to Tune Its Adsorption and Reactivity at Electrified Interfaces," *Acc. Chem. Res.*, 54 (2021) 1034-1042
- [86] Y. Yamada, K. Usui, K. Sodeyama, S. Ko, Y. Tateyama and A. Yamada, "Hydrate-melt electrolytes for high-energy-density aqueous batteries," *Nat. Energy*, 1 (2016) 1-9
- [87] D. Reber, R. Figi, R. Kühnel and C. Battaglia, "Stability of aqueous electrolytes based on LiFSI and NaFSI," *Electrochim Acta*, 321 (2019) 134644-134649
- [88] A. Triolo, V. Di Lisio, F. Lo Celso, G. Appetecchi, B. Fazio, P. Chater, A. Martinelli, F. Sciubba and O. Russina, "Liquid Structure of a Water-in-Salt Electrolyte with a Remarkably Asymmetric Anion," *J. Phys. Chem. B*, 125 (2021) 12500-12517
- [89] M. McEldrew, Z. Goodwin, S. Bi, A. Kornyshev and M. Bazant, "Ion Clusters and Networks in Water-in-Salt Electrolytes," *J. Electrochem. Soc.*, 168 (2021) 50514-50527
- [90] K. Gering, "Prediction of electrolyte viscosity for aqueous and non-aqueous systems: Results from a molecular model based on ion solvation and a chemical physics framework," *Electrochim. Acta*, 51 (2006) 3125-3138
- [91] H. Al-Salih, E. Baranova and Y. Abu-Lebdeh, "Unraveling the phase diagram-ion transport relationship in aqueous electrolyte solutions and correlating conductivity with concentration and temperature by semi-empirical modeling," *Commun. Chem.*, 195 (2023) 1-13
- [92] C. Yim, J. Tam, H. Soboleski and H. Abu-Lebdeh, "On the Correlation between Free Volume, Phase Diagram and Ionic Conductivity of Aqueous and Non-Aqueous Lithium Battery Electrolyte Solutions over a Wide Concentration Range," *J. Electrochem. Soc.*, 164 (2017) A1002-A1011
- [93] J. Yue, J. Zhang, Y. Tong, M. Chen, L. Liu, L. Jiang, T. Lv, Y. Hu, H. Li, X. Huang, L. Gu, G. Feng, K. Xu, L. Suo and L. Chen, "Aqueous interphase formed by CO₂ brings electrolytes back to salt-in-water regime," *Nat. Chem.*, vol. 13, pp. 1061-1069, 2021.
- [94] J. Han, A. Mariani, H. Zhang, M. Zarrabeitia, X. Gao, D. Carvalho, A. Varzi and S. Passerini, "Gelified acetate-based water-in-salt electrolyte stabilizing hexacyanoferrate cathode for aqueous potassium-ion batteries," *Energy Storage Mater.*, 30 (2020) 196-205
- [95] H. Chen, Z. Zhang, W. Wei, G. Chen, X. Yang, C. Wang and F. Du, "Use of a water-in-salt electrolyte to avoid organic material dissolution and enhance the kinetics of aqueous potassium ion batteries," *Sustainable Energy Fuels*, 4 (2020) 128-131
- [96] D. Weingarh, H. Noh, A. Foelske-Schmitz, A. Wokaun and R. Kötz, "A reliable determination method of stability limits for electrochemical double layer capacitors," *Electrochim. Acta*, 103 (2013) 119-124

- [97] D. Xiao, Q. Wu, X. Liu, Q. Dou, L. Liu, B. Yang and H. Yu, "Aqueous Symmetric Supercapacitors with Carbon Nanorod Electrodes and Water-in-Salt Electrolyte," *ChemElectroChem*, 6 (2019) 439-446
- [98] X. Bu, L. Su, Q. Dou, S. Lei and X. Yan, "A low-cost "water-in-salt" electrolyte for a 2.3 V high-rate carbon-based supercapacitor," *J. Mater. Chem. A*, 7 (2019) 7541-7547
- [99] E. Pamet , B. Gorska and F. B guin, "Electrical Double-Layer Capacitors Based on a Ternary Ionic Liquid Electrolyte Operating at Low Temperature with Realistic Gravimetric and Volumetric Energy Outputs," *ChemSusChem*, 14 (2021) 1196-1208
- [100] J. Vatamanu and O. Borodin, "Ramifications of Water-in-Salt Interfacial Structure at Charged Electrodes for Electrolyte Electrochemical Stability," *J. Phys. Chem. Lett.*, 8 (2017) 4362-4367
- [101] M. McEldrew, Z. Goodwin, A. Kornyshev and M. Bazant, "Theory of the Double Layer in Water-in-Salt Electrolytes," *J. Phys. Chem. Lett.*, 9 (2018) 5840-5846
- [102] L. K ps, F. Kreth, A. Bothe and A. Balducci, "High voltage electrochemical capacitors operating at elevated temperature based on 1,1-dimethylpyrrolidinium tetrafluoroborate," *Energy Stor. Mater.*, 44 (2022) 66-72
- [103] P. Azais, L. Duclaux, P. Florian, D. Massiot, M. Lillo-Rodenas, J. Linares-Solano, C. Jehoulet and F. B guin, "Causes of supercapacitors ageing in organic electrolyte," *J. Power Sources*, 171 (2007) 1046-1053
- [104] M. Ue, K. Ido and S. Mori, "Electrochemical properties of organic liquid electrolytes based on quaternary onium salts for electrical double-layer capacitors," *J. Electrochem. Soc.*, 141 (1994) 2989-2996
- [105] J. Garche, C. Dyer, P. Moseley, Z. Ogumi, D. Rand and B. Scrosati, *Encyclopedia of Electrochemical Power Sources*, Amsterdam: Elsevier, 2009.
- [106] P. Ruch, D. Cericola, A. Foelske, R. K tz and A. Wokaun, "A comparison of the aging of electrochemical double layer capacitors with acetonitrile and propylene carbonate-based electrolytes at elevated voltages," *Electrochim. Acta*, 55 (2010) 2352-2357
- [107] K. Naoi, "Nanohybrid Capacitor: The Next Generation Electrochemical Capacitors," *Fuel cells*, 10 (2010) 825-833
- [108] H. Duncan, N. Salem and Y. Abu-Lebdeh, "Electrolyte Formulations Based on Dinitrile Solvents for High Voltage Li-Ion Batteries," *J. Electrochem. Soc.*, 160 (2013) A838-A848
- [109] M. Nagahama and N. Hasegawa, "High Voltage Performances of Li₂NiPO₄F Cathode with Dinitrile-Based Electrolytes," *J. Electrochem. Soc.*, 157 (2010) A748-A752
- [110] A. Brandt and A. Balducci, "The Influence of Pore Structure and Surface Groups on the Performance of High Voltage Electrochemical Double Layer Capacitors Containing Adiponitrile-Based Electrolyte," *J. Electrochem. Soc.*, 159 (2012) A2053-A2059
- [111] G. Wang, L. Zhang and J. Zhang, "A review of electrode materials for electrochemical supercapacitors," *Chem. Soc. Rev.*, 41 (2021) 797-828
- [112] A. Balducci, R. Dugas, P. Taberna, P. Simon, D. Plee and P. S. Mastragostino, "High temperature carbon-carbon supercapacitor using ionic liquid as electrolyte," *J. Power Sources*, 165 (2007) 922-927

- [113] H. Nguyen, J. Kim and K. Lee, "High-voltage and intrinsically safe supercapacitors based on a trimethyl phosphate electrolyte," *J. Mater. Chem. A*, 9 (2021) 20725-20736
- [114] J. M. Griffin, A. C. Forse, W.-Y. Tsai, P.-L. Taberna, P. Simon and C. P. Grey, "In situ NMR and electrochemical quartz crystal microbalance techniques reveal the structure of the electrical double layer in supercapacitors," *Nat. Mater*, 14 (2015) 812-819
- [115] M. Deschamps, E. Gilbert, P. Azais, E. Raymundo-Piñero, M. Ammar, P. Simon, D. Massiot and F. Béguin, "Exploring electrolyte organization in supercapacitor electrodes with solid-state NMR," *Nature Mater*, 12 (2013) 351-358
- [116] J. Griffin, A. Forse, H. Wang, N. Trease, P.-L. Taberna, P. Simon and C. Grey, "Ion counting in supercapacitor electrodes using NMR spectroscopy," *Faraday Discuss*, 176 (2014) 49-68
- [117] A. Forse, J. Griffin, C. Merlet, P. Bayley, H. Wang, P. Simon and C. Grey, "NMR Study of Ion Dynamics and Charge Storage in Ionic Liquid Supercapacitors," *J. Am. Chem. Soc.*, 137 (2015) 7231-7242
- [118] W.-Y. Tsai, P.-L. Taberna and P. Simon, "Electrochemical Quartz Crystal Microbalance (EQCM) Study of Ion Dynamics in Nanoporous Carbons," *J. Am. Chem. Soc.*, 136 (2014) 8722-8728
- [119] M. D. Levi, N. Levy, S. Sigalov, G. Salitra, D. Aurbach and J. Maier, "Electrochemical Quartz Crystal Microbalance (EQCM) Studies of Ions and Solvents Insertion into Highly Porous Activated Carbons," *J. Am. Chem. Soc.*, 132 (2010) 13220-13222
- [120] Z. Bo, J. Yang, H. Qi, K. Cen and Z. Han, "Revealing ion transport in supercapacitors with Sub-2 nm two-dimensional graphene channels," *Energy Storage Mater.*, 31 (2020) 64-71
- [121] M. Levi, G. Salitra, N. Levy, D. Aurbach and J. Maier, "Application of a quartz-crystal microbalance to measure ionic fluxes in microporous carbons for energy storage," *Nature Mater.*, 8 (2009) 872-875
- [122] Y. Wang, C. Malveau and D. Rochefort, "Solid-state NMR and electrochemical dilatometry study of charge storage in supercapacitor with redox ionic liquid electrolyte," *Energy Storage Mater.*, 20 (2019) 80-88
- [123] P. Bujewska, P. Galek and K. Fic, "Monitoring the ion population at a carbon electrode/aqueous electrolyte interface at various pHs using electrochemical dilatometry," *Energy Storage Mater.*, 63 (2023) 103003-103010
- [124] N. Jäckel, S. Emge, B. Krüner, B. Roling and V. Presser, "Quantitative Information about Electrosorption of Ionic Liquids in Carbon Nanopores from Electrochemical Dilatometry and Quartz Crystal Microbalance Measurements," *J. Phys. Chem. C*, 121 (2017) 19120-19128
- [125] H. Yin, H. Shao, B. Daffos, P.-L. Taberna and P. Simon, "The effects of local graphitization on the charging mechanisms of microporous carbon supercapacitor electrodes," *Electrochem. commun.*, 137 (2022) 107258-107262
- [126] L. Caizan-Juanareana, M. Arnaiz, E. Gucciardi, L. Oca, E. Bekaert, I. Gandiaga and J. Ajuria, "Unraveling the Technology behind the Frontrunner LIC ULTIMO to Serve as a Guideline for Optimum Lithium-Ion Capacitor Design, Assembly, and Characterization," *Adv. Energy Mater.*, 11 (2021) 2100912-2100925

- [127] T. Aida, K. Yamada and M. Morita, "An Advanced Hybrid Electrochemical Capacitor That Uses a Wide Potential Range at the Positive Electrode," *Electrochem. Solid-State Lett.*, 9 (2006) A534-A536
- [128] D. Cericola and R. Kötz, "Hybridization of rechargeable batteries and electrochemical capacitors: Principles and limits," *Electrochim. Acta.*, 72 (2012) 1-17
- [129] A. Chojnacka and F. Béguin, "Recent progress in the realization of metal-ion capacitors with alloying anodic hosts: A mini review," *Electrochem. commun.*, 139 (2022) 107305-107310
- [130] S. Zhang, "Dual-Carbon Lithium-Ion Capacitors: Principle, Materials, and Technologies," *Batter. Supercaps*, 3 (2020) 1137-1146
- [131] H. Yoo, E. Markevich, G. Salitra, D. Sharon and D. Aurbach, "On the challenge of developing advanced technologies for electrochemical energy storage and conversion," *Mater. Today*, 17 (2014) 110-121
- [132] J. Zheng, "Energy Density Theory of Lithium-Ion Capacitors," *J. Electrochem. Soc.*, 168 (2021) 80503-80510
- [133] D. Dewar and A. Glushenkov, "Optimisation of sodium-based energy storage cells using pre-sodiation: a perspective on the emerging field," *Energy Environ. Sci.*, 14 (2021) 1380-1401
- [134] M. Endo, T. Maeda, T. Takeda, Y. J. Kim, K. H. H. Koshiba and M. S. Dresselhaus, "Capacitance and Pore-Size Distribution in Aqueous and Nonaqueous Electrolytes Using Various Activated Carbon Electrodes," *J. Electrochem. Soc.*, 148 (2001) A910A-914
- [135] J.-C. Soetens, C. Millot and B. Maigret, "Molecular Dynamics Simulation of Li+BF4- in Ethylene Carbonate, Propylene Carbonate, and Dimethyl Carbonate Solvents," *J. Phys. Chem. A*, 102 (1998) 1055-1061
- [136] X. Wang, L. Liu and Z. Niu, "Carbon-based materials for lithium-ion capacitors," *Mater. Chem. Front.*, 3 (2019) 1265-1279
- [137] K. Subramayan, M. Divya and V. Aravindan, "Dual-carbon Na-ion capacitors: progress and future prospects," *J. Mater. Chem. A*, 9 (2021) 9431-9450
- [138] P. Cai, K. Wang, T. Wang, H. Li, M. Zhou, W. Wang and K. Jiang, "Comprehensive Insights into Potassium-Ion Capacitors: Mechanisms, Materials, Devices and Future Perspectives," *Adv. Energy Mater.*, 14 (2024) 2401183-2401262
- [139] R. Yazami and P. Touzain, "A reversible graphite-lithium negative electrode for electrochemical generators," *J. Power Sources*, 9 (1983) 365-371
- [140] D. Aurbach, B. Markovsky, I. Weissman, E. Levi and Y. Ein-Eli, "On the correlation between surface chemistry and performance of graphite negative electrodes for Li ion batteries," *Electrochim. Acta*, 45 (1999) 67-86
- [141] D. Guerard and A. Herold, "Intercalation of lithium into graphite and other carbons," *Carbon*, 13 (1975) 337-345
- [142] W. Rüdorff, "Graphite Intercalation Compounds," *Adv. Inorg. Chem. Radiochem.*, 1 (1959) 223-266

- [143] J. Asenbauer, T. Eisenmann, M. Kuenzel, A. Kazzazi, Z. Chen and D. Bresser, “The success story of graphite as a lithium-ion anode material – fundamentals, remaining challenges, and recent developments including silicon (oxide) composites,” *Sustainable Energy Fuels*, 4 (2020) 5387-5416
- [144] N. Daumas and A. Herold, “Relations between phase concept and reaction mechanics in graphite insertion compounds,” *C. R. Acad. Sci. Ser. C.*, 268 (1969) 373-375
- [145] C. Sole, N. Drewett and L. Hardwick, “In situ Raman study of lithium-ion intercalation into microcrystalline graphite,” *Faraday Discuss.*, 172 (2014) 223-237
- [146] H. Michael, F. Iacoviello, M. Heenan, A. Lelewellyn, J. Weaving, R. Jervis and D. S. P. Brett, “A Dilatometric Study of Graphite Electrodes during Cycling with X-ray Computed Tomography,” *J. Electrochem. Soc.*, 168 (2021) 10507-10513
- [147] S. Schweidler, L. De Biasi, A. Schiele, P. Hartmann, T. Brezesinski and J. Janek, “Volume changes of graphite anodes revisited: a combined operando X-ray diffraction and in situ pressure analysis study,” *J. Phys. Chem. C.*, 122 (2018) 8829-8835
- [148] P. Ge and M. Foulletier, “Electrochemical intercalation of sodium in graphite Pascal GE and Mireille Foulletier,” *Solid State Ion.*, 28 (1988) 1172-1175
- [149] M. Doeff, Y. Ma, S. Visco and L. De Jonghe, “Electrochemical Insertion of Sodium into Carbon,” *J. Electrochem. Soc.*, 140 (1993) L196-L197
- [150] H. Moriwake, A. Kuwabara, C. Fisher and Y. Ikuhara, “Why is sodium-intercalated graphite unstable?,” *RSC Adv.*, 7 (2017) 36550-36554
- [151] Z. Jian, W. Luo and X. Ji, “Carbon electrodes for K-Ion batteries,” *J. Am. Chem. Soc.*, 137 (2015) 11566-11569
- [152] S. Saju, S. Chattopadhyay, J. Xu, S. Alhashim, A. Pramnik and P. Ajayan, “Hard carbon anode for lithium-, sodium-, and potassium-ion batteries: Advancement and future perspective,” *Cell Rep. Phys. Sci.*, 5 (2024) 101851-101888
- [153] K. Sato, M. Noguchi, A. Demachi, N. Oki and M. Endo, “A Mechanism of Lithium Storage in Disordered Carbons,” *Science*, 264 (1994) 556-558
- [154] M. Winter, J. Besenhard, M. Spahr and P. Novák, “Insertion Electrode Materials for Rechargeable Lithium Batteries,” *Adv. Mater.*, 10 (1998) 725-763
- [155] A. Satoh, N. Takami, T. Ohsaki, M. Oguchi and H. Sasaki, “⁷Li NMR and ESR analysis of Lithium storage in hard carbon materials,” *Denki Kagaku*, 66 (1998) 1260-1269
- [156] D. Stevens and J. Dahn, “High capacity anode materials for rechargeable sodium-ion batteries,” *J. Electrochem. Soc.*, 147 (2000) 1271-1273
- [157] M. Letellier, F. Chevallier, C. Clinard, E. Frąckowiak, J. Rouzaud, F. Béguin, M. Morcrette and J. Tarascon, “The first in situ ⁷Li nuclear magnetic resonance study of lithium insertion in hard-carbon anode materials for Li-ion batteries,” *J. Chem. Phys.*, 118 (2003) 6038-6045
- [158] M. Letellier, F. Chevallier, F. Béguin and J. Rouzaud, “The first in situ ⁷Li NMR study of the reversible lithium insertion mechanism in disorganised carbons,” *J. Phys. Chem. Solids*, 65 (2004) 245-251
- [159] J. Stratford, P. Allan, O. Pecher, O. Chater, P. Chater and C. Grey, “Mechanistic insights into sodium storage in hard carbon anodes using local structure probes,” *Chem. Commun.*, 52 (2016) 12430-12433

- [160] P. Tsai, S. Chung, S. Lin and A. Yamada, “Ab initio study of sodium intercalation into disordered carbon,” *J. Mater. Chem. A*, 3 (2015) 9763-9768
- [161] H. Alptekin, H. Au, A. Jensen, E. Olsson, M. Goktas, T. Headen, P. Adelhelm, Q. Cai, A. Drew and M. Titirici, “Sodium Storage Mechanism Investigations through Structural Changes in Hard Carbons,” *ACS Appl. Energy Mater.*, 3 (2020) 9918-9927
- [162] X. Lin, J. Huang and B. Zhang, “Correlation between the microstructure of carbon materials and their potassium ion storage performance,” *Carbon*, 143 (2019) 138-146
- [163] M. Arnaiz and J. Ajuria, “Pre-Lithiation Strategies for Lithium Ion Capacitors: Past, Present, and Future,” *Batteries Supercaps*, 4 (2021) 733-748
- [164] K. Xu, “Nonaqueous Liquid Electrolytes for Lithium-Based Rechargeable Batteries,” *Chem. Rev.*, 104 (2004) 4303-4417
- [165] E. Peled, “The Electrochemical Behavior of Alkali and Alkaline Earth Metals in Nonaqueous Battery Systems—The Solid Electrolyte Interphase Model,” *J. Electrochem. Soc.*, 126 (1979) 2047-2051
- [166] A. Ponrouch, E. Marchante, M. Courty, J. Tarascon and M. Palancin, “In search of an optimized electrolyte for Na-ion batteries,” *Energy Environ. Sci.*, 5 (2012) 8572-8583
- [167] M. Dubois, J. Ghanbaja and D. Billaud, “Electrochemical intercalation of sodium ions into poly(para-phenylene) in carbonate-based electrolytes,” *Synth. Met.*, 90 (1997) 127-134
- [168] J. Vetter, P. Novak, M. Wagner, C. Veit, K. Möller, J. Besenhard, M. Winter, M. Wohlfahrt-Mehrens, C. Vogler and Hammouche, “Ageing mechanisms in lithium-ion batteries,” *J. Power Sources*, 147 (2005) 269-281
- [169] D. Aurbach, “Review of selected electrode–solution interactions which determine the performance of Li and Li ion batteries,” *J. Power Sources*, 89 (2000) 206-218
- [170] N. Singh, R. Singh and N. Singh, “Organic solid state reactivity,” *Tetrahedron*, 50 (1994) 6441-6493
- [171] F. Cheng, M. Cao, Q. Li, C. Fang, J. Han and Y. Huang, “Electrolyte Salts for Sodium-Ion Batteries: NaPF₆ or NaClO₄,” *ACS Nano*, 17 (2023) 18608-18615
- [172] H. Kim, J. Hong, K. Park, H. Kim, S. Kim and K. Kang, “Aqueous Rechargeable Li and Na Ion Batteries,” *Chem. Rev.*, 114 (2014) 11788-11827.
- [173] N. Yabuuchi, K. Kubota, M. Dahbi and S. Komaba, “Research Development on Sodium-Ion Batteries,” *Chem. Rev.*, 114 (2014) 11636-11682
- [174] M. Winter, “The Solid Electrolyte Interphase – The Most Important and the Least Understood Solid Electrolyte in Rechargeable Li Batteries,” *Zeitschrift für Physikalische Chemie*, 223 (2009) 1395-1406
- [175] H. Wang, D. Zhai and F. Kang, “Solid electrolyte interphase (SEI) in potassium ion batteries,” *Energy Environ. Sci.*, 13 (2020) 4583-4608
- [176] F. Li, Y. Cao, W. Wu, G. Wang and D. Qu, “Prelithiation Bridges the Gap for Developing Next-Generation Lithium-Ion Batteries/Capacitors,” *Small Methods*, 6 (2022) 2200411-2200422
- [177] Z. Zhang, R. Wang, B. He, J. Jin, Y. Gong and H. Wang, “Recent advances on pre-sodiation in sodium-ion capacitors: A mini review,” *Electrochem. commun.*, 129 (2021) 107090-107095

- [178] C. Deacux, G. Lota, E. Raymundo-Piñero, E. Frackowiak and F. Béguin, “Electrochemical performance of a hybrid lithium-ion capacitor with a graphite anode preloaded from lithium bis(trifluoromethane)sulfonimide-based electrolyte,” *Electrochim. Acta*, 86 (2012) 282-286
- [179] A. Mackowiak, P. Jezowski, Y. Matsui, M. Ishikawa and K. Fic, “Redox-active electrolytes as a viable approach for the one-step assembly of metal-ion capacitors,” *Energy Storage Mater.*, 65 (2024) 103163-103176
- [180] M. Park, Y. Lim, J. Kim, Y. Kim, J. Cho and J. Kim, “A Novel Lithium-Doping Approach for an Advanced Lithium Ion Capacitor,” *Adv. Energy Mater.*, 1 (2011) 1002-1006
- [181] M. Park, Y. Lim, S. Hwang, J. Kim, J. Kim, S. Dou, J. Cho and Y. Kim, “Scalable Integration of Li₅FeO₄ towards Robust, High-Performance Lithium-Ion Hybrid Capacitors,” *ChemSusChem*, 7 (2014) 3138-3144
- [182] Y. Lim, D. Kim, J. Lim, J. Kim, J. Yu, Y. Kim, D. Byun, M. Cho, K. Cho and M. Park, “Anti-fluorite Li₆CoO₄ as an alternative lithium source for lithium ion capacitors: an experimental and first principles study,” *J. Mater. Chem. A*, 3 (2015) 12377-12385
- [183] P. Jezowski, K. Fic, O. Crosnier, T. Brousse and F. Béguin, “Lithium rhenium(vii) oxide as a novel material for graphite pre-lithiation in high performance lithium-ion capacitors,” *J. Mater. Chem. A*, 4 (2016) 12609-12615
- [184] P. Jezowski, O. Crosnier, E. Deunf, P. Poizot, F. Béguin and T. Brousse, “Safe and recyclable lithium-ion capacitors using sacrificial organic lithium salt,” *Nat. Mater.*, vol. 17, pp. 167-173, 2018.
- [185] P. Jezowski, A. Chojnacka, X. Pan and F. Béguin, “Sodium amide as a “zero dead mass” sacrificial material for the pre-sodiation of the negative electrode in sodium-ion capacitors,” *Electrochim. Acta*, 375 (2021) 137980-137987
- [186] K. Zou, W. Deng, P. Cai, X. Deng, B. Wang, C. Liu, J. Li, H. Hou, G. Zou and X. Ji, “Pre-lithiation/Presodiation Techniques for Advanced Electrochemical Energy Storage Systems: Concepts, Applications, and Perspectives,” *Adv. Funct. Mater.*, 31 (2021) 2005581-2005594
- [187] X. Pan, A. Chojnacka and F. Béguin, “Advantageous carbon deposition during the irreversible electrochemical oxidation of Na₂C₄O₄ used as a presodiation source for the anode of sodium-ion systems,” *Energy Stor. Mater.*, 40 (2021) 22-30
- [188] X. Pan, A. Chojnacka, P. Jezowski and F. Béguin, “Na₂S sacrificial cathodic material for high performance sodium-ion capacitors,” *Electrochim. Acta*, 318 (2019) 471-478.
- [189] M. Park, Y. Lim, J. Kim, Y. Kim, J. Cho and J. Kim, “A Novel Lithium-Doping Approach for an Advanced Lithium Ion Capacitor,” *Adv. Energy Mater.*, 1 (2011) 1002-1006
- [190] P. Jezowski, K. Fic, O. Crosnier, T. Brousse and F. Béguin, “Use of sacrificial lithium nickel oxide for loading graphitic anode in Li-ion capacitors,” *Electrochim. Acta*, 206 (2016) 440-445
- [191] S. Zhang, “Eliminating pre-lithiation step for making high energy density hybrid Li-ion capacitor,” *J. Power Sources*, 343 (2017) 322-328

- [192] C. Liu, T. Li, H. Zhang, Z. Song, C. Qu, G. Hou, H. Zhang, C. Ni and X. Li, "DMF stabilized Li₃N slurry for manufacturing self-prelithiatable lithium-ion capacitors," *Sci. Bull.*, 65 (2020) 434-442
- [193] M. Arnaiz, D. Shanmukaraj, D. Carriazo, D. Bhattacharjya, A. Villaverde, M. Armand and J. Ajuria, "A transversal low-cost pre-metallation strategy enabling ultrafast and stable metal ion capacitor technologies," *Energy Environ. Sci.*, 13 (2020) 2441-2449
- [194] P. Jeżowski, O. Crosnier and T. Brousse, "Sodium borohydride (NaBH₄) as a high-capacity material for next-generation sodium-ion capacitors," *ChemistryOpen*, 19 (2021) 432-441
- [195] Y. Niu, Y. Guo, Y. Yin, S. Zhang, T. Wang, P. Wang, S. Xin and Y. Gou, "High-Efficiency Cathode Sodium Compensation for Sodium-Ion Batteries," *Adv Mater*, 32 (2020) 2001419-2001425
- [196] B. Shen, R. Zhan, Y. Li, L. Hu, Y. Niu, J. Jiang, Q. Wang and M. Xu, "Manipulating irreversible phase transition of NaCrO₂ towards an effective sodium compensation additive for superior sodium-ion full cells," *J. Colloid Interface Sci.*, 553 (2019) 524-529
- [197] C. Angell, "Liquid fragility and the glass transition in water and aqueous solutions," *Chem. Rev.*, 102 (2002) 2627-2650
- [198] J. Lim, K. Park, H. J. K. Lee, K. Kwak and M. Cho, "Nanometric Water Channels in Water-in-Salt Lithium Ion Battery Electrolyte," *J. Am. Chem. Soc.*, 140 (2018) 15661-15667
- [199] V. Khomenko, E. Raymundo-Piñero and F. Béguin, "High-energy density graphite/AC capacitor in organic electrolyte," *J. Power Sources*, 177 (2008) 643-651
- [200] A. Slesinski and E. Frackowiak, "Determination of accurate electrode contribution during voltammetry scan of electrochemical capacitors," *J. Solid State Electrochem.*, 22 (2018) 2135-2139

Scientific achievements

1. Publications

1.1. **Andres Camilo Parejo-Tovar**, François Béguin and, Paula Ratajczak, “Comprehensive potentiodynamic analysis of electrodes performance in hybrid capacitors”, *Electrochem. commun.* 147 (2023) 107436_1-107436_6

<https://doi.org/10.1016/j.elecom.2023.107436>

(IF₂₀₂₃ = 4.7; MEiN = 100)

1.2. **Andres Camilo Parejo-Tovar** and, François Béguin, “The NaClO₄-water eutectic electrolyte for environmentally friendly electrical double-layer capacitors operating at low temperature”, *Energy Storage Mater.* 69 (2024) 103387_1-103387_14

<https://doi.org/10.1016/j.ensm.2024.103387>

(IF₂₀₂₃ = 18.9; MEiN = 200)

1.3. **Andres Camilo Parejo-Tovar** and, François Béguin, “Ideally realized sodium-ion capacitor via irreversible oxidation of sodium azide to pre-metalate the anodic host”, *J. Power Sources* 609 (2024) 234637_1-234637_12

<https://doi.org/10.1016/j.jpowsour.2024.234637>

(IF₂₀₂₃ = 8.1; MEiN = 140)

1.4. Masoud Foroutan Koudahi, **Andres Camilo Parejo-Tovar**, François Béguin and, Elżbieta Frąckowiak, “Charge storage and operando electrochemical dilatometry of MXene electrodes in ionic liquids”, *Energy Storage Mater.* 72 (2024) 103771_1-103771_13

<https://doi.org/10.1016/j.ensm.2024.103771>

(IF₂₀₂₃ = 18.9; MEiN = 200)

1.5. **Andres Camilo Parejo-Tovar**, Céline Merlet, Paula Ratajczak and, François Béguin, “Operando tracking of ion population changes in the EDL electrode of a lithium-ion capacitor during its charge/discharge”, *Energy Storage Mater.* 73 (2024)

(Accepted)

(IF₂₀₂₃ = 18.9; MEiN = 200)

Total Impact Factor: 69.5

Total Impact Factor including Co-authors: 24.5

Total MEiN points: 840

2. Oral Presentations

2.1. **Andres Camilo Parejo-Tovar***, François Béguin, Mirosława Pawlyta and, Paula Ratajczak, “Impact of the Negative Electrode Structure/Texture on the Electrochemical Performance of Carbon-based Metal-ion capacitor analyzed through CV and EIS”, *NanoTech Poland 2022*, Poznan, Poland, 01.06.2022

2.2. **Andres Camilo Parejo-Tovar***, François Béguin and, Paula Ratajczak; “Comprehensive Analysis of Electrodes Performance in Carbon-based Hybrid Capacitors by Cyclic Voltammetry”, *ISEEcap 2022*, Bologna, Italy, 11.06.2022

2.3. **Andres Camilo Parejo-Tovar***, François Béguin, Mirosława Pawlyta and, Paula Ratajczak, “Realization of sodium ion capacitor by pre-metalation of a hard carbon anode using sodium azide as sacrificial cathodic material”, *NanoTech Poland 2023*, Poznan, Poland, 14.06.2023

2.4. **Andres Camilo Parejo-Tovar***, Paula Ratajczak and, François Béguin; “Insights into the charging mechanism of the positive electrode in Lithium-ion Capacitors”, *The 74th Annual Meeting of the International Society of Electrochemistry*, Lyon, France, 03.09.2023

2.5. **Andres Camilo Parejo-Tovar**, Saida Gharouel and, François Béguin*; “EDLCs operating outstandingly at low temperature with an aqueous eutectic electrolyte”, *7th International Conference on Advanced Capacitors*, Kamakura, Japan, 26.09.2023

2.6. **Andres Camilo Parejo-Tovar** and, François Béguin*; “Environmentally friendly EDLC operating at low temperature with the NaClO₄-water eutectic electrolyte” *ISEEcap 2024*, Vitoria Gateiz, Spain, 08.07.2024

* **Speaker**

3. Poster presentations

3.1. **Andres Camilo Parejo-Tovar**, Zhuanpei Wang, François Béguin and, Paula Ratajczak; “Simulation and Experimental Studies on Imidazolium-based Ionic Liquids as Electrolytes for Electrochemical Capacitors” *72th Annual Meeting of the International Society of Electrochemistry*, Jeju, South Korea, 05.08.2022

3.2. **Andres Camilo Parejo-Tovar**, François Béguin and, Paula Ratajczak; “Assessment of Electrodes Operation in Carbon-based Na-ion Capacitors by Potentiostatic Electrochemical Impedance Spectroscopy”, *ISEEcap 2022*, Bologna, Italy, 11.06.2022

3.3. **Andres Camilo Parejo-Tovar**, François Béguin and, Paula Ratajczak; “A novel concept of sustainable capacitor based on the carbon-ion technology - CARBionCAP”, *4th Interdisciplinary FNP Scientific Conference*, Warsaw, Poland, 06.10.2022

3.4. **Andres Camilo Parejo-Tovar**, François Béguin, Mirosława Pawlyta and, Paula Ratajczak; “Analysis of Charging Mechanisms in Lithium-ion Capacitors By Electrochemical Dilatometry”, *The 74th Annual Meeting of the International Society of Electrochemistry*, Lyon, France, 03.09.2023

4. Participation in scientific project

4.1. POWROTY Project (POIR.04.04.00-00-5EF5/18-00)

Project funded by the Polish Foundation for Science (FNP)

Project leader: Dr. Eng. Paula Ratajczak

5. Awards

5.1. **ISEECap Poster Presentation Awarded by the International Society of Electrochemistry (ISE)**; Andrés Camilo Parejo-Tovar, François Béguin, Paula Ratajczak ; “Assessment of Electrodes Operation in Carbon-based Na-ion Capacitors by Potentiostatic Electrochemical Impedance Spectroscopy”, *ISEECap 2022*, Bologna, Italy, 11.06.2022

6. Grants

6.1. France Excellence scholarship: **SSHN - research stay** to develop the project entitled “Understanding charging/discharging mechanism of the positive electrode in metal-ion capacitor via molecular dynamics simulations” under the supervision of Dr. Céline Merlet, Centre interuniversitaire de recherche et d'ingénierie des matériaux – CIRIMAT, Toulouse, France, 18.09.2023

Abstract

Enhancing the performance of symmetric and hybrid electrochemical capacitors is crucial for the advancement of energy storage technologies. Strategies aimed at improving energy density, power density, safety, operational temperature range, self-discharge rates, lifespan, and cost-effectiveness are essential to keep pace with the growing energy demands of modern society. In this context, this dissertation addresses several key challenges in this area to improve the performance of symmetric and hybrid electrochemical capacitors. First, the selection and design of high-conductivity Water-in-Salt (WIS) electrolytes for use in Electrical double-layer capacitors (EDLCs) is explored, aiming to achieve higher nominal voltage values and extended cycle life across a wide temperature range. Second, the ideal realization of metal ion capacitors (MICs) through the irreversible oxidation of a carefully selected sacrificial material that permits the *in situ* pre-metalation of the anodic host is examined. Third, the focus is placed on understanding of the potentiodynamic behaviour of MIC electrodes during cycling, and finally, investigating the ion population changes occurring in the positive electrode of a MIC during its charge/discharge. The dissertation is organized into five chapters.

Chapter I provides a comprehensive literature review on electrochemical capacitors featuring carbon-based electrodes. It begins by outlining the principles and characteristics of electrical double-layer capacitors (EDLCs) and common electrode materials, emphasizing how the textural and structural properties of carbon influence the capacitive performance of electrodes. Additionally, it compares organic electrolytes, ionic liquids, and aqueous media used in EDLCs, with special attention to emerging water-in-salt electrolytes. The chapter also discusses the ion population changes in EDLC electrodes during charging. In the second part, the focus shifts to carbon-based metal-ion capacitors (MICs), exploring their operation principles. It examines the pairing of an EDL-type positive electrode with a battery-type negative electrode in terms of output energy and reviews materials commonly used for both electrodes. This section also reviews the solid electrolyte interphase (S.E.I.) formation on the negative electrode (as crucial factor for a reliable MIC operation), then discussing the various electrolytes used to promote S.E.I. formation and the common methods for pre-metalating the negative electrode, aimed at enhancing MIC performance.

Chapter II addresses the challenge of implementing Water-in-Salt (WIS) electrolytes in EDLCs for sub-ambient temperature applications through the publication titled "*The NaClO₄-Water Eutectic Electrolyte for Environmentally Friendly Electrical Double-Layer Capacitors Operating at Low Temperature.*" This study investigated the transport properties of an 8.84 mol kg⁻¹ NaClO₄ WIS eutectic electrolyte down to -35 °C. The NaClO₄-water eutectic electrolyte

showed an ionic conductivity of 180 mS cm^{-1} and a dynamic viscosity of $2.48 \text{ mPa}\cdot\text{s}$ at room temperature ($25 \text{ }^\circ\text{C}$, RT). At $-30 \text{ }^\circ\text{C}$, the conductivity remained high at 23.7 mS cm^{-1} , with viscosity increasing to $24.8 \text{ mPa}\cdot\text{s}$. Molecular dynamics simulations revealed that the local structure of the solution remains stable from RT to $-35 \text{ }^\circ\text{C}$, with hydrogen-bonded water molecules forming channel-like domains that enhance the ionic diffusion. The electrochemical stability window (*ESW*) of activated carbon (AC) electrodes in the 8.84 m NaClO_4 electrolyte increases from 1.8 V at RT to 2.1 V at $-35 \text{ }^\circ\text{C}$. These high values are attributed to the electrolyte's near-neutral pH and reduction of free water in the Stern layer under positive polarization. Electrochemical investigations on laminate AC//AC cells in the 8.84 m NaClO_4 electrolyte demonstrated low resistive components down to $-30 \text{ }^\circ\text{C}$, and the possibility to achieve operational voltages of 2.0 V at $-30 \text{ }^\circ\text{C}$ and 1.7 V at RT. Notably, at $-30 \text{ }^\circ\text{C}$ and under constant power discharge up to 10 kW kg^{-1} , the AC//AC capacitor in NaClO_4 -water eutectic electrolyte exceeded the energy output of traditional AC//AC cells in the 1 mol L^{-1} TEABF₄/ACN electrolyte. These findings underscore the potential of environmentally friendly EDLCs in the NaClO_4 -water eutectic electrolyte to effectively compete with traditional organic electrolyte devices under sub-ambient temperature conditions.

Chapter III presents a study entitled “*Ideally Realized Sodium-Ion Capacitor via Irreversible Oxidation of Sodium Azide to Pre-Metalate the Anodic Host*”. Herein, sodium azide (NaN_3) is used as a sacrificial cathodic material to resolve the metal deficiency in the anodic host of sodium-ion capacitors (NICs). *Operando* electrochemical mass spectroscopy at C/40 (theoretical capacity of NaN_3) on a NaN_3 -C65 electrode (percolated by the conductive additive C65) demonstrated a complete irreversibility of the azide oxidation, producing N_2 as the sole by-product. Gas adsorption analysis on pristine and oxidized NaN_3 -AC (activated carbon) electrodes revealed notable regeneration of the porous texture of activated carbon after oxidation. Laminated NaN_3 -AC//HCM cells (HCM: hard carbon) were fabricated, and sodium was transferred to the HCM negative electrode through electrochemical oxidation of NaN_3 , resulting in AC// Na_xHCM sodium-ion capacitors. These NICs demonstrated impressive capacitance retention of 90% and energy efficiency of 95% after 15,000 galvanostatic cycles over a voltage range of 2.0 V to 3.8 V . They exhibited an output energy of 38 Wh kg^{-1} up to 4 kW kg^{-1} , demonstrating the effectiveness of sodium azide as a "zero dead mass" sacrificial material for the cost-effective realization of NICs with attractive electrochemical properties.

The publication entitled “*Comprehensive Potentiodynamic Analysis of Electrode Performance in Hybrid Capacitors*” is presented in **Chapter IV**. It introduces a straightforward methodology

for assessing the potentiodynamic information of individual electrodes in hybrid capacitors by dynamically adjusting the potential sweep rates during cyclic voltammetry (CV). This experimental and calculation procedure was tested on a lithium-ion capacitor (LIC) with AC and Li_xC_6 electrodes, and compared to a symmetric AC//AC EDLC. It was confirmed that during the potentiodynamic analysis of a LIC, the scan rate of the electrodes is not constant over time. Specifically, the scan rate of the negative electrode tends to decrease to zero, while the scan rate of the positive electrode approaches the rate of the imposed voltage sweep. Changing the graphite-to-AC mass ratio impacted the stabilization time, with a 2:1 ratio speeding it up and a 0.5:1 ratio slowing it down. This proposed methodology is fundamental for identifying any imbalances in the contributions of the electrodes and providing an accurate representation of their current profiles during the potentiodynamic analysis of a MIC.

Chapter V presents the publication titled "*Operando Tracking of Ion Population Changes in the EDL Electrode of a Lithium-Ion Capacitor During Its Charge/Discharge*," which elucidates the charge exchange processes in an activated carbon (AC) based electrode operating within an extended potential range, akin to the positive electrode of a lithium-ion capacitor (LIC). Molecular dynamics simulations applied to the battery-type electrolyte (LiPF_6 in EC/DMC), both in bulk and adsorbed within a model porous carbon, revealed partial solvation of Li^+ cations in pores and complete desolvation of PF_6^- anions in both states. *Operando* and *in situ* methods applied to the AC electrode confirm: (i) ionic exchange followed by anion adsorption during the initial hole injection from the point of zero charge (*PZC*) to 4.5 V vs. Li/Li^+ ; (ii) desorption and peak liberation of trapped PF_6^- at 3.2 V vs. Li/Li^+ during hole withdrawal; (iii) perm-selective adsorption of partially solvated Li^+ during electron injection down to 2.2 V vs. Li/Li^+ ; and (iv) cation desorption during electron withdrawal up to *PZC*, followed by similar ionic exchange and anion adsorption at potentials above *PZC*, however with peak liberation of some trapped Li^+ at 3.8 V vs. Li/Li^+ . The high polarization required to extract trapped ions from the porosity may explain the reduced lifespan of LICs (due to structural damages of the AC host), suggesting the need of further works to eliminate ion trapping by optimizing the porous texture.

In summary, this dissertation provides significant contributions to improving the performance of symmetric and hybrid electrochemical capacitors by addressing key challenges in energy density, cycle life, and temperature range. It explores innovative electrolyte designs, electrode dynamics, and ion behaviour, with a focus on water-in-salt electrolytes and pre-metalation using sacrificial materials. The presented findings allow efficiency, durability, and

environmental sustainability to be enhanced, offering promising solutions for high-performance energy storage, particularly in extreme conditions. Ultimately, the research paves the way for more effective and scalable technologies to meet the world's growing energy needs.

Streszczenie

Poprawa wydajności symetrycznych i hybrydowych kondensatorów elektrochemicznych ma kluczowe znaczenie dla rozwoju technologii magazynowania energii. Strategie mające na celu poprawę gęstości energii, gęstości mocy, bezpieczeństwa, zakresu temperatur pracy, szybkości samowyładowania, żywotności i opłacalności są niezbędne, aby dotrzymać kroku rosnącemu zapotrzebowaniu na energię współczesnego społeczeństwa. W tym kontekście niniejsza rozprawa doktorska dotyczy kilku kluczowych wyzwań w tym obszarze w celu poprawy wydajności symetrycznych i hybrydowych kondensatorów elektrochemicznych. Po pierwsze, badany jest wybór i projektowanie elektrolitów o wysokiej przewodności typu woda w soli (z *ang.* Water-in-Salt, WIS) do stosowania w kondensatorach podwójnej warstwy elektrycznej (z *ang.* Electrical Double Layer Capacitors, EDLC), w celu osiągnięcia wyższych wartości napięcia nominalnego i wydłużenia żywotności cyklu w szerokim zakresie temperatur. Po drugie, badana jest idealna realizacja kondensatorów metalowo-jonowych (z *ang.* Metal-Ion Capacitors, MIC) poprzez nieodwracalne utlenianie starannie dobranego materiału zużywalnego (z *ang.* sacrificial material), który umożliwia wstępną metalizację *in situ* anodowego nośnika. Po trzecie, skupiono się na zrozumieniu zachowania potencjodynamicznego elektrod MIC podczas cyklicznego ładowania i wyładowywania, a także na zbadaniu zmian populacji jonów zachodzących w elektrodzie dodatniej MIC podczas ładowania/wyładowywania. Rozprawa składa się z pięciu rozdziałów.

Rozdział I zawiera kompleksowy przegląd literatury na temat kondensatorów elektrochemicznych z elektrodami węglowymi. Rozpoczyna się od nakreślenia zasad i charakterystyki EDLC i popularnych materiałów elektrodowych, podkreślając, w jaki sposób teksturalne i strukturalne właściwości węgla wpływają na wydajność pojemnościową elektrod. Ponadto porównano elektrolity organiczne, ciecze jonowe i media wodne stosowane w EDLC, ze szczególnym uwzględnieniem ostatnio często pojawiających się elektrolitów typu WIS. W rozdziale tym omówiono również zmiany populacji jonów w elektrodach EDLC podczas pracy ogniwa. W drugiej części skupiono się na kondensatorach MIC na bazie węgla, badając zasady ich działania. Przeanalizowano połączenie elektrody dodatniej typu EDL z elektrodą ujemną typu baterijnego pod względem energii wyjściowej i dokonano przeglądu materiałów powszechnie stosowanych w obu elektrodach. W tej części omówiono również tworzenie się stałej interfazy elektrolitu (z *ang.* Solid Electrolyte Interphase, S.E.I.) na elektrodzie ujemnej (jako kluczowy czynnik niezawodnego działania MIC), a następnie omówiono różne elektrolity stosowane do promowania tworzenia S.E.I. oraz powszechne metody wstępnego metalizowania elektrody ujemnej, mające na celu zwiększenie wydajności MIC.

Rozdział II dotyczy wyzwania, jakim jest wdrożenie elektrolitów typu woda w soli w EDLC do zastosowań w temperaturach poniżej temperatury otoczenia poprzez publikację zatytułowaną "*The NaClO₄-Water Eutectic Electrolyte for Environmentally Friendly Electrical Double-Layer Capacitors Operating at Low Temperature*" („Elektrolit eutektyczny NaClO₄-woda dla przyjaznych dla środowiska elektrycznych kondensatorów dwuwarstwowych pracujących w niskich temperaturach”). W badaniu tym zbadano właściwości transportowe eutektycznego elektrolitu NaClO₄ WIS o stężeniu 8,84 mol kg⁻¹ do temperatury -35 °C. Elektrolit eutektyczny NaClO₄-woda wykazał przewodność jonową 180 mS cm⁻¹ i lepkość dynamiczną 2,48 mPa·s w temperaturze pokojowej (25 °C, RT). W temperaturze -30 °C przewodnictwo pozostało na wysokim poziomie 23,7 mS cm⁻¹, a lepkość wzrosła do 24,8 mPa·s. Symulacje dynamiki molekularnej wykazały, że lokalna struktura roztworu pozostaje stabilna od RT do -35 °C, z cząsteczkami wody połączonymi wiązaniami wodorowymi, tworzącymi domeny przypominające kanały, które zwiększają dyfuzję jonów. Okno stabilności elektrochemicznej (z ang. Electrochemical Stability Window, ESW) elektrod z węglem aktywnym (AC) w elektrolicie NaClO₄ o stężeniu 8,84 m wzrasta z 1,8 V w temperaturze pokojowej do 2,1 V w temperaturze -35°C. Te wysokie wartości przypisuje się niemal neutralnemu pH elektrolitu i redukcji wolnej wody w warstwie Sterna pod wpływem dodatniej polaryzacji. Badania elektrochemiczne ogniw laminatowych AC//AC w elektrolicie NaClO₄ o stężeniu 8,84 m wykazały niską rezystywność do -30 °C oraz możliwość osiągnięcia napięcia roboczego 2,0 V w temperaturze -30 °C i 1,7 V w temperaturze RT. W szczególności, w temperaturze -30 °C i przy stałym wyładowaniu z mocą do 10 kW kg⁻¹, kondensator AC//AC w elektrolicie eutektycznym NaClO₄-woda przewyższał wydajność energetyczną tradycyjnych ogniw AC//AC w elektrolicie TEABF₄/ACN o stężeniu 1 mol L⁻¹. Odkrycia te podkreślają potencjał przyjaznych dla środowiska ogniw EDLC w elektrolicie eutektycznym NaClO₄-woda, aby skutecznie konkurować z tradycyjnymi urządzeniami z elektrolitem organicznym w warunkach poniżej temperatury otoczenia.

Rozdział III przedstawia badanie zatytułowane "*Ideally Realized Sodium-Ion Capacitor via Irreversible Oxidation of Sodium Azide to Pre-Metalate the Anodic Host*" („Idealnie zrealizowany kondensator sodowo-jonowy poprzez nieodwracalne utlenianie azydku sodu w celu wstępnego zmetalizowania hosta anodowego”). Azydek sodu (NaN₃) został tu wykorzystany jako katodowy materiał zużywalny w celu usunięcia niedoboru metalu w anodowym nośniku kondensatorów sodowo-jonowych (z ang. Sodium-Ion Capacitors, NIC). Elektrochemiczna spektroskopia masowa w trybie *operando* przy C/40 (teoretyczna

pojemność NaN_3) na elektrodzie $\text{NaN}_3\text{-C65}$ (perkolowanej przez przewodzący dodatek C65) wykazała całkowitą nieodwracalność utleniania azydku, wytwarzając N_2 jako jedyny produkt uboczny. Analiza adsorpcji gazu na czystych i utlenionych elektrodach $\text{NaN}_3\text{-AC}$ (węgiel aktywny) wykazała znaczną regenerację porowatej tekstury węgla aktywnego po utlenieniu. Wyprodukowano laminowane ogniwa $\text{NaN}_3\text{-AC//HCM}$ (HCM: twardy węgiel), a sól została przeniesiona na elektrodę ujemną HCM poprzez elektrochemiczne utlenianie NaN_3 , w wyniku czego powstały kondensatory sodowo-jonowe AC// Na_xHCM . Te NIC wykazały imponującą retencję pojemności na poziomie 90% i wydajność energetyczną na poziomie 95% po 15 000 cykli galwanostatycznych w zakresie napięć od 2,0 V do 3,8 V. Kondensatory te wykazały energię wyjściową na poziomie 38 Wh kg^{-1} przy mocy do 4 kW kg^{-1} , co potwierdza skuteczność azydku sodu jako materiału zużywalnego o "zerowej masie własnej" do opłacalnej realizacji NIC o atrakcyjnych właściwościach elektrochemicznych.

Rozdział IV przedstawia publikację zatytułowaną „*Comprehensive Potentiodynamic Analysis of Electrode Performance in Hybrid Capacitors*” („Kompleksowa analiza potencjodynamiczna pracy elektrod w kondensatorach hybrydowych”). W tym rozdziale wprowadzono metodologię oceny potencjodynamicznej wydajności poszczególnych elektrod w kondensatorach hybrydowych poprzez dynamiczne dostosowywanie szybkości zmiany potencjału podczas woltamperometrii cyklicznej (z ang. Cyclic Voltammetry, CV). Ta procedura eksperymentalna i obliczeniowa została przetestowana na kondensatorze litowo-jonowym (z ang. Lithium-Ion Capacitor, LIC) z elektrodami AC i Li_xC_6 , a następnie porównana z symetrycznym kondensatorem EDLC AC//AC. Potwierdzono, że podczas analizy potencjodynamicznej LIC szybkość skanowania elektrod nie jest stała w czasie. Szybkość skanowania elektrody ujemnej maleje do zera, natomiast szybkość skanowania elektrody dodatniej zbliża się do narzuconej szybkości zmiany napięcia. Zmiana stosunku masy grafitu do AC wpłynęła na czas stabilizacji: stosunek 2:1 przyspieszał go, a stosunek 0,5:1 spowalniał. Zaproponowana metodologia jest kluczowa dla identyfikacji nierównowagi w udziale elektrod oraz dokładnej reprezentacji ich profili prądowych podczas analizy potencjodynamicznej MIC.

Rozdział V przedstawia publikację zatytułowaną „*Operando Tracking of Ion Population Changes in the EDL Electrode of a Lithium-Ion Capacitor During Its Charge/Discharge*” („Śledzenie w trybie *operando* zmian populacji jonów w elektrolicie EDL kondensatora litowo-jonowego podczas jego ładowania/wyładowywania”), która wyjaśnia procesy wymiany ładunków w elektrodzie z węglem aktywnym pracującej w rozszerzonym zakresie potencjałów, podobnie jak dodatnia elektroda kondensatora LIC. Symulacje dynamiki molekularnej

zastosowane do elektrolitu typu bateryjnego (LiPF_6 w EC/DMC), zarówno w stanie objętościowym, jak i zaadsorbowanego w modelowym porowatym węglu, ujawniły częściową solwatację kationów Li^+ w porach oraz całkowitą desolvatację anionów PF_6^- . Metody *operando* oraz *in situ* zastosowane do elektrody AC potwierdziły: (i) wymianę jonów, a następnie adsorpcję anionów podczas początkowego generowania dziur od punktu zerowego ładunku (*z ang.* Point of Zero Charge, PZC) do 4,5 V względem Li/Li^+ ; (ii) desorpcję oraz maksymalne uwalnianie uwięzionego PF_6^- przy 3,2 V względem Li/Li^+ podczas rekombinacji dziur; (iii) perm-selektywną adsorpcję częściowo rozpuszczonego Li^+ podczas wprowadzania elektronów do 2,2 V względem Li/Li^+ ; oraz (iv) desorpcję kationów podczas wycofywania elektronów do PZC, a następnie podobną wymianę jonów i adsorpcję anionów przy potencjałach powyżej PZC, jednak z uwolnieniem niektórych uwięzionych kationów Li^+ przy 3,8 V względem Li/Li^+ . Wysoka polaryzacja wymagana do uwolnienia uwięzionych jonów z porów może wyjaśniać skróconą żywotność LIC (spowodowaną uszkodzeniami strukturalnymi węgla aktywnego), co sugeruje konieczność dalszych badań nad eliminacją „pułapkowania” jonów poprzez optymalizację porowatej tekstury.

Podsumowując, niniejsza rozprawa doktorska wnosi znaczący wkład w poprawę wydajności symetrycznych i hybrydowych kondensatorów elektrochemicznych poprzez rozwiązanie kluczowych wyzwań związanych z gęstością energii, żywotnością cyklu oraz zakresem temperatur pracy. Badania obejmują innowacyjne projekty elektrolitów, dynamikę elektrod i zachowania jonów, z naciskiem na elektrolity typu woda w soli oraz wstępną metalizację z wykorzystaniem katodowych materiałów zużywalnych. Przedstawione odkrycia przyczyniają się do zwiększenia wydajności, trwałości i równoważności środowiskowej, oferując obiecujące rozwiązania dla wysokowydajnych systemów magazynowania energii, zwłaszcza w ekstremalnych warunkach. Badania te torują drogę do bardziej efektywnych i skalowalnych technologii, które zaspokoją rosnące potrzeby energetyczne na świecie.

Co-authorship statements



POLITECHNIKA POZNAŃSKA

Andres Parejo-Tovar

Instytut Chemii i Elektrochemii Technicznej
ul. Berdychowo 4, 60-965 Poznań
tel. +48 519 620 154
e-mail: andres.parejotovar@doctorate.put.poznan.pl



Poznan, 24.09.2024

Declaration of individual contribution in publications

As the co-author of the following paper, I hereby declare that my contribution to this work was:

Article: *Comprehensive potentiodynamic analysis of electrodes performance in hybrid capacitors*

Authors: **Andres Parejo-Tovar**, François Béguin, Paula Ratajczak

Journal: Electrochemistry Communications

DOI: [10.1016/j.elecom.2023.107436](https://doi.org/10.1016/j.elecom.2023.107436)

Contribution: Conceptualization (development of the method to analyse the potentiodynamic behaviour of the electrodes), Methodology, Investigation (preparation of electrodes, electrochemical investigations), Formal analysis, Data curation, Writing – original draft, Visualization.



Signature



POLITECHNIKA POZNAŃSKA

Professor François Béguin

Institut Chemii i Elektrochemii Technicznej
ul. Berdychowo 4, 60-965 Poznań
tel. +48 61 647 5985
e-mail: francois.beguin@put.poznan.pl



Poznan, 24.09.2024

Declaration of individual contribution in publications

As the co-author of the following paper, I hereby declare that my contribution to this work was:

Article: *Comprehensive potentiodynamic analysis of electrodes performance in hybrid capacitors*

Authors: **Andres Parejo-Tovar**, François Béguin, Paula Ratajczak

Journal: Electrochemistry Communications

DOI: <https://doi.org/10.1016/j.elecom.2023.107436>

Contribution: Resources, Supervision, Validation, Writing – review & editing.



Signature



POLITECHNIKA POZNAŃSKA

Dr inż. Paula Ratajczak

Instytut Chemii i Elektrochemii Technicznej
ul. Berdychowo 4, 60-965 Poznań
tel. +48 61 647 5985
e-mail: francois.beguिन@put.poznan.pl



Poznan, 24.09.2024

Declaration of individual contribution in publications

As the co-author of the following paper, I hereby declare that my contribution to this work was:

- Article:** *Comprehensive potentiodynamic analysis of electrodes performance in hybrid capacitors*
- Authors:** Andres Parejo-Tovar, François Béguin, **Paula Ratajczak**
- Journal:** Electrochemistry Communications
- DOI:** 10.1016/j.elecom.2023.107436
- Contribution:** Conceptualization, Validation, Visualization, Writing – review & editing, Supervision, Project administration, Funding acquisition.


Signature



POLITECHNIKA POZNAŃSKA

Andres Parejo-Tovar

Instytut Chemii i Elektrochemii Technicznej
ul. Berdychowo 4, 60-965 Poznań
tel. +48 519 620 154
e-mail: andres.parejotovar@doctorate.put.poznan.pl



Poznan, 24.09.2024

Declaration of individual contribution in publications

As the co-author of the following paper, I hereby declare that my contribution to this work was:

Article: *The NaClO₄-water eutectic electrolyte for environmentally friendly electrical double-layer capacitors operating at low temperature*

Authors: **Andres Parejo-Tovar**, François Béguin

Journal: Energy Storage Materials

DOI: [10.1016/j.ensm.2024.103387](https://doi.org/10.1016/j.ensm.2024.103387)

Contribution: Writing – original draft, Visualization, Investigation (planning experiments, preparation of samples, physicochemical characterization of the samples, realization of DSC experiments, realization gas adsorption experiments, electrochemical investigations), Formal analysis, Data curation, Realization of molecular dynamic simulations.



Signature



POLITECHNIKA POZNAŃSKA

Professor François Béguin

Institut Chemii i Elektrochemii Technicznej
ul. Berdychowo 4, 60-965 Poznań
tel. +48 61 647 5985
e-mail: francois.beguin@put.poznan.pl



Poznan, 24.09.2024

Declaration of individual contribution in publications

As the co-author of the following paper, I hereby declare that my contribution to this work was:

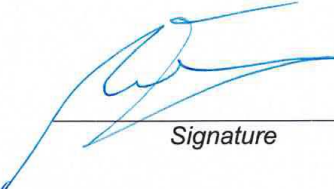
Article: *The NaClO₄-water eutectic electrolyte for environmentally friendly electrical double-layer capacitors operating at low temperature*

Authors: **Andres Parejo-Tovar**, François Béguin

Journal: Energy Storage Materials

DOI: <https://doi.org/10.1016/j.ensm.2024.103387>

Contribution: Writing – review & editing, Visualization, Validation, Supervision, Project administration, Funding acquisition, Conceptualization.



Signature



POLITECHNIKA POZNAŃSKA

Andres Parejo-Tovar

Instytut Chemii i Elektrochemii Technicznej
ul. Berdychowo 4, 60-965 Poznań
tel. +48 519 620 154
e-mail: andres.parejotovar@doctorate.put.poznan.pl



Poznan, 24.09.2024

Declaration of individual contribution in publications

As the co-author of the following paper, I hereby declare that my contribution to this work was:

Article: *Ideally realized sodium-ion capacitor via irreversible oxidation of sodium azide to pre-metalate the anodic host*

Authors: **Andres Parejo-Tovar**, François Béguin

Journal: Journal of Power Sources

DOI: [10.1016/j.jpowsour.2024.234637](https://doi.org/10.1016/j.jpowsour.2024.234637)

Contribution: Writing – original draft, Visualization, Investigation (planning experiments, preparation of the samples and electrodes, physicochemical analysis of the samples, realization of mass spectroscopy experiments, realization of gas adsorption experiments, electrochemical investigations, concept of pouch cells connected to peristaltic pump for gas evacuation), Formal analysis, Data curation.


Signature



POLITECHNIKA POZNAŃSKA

Professor François Béguin

Institut Chemii i Elektrochemii Technicznej
ul. Berdychowo 4, 60-965 Poznań
tel. +48 61 647 5985
e-mail: francois.beguin@put.poznan.pl



Poznan, 24.09.2024

Declaration of individual contribution in publications

As the co-author of the following paper, I hereby declare that my contribution to this work was:


Article: *Ideally realized sodium-ion capacitor via irreversible oxidation of sodium azide to pre-metalate the anodic host*

Authors: Andrés Parejo-Tovar, François Béguin

Journal: Journal of Power Sources

DOI: <https://doi.org/10.1016/j.jpowsour.2024.234637>

Contribution: Writing – review & editing, Visualization, Validation, Supervision, Project administration, Funding acquisition, Conceptualization..



Signature



POLITECHNIKA POZNAŃSKA

Andres Parejo-Tovar

Instytut Chemii i Elektrochemii Technicznej
ul. Berdychowo 4, 60-965 Poznań
tel. +48 519 620 154
e-mail: andres.parejotovar@doctorate.put.poznan.pl



Poznan, 24.09.2024

Declaration of individual contribution in publications

As the co-author of the following paper, I hereby declare that my contribution to this work was:

Article: *Operando tracking of ion population changes in the EDL electrode of a lithium-ion capacitor during its charge/discharge*

Authors: **Andres Parejo-Tovar**, Céline Merlet, Paula Ratajczak,
François Béguin

Journal: Energy Storage Materials

DOI:

Contribution: Investigation (planning experiments, preparation of electrodes, physicochemical characterization of samples, realization of gas adsorption, realization of operando ECD, operando Raman spectroscopy, in situ PEIS experiments); Formal Analysis; Data Curation; Visualization; Writing – Original Draft; Software (Realization of molecular dynamic simulations).



Signature



Centre Inter-universitaire de Recherche et d'Ingénierie des Matériaux – UMR CNRS 5085



Dr Céline Merlet
CNRS Researcher
CIRIMAT – Université Toulouse III - Paul Sabatier

Toulouse, 25.09.2024

Declaration of individual contribution in publications

As the co-author of the following paper, I hereby declare that my contribution to this work was:

Article: *Operando tracking of ion population changes in the EDL electrode of a lithium-ion capacitor during its charge/discharge*

Authors: Andres Parejo-Tovar, Céline Merlet, Paula Ratajczak, François Béguin

Journal: Energy Storage Materials

Contribution: Software; Validation; Writing – review & editing

Dr Céline MERLET



POLITECHNIKA POZNAŃSKA

Dr inż. Paula Ratajczak

Instytut Chemii i Elektrochemii Technicznej

ul. Berdychowo 4, 60-965 Poznań

tel. +48 61 647 5985

e-mail: francois.beguिन@put.poznan.pl



Poznan, 24.09.2024

Declaration of individual contribution in publications

As the co-author of the following paper, I hereby declare that my contribution to this work was:

Article: *Operando tracking of ion population changes in the EDL electrode of a lithium-ion capacitor during its charge/discharge*

Authors: Andres Parejo-Tovar, Céline Merlet, **Paula Ratajczak**, François Béguin

Journal: Energy Storage Materials

Contribution: Validation; Funding Acquisition; Project Administration;


Signature



POLITECHNIKA POZNAŃSKA

Professor François Béguin

Instytut Chemii i Elektrochemii Technicznej
ul. Berdychowo 4, 60-965 Poznań
tel. +48 61 647 5985
e-mail: francois.beguin@put.poznan.pl



Poznan, 24.09.2024

Declaration of individual contribution in publications

As the co-author of the following paper, I hereby declare that my contribution to this work was:

Article: *Operando tracking of ion population changes in the EDL electrode of a lithium-ion capacitor during its charge/discharge*

Authors: Andres Parejo-Tovar, Céline Merlet, Paula Ratajczak, François Béguin

Journal: Energy Storage Materials

DOI:

Contribution: Conceptualization, Methodology, Resources, Writing –review & editing, Visualization, Supervision, Project Administration, Funding Acquisition.



Signature

